ULTRA SENSITIVE MOLECULAR DETECTION USING OPEN CIRCUIT POTENTIAL

Kanokwan CHAROENKITAMORN

Japan Advanced Institute of Science and Technology

Doctoral Dissertation

ULTRA SENSITIVE MOLECULAR DETECTION USING OPEN CIRCUIT POTENTIAL

Kanokwan CHAROENKITAMORN

Supervisor: Professor Yuzuru Takamura

School of Materials Science

Japan Advanced Institute of Science and Technology

March 2018

Ultra-sensitive molecular detection using open circuit potential

Kanokwan CHAROENKITAMORN

Student ID: 1540012

School of Materials Science, Japan Advanced Institute of Science and Technology, 1-1 Asahidai, Nomi City, Ishikawa 923-1292, Japan

Abstract

This work presents the new approach to investigate metal nanoparticles (MNPs) labeled antibody for human chorionic gonadotropin hormone (hCG) detection by open circuit potential (OCP) measurement. OCP has drawn much attention for investigating various electrochemical processes because it can miniaturize electrochemical system for integration in compact analytical device. In this work, OCP was successfully used as detection method for the quantitative analysis of protein biomarker by using MNPs. The detection of pregnancy marker, human chorionic gonadotropin hormone (hCG), was developed. For gold nanoparticles based OCP detection, after preparation of sandwich-type immunosystem, a space between the AuNPs and electrode surface exists due to the formation of immunocomplexes that may hinder electron transfer process and cause unsuccessful detection of AuNPs at the secondary antibody. In order to overcome this issue, pre-oxidation and reduction processes were applied to the system to cancel/clear the gap. As a result, the detection of AuNPs at secondary antibody was significantly improved. However, this method requires the application of both oxidation and reduction potentials to achieve detectable signal, which makes it not simplified as OCP method should be. To simplify OCP measurement, we are interested in the use of PtNPs in a hydrazine solution, solution of redox molecules. Because the reaction of interest, the oxidation of hydrazine, was good electrocatalyzed at the PtNPs, the new simple electrochemical immunoassay based on PtNPs was developed in this chapter. The detection of hCG was demonstrated by direct electrical detection of PtNPs in a hydrazine solution using OCP measurement without any application of external potential procedure. The limit of detection of both developed method was found in pg/mL range with an acceptable sensitivity and reproducibility. Finally, the fabrication of micro-nano sized carbon electrode array was studied to approach the application of single molecule detection. A novel approach in which the direct pyrolysis of SAL601-SR2 electron beam resist after patterning was performed to obtain nano-sized carbon electrode array. This method enabled simple sub-micrometer fabrication of carbon dot (below 200 nm). This work shows the simplified and improved electrochemical assay for protein biomarker detection by OCP technique, and possibility to fabricate sub-micrometer sized carbon electrode array for single molecule isolating and counting application.

Keywords: human chorionic gonadotropin, carbon electrode, metal nanoparticles, open circuit potential, electrochemical immunosensor

Contents

Page

Page

This dissertation was prepared according to the curriculum for the Collaborative Education Program organized by Japan Advanced Institute of Science and Technology and Chulalongkorn University.

Chapter I

GENERAL INTRODUCTION

1.1 Introduction

A biomarker, or biological marker, generally refers to a measurable indicator of some biological state or condition. In the clinical field, protein biomarkers are used to differentiate between healthy and disease states, and to monitor disease progression. Many biomarkers exist near or below the limit of detection of current state-of-the-art analytical methods, especially in healthy individuals. For a long time, the conventional biochemical techniques have been explored for detection of biomolecules such as gel electrophoresis [1], enzyme-linked immonosorbant assay (ELISA) [2], and colorimetric assay [3]. Recently, fluorescence based ELISA are widely used in the development of ultrasensitive biosensors. Either absorbance or fluorescence is used as optical based method for analysis. Fluorescence is more sensitive because each fluorophore emits thousands are amplified to perhaps a million photons before it is photobleached. With both optical based method, the more of the absorbing or fluorescing species present, the higher the absorbance or fluorescence signal. However, although the optical detection is effective and highly sensitive method, several drawbacks associated can suffer from this type of measurement. These consist a requirement for generally complicated bulky instrument and power-intensive light sources, detectors, and monochromators, and potential false signals arising from complex colored samples. Moreover, the sensitivity of optical method is dependent on the Lambert–Beer law. Therefore, it requires some sample volume and path length to achieve certain performances [1]. In this context, electrochemical method is effective method for using as detector because of high sensitivity, ease of use, a possible automation and integration in compact analytical devices, mostly cheap and relatively simple technology of its production. For point-of-care testing (POCT) diagnostic systems, it requires portable, rapid, accurate, quantitative devices and easy-to-use systems that could be run by a non-expert, with minimum user interventions. Thus, electrochemical detection has great potential in POCT for early detection of diseases which can diagnose the disease while it is asymptomatic, with no signs or symptoms. The earlier detection of disease may lead to more cures or longer survival.[4].

Among electrochemical techniques, amperometry and voltammetry are frequently used to screen various kinds of analytes with high sensitivity such as α-fetoprotein (LOD~10 pg/ml) [5, 6], anthrax protective antigen toxin (LOD~50 pg/ml) [7], and hCG (LOD~36 pg/ml) [8].

Although the amperometry and voltammetry methods can provide LOD in the pg/mL range, the complexity of biological system makes them ineffective for the single molecule detection. This is because the amperometric and voltammetric methods detect signal by scanning a specific potential for a particular analyte. The potential scans from multiple electrodes would result in the crossed signal interference. Moreover, the scanning of potential makes the whole system complicated in design and operation. Therefore, the development of electrochemical method for immunoassay without any interference is needed. In this regard, open circuit potential (OCP) appears as a suitable technique since it simply measures the voltage difference between working electrode immersed in medium solution and a suitable reference electrode without application of neither potential nor current to the system. Compared to the voltammetry and amperometry, the OCP technique possesses several main advantages such as (i) spontaneous measurement of the electrode potential built by electrochemical reactions on the electrode surface, (ii) no perturbation on the solution, and (iii) easily acquiring multiple electrode potentials at once. Thus, OCP is suitable for simple detections of protein biomarkers [9, 10]. Previsouly, Ahammad and co-workers [11] have developed gold nanoparticle-modified indium tin oxide electrode for immobilizing horseradish peroxidase -conjugated antibody and applied to cardiac biomarker troponin I detection by the OCP. However, this system was not able to provide high sensitivity in pg/mL level, which is essential for single molecule detection.

In this work, we aim to develop a new method to build OCP based on antigen-antibody reaction, and highly-sensitive detection is demonstrated for protein biomarker measurement using metal nanoparticles as electrochemical label. Moreover, we aim to use the developed system for isolating and counting single molecule, and apply for earlier diagnosis.

To use the electrochemical method for isolating and counting single molecule, it is necessary to find a suitable material and method for fabrication of nano-micro electrode array. For this propose, carbon film is selected because of its high electrical conductivity with scaling-down possibility to nanometer order. The unique point of this research is the development of ultrahigh sensitive OCP-based electrochemical method for realization of isolating and counting single biomarker molecule.

1.2 Electrochemistry

The electrochemical techniques provide information on the processes taking place when an electric potential is applied to the system under study. Electrochemistry can be used to studies the oxidation (loss of electrons) or reduction (gain of electrons) that a material

undergoes during the electrical stimulation. These redox reactions (reduction and oxidation reactions) can provide information about the concentration, reaction mechanisms, kinetics, chemical status and other behavior of a species in solution. Generally, there are two kinds of electrochemical cells which are galvanic cell and electrolytic cell. Galvanic cell produces an electric current from energy released by a spontaneous redox reaction. On the other hand, electrolytic cell requires an external source of electrical energy to induce a chemical reaction. Electrolytic method have many advantages, for instance, high sensitivity with a wide linear dynamic range of concentration for both inorganic and organic species, simplicity, rapid analysis time and simultaneous detection of various target analytes. The selection of the electrochemical techniques depends on the nature of ions or compounds of interest and its interferences in surrounding environment [12, 13].

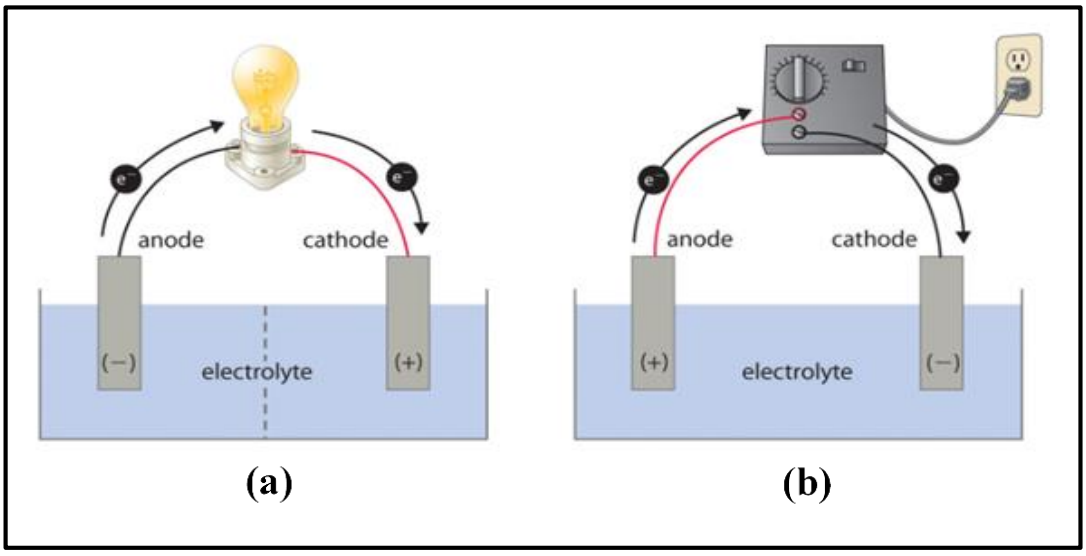

Figure 1. Electrochemical cells (a) galvanic cell, (b) electrolytic cell [14]

1.2.1 Fundamental of electrochemistry [15]

The redox reaction occurs only on the surface area of an electrode. There are four main factors that direct to the reaction rate and current at the electrodes: mass transfer to the electrode surface, kinetics of electron transfer, preceding and ensuring reactions, and surface reactions (adsorption) as shown in Figure 2. A simple reaction is represented by:

$$O + ne^- \rightleftharpoons R$$

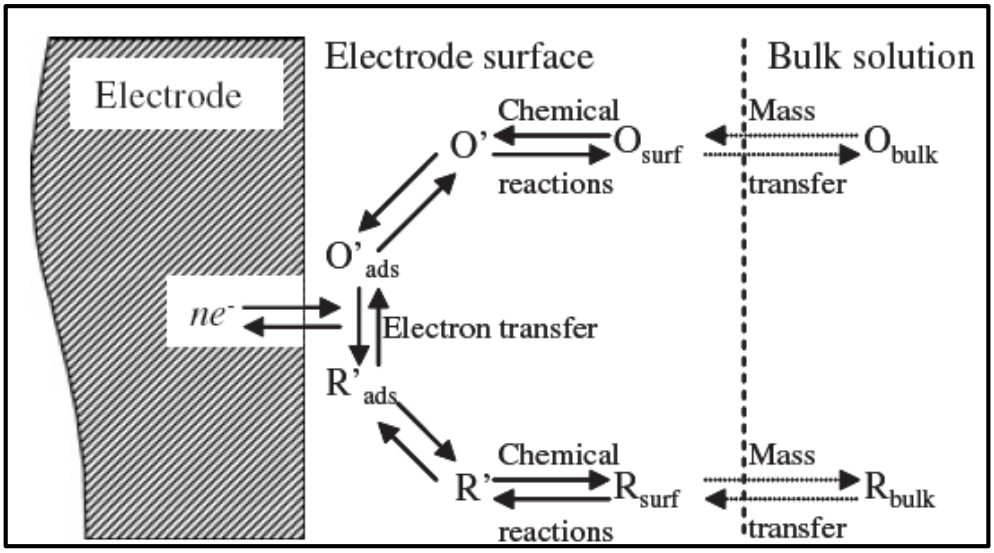

Figure 2. Process in electrode reaction [15]

O and R are the oxidized and reduced form of a redox reaction. For a system controlled by the laws of thermodynamics, the potential of the electrode can be used to determine the concentration of electroactive species by Nernst Equation:

$$E=E^0+\frac{2.3\ RT}{nF}\ \log\frac{C_0(0,t)}{C_R\ (0,t)}$$

Where E^0 is the standard potential for the redox reaction, $C_o\ (0,t)$ and $C_R\ (0,t)$ are the concentration of the oxidized and reduced form, respectively. R is the universal gas constant (8.314 $JK^{-1}mol^{-1}$), T is the Kelvin temperature, n is number of electrons transferred in the redox reaction, and F is the Faraday constant (96,487 coulombs).

1.2.1.1 Mass transfer [13, 16]

Mass transfer process is one of the main fundamental electrochemistrys to describe charge transfer on the surface area of the electrode. The mass transfer consists of three processes: migration, diffusion and convection.

(i) Migration

The movement of ion under the electrical field in solution, positive charge will be attracted to negative charge and the negative charge will be also attracted to opposite way (Figure 3). The increased or decreased velocity of ion depends on the potential at the surface of electrode. Migration of all ion species in solution can take place; therefore, the current of ion from analyte might be suppressed. To solve this problem, the addition of a large concentration of electrolyte usually applies.

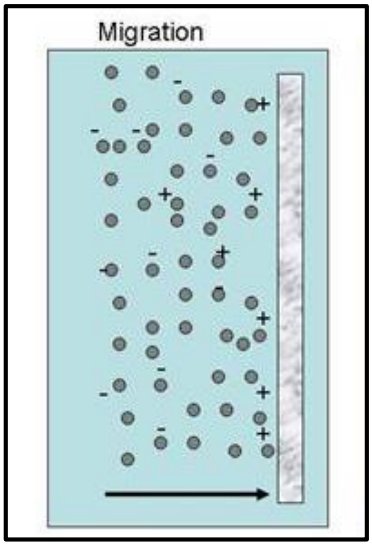

Figure 3. Migration of ion in solution [17]

(ii) Diffusion

The movement of ion or molecule in solution occurs from different concentrations between two regions. Ion will move from higher concentration region lower ones as shown in Figure 4.

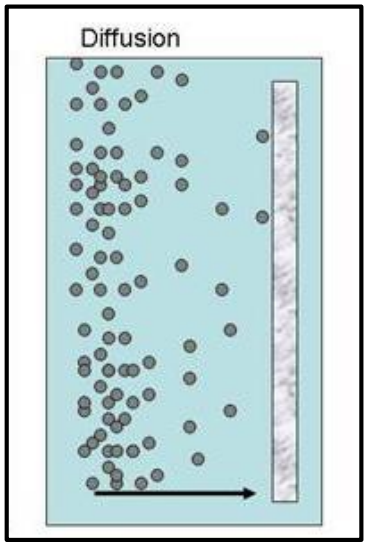

Figure 4. Diffusion from a different concentration [17]

(iii) Convection

The movement of fluids is described by hydrodynamics. The convection is generated by the difference of temperature and density of solution from external mechanisms such as stirring, vibration, and flowing. The mass transfer is accelerated by the convection.

1.2.2 Voltammetry [16, 18]

Voltammetry is an electrochemical technique which is based on the application of a potential to an electrode surrounded with an electrolyte containing electro-active species and measuring the signal as a current flowing through that electrode. Voltammetric electrochemical cell consists of three electrodes which are working electrode (WE), counter electrode (CE) and reference electrode (RE). Each electrode have their specific characteristics. Working electrode is the most important electrode of electrochemical cell because the interested reaction will occur at the surface of this electrode. Next, counter electrode or auxiliary electrode is an electrode used in a three electrode electrochemical cell for voltammetric analysis or other reactions in which an electric current is expected to flow. This electrode will make the potential of reference electrode remain constant since no electron flow through. Lastly, reference electrode is an electrode which has a constant and well-known electrode potential. The high stability of the electrode potential is usually achieved by using a redox system with constant (buffered or saturated) concentrations of each species of the redox reaction. Occasionally, the potential that applied in the system changed as a function of time was controlled.

1.2.2.1 Cyclic Voltammetry [13, 18]

Cyclic Voltammetry (CV) is the most commonly known technique for studying qualitative information of substances, for instance, redox processes, reaction intermediates, and stability of reaction products. Thus, cyclic voltammetry is the first step to perform when electrochemical technique is applied. This technique is based on changing the applied potential of the working electrode in both forward and backward direction (opposite direction) at constant scan rate while monitoring the signal current. Electrochemical behavior of the system can be obtained from this simple technique that requires relatively small experimental attempt. Unfortunately, it is difficult to get quantitative information from this technique. Cyclic voltammetry experiment comprises of linear scan potential of a working electrode in an equilibrium unstirred solution by a triangular potential waveform shown in Figure 5. The potential waveform illustrates the forward scan and then backward scan. The measured current at working electrode is plotted versus the applied potential called cyclic voltammograms. Normally, a voltammogram of reversible redox couple during one cycle shows cathodic current (i_{pc}) in the forward scan (from positive potential to negative potential) and anodic current (i_{pa}) in the reverse scan (from negative potential to positive potential) at the applied potential approached to the standard potential E^0 for that redox process. The corresponding peak

potential occurring at i_{pc} and i_{pa} named cathodic peak potential (E_{pc}) and anodic peak potential (E_{pa}), respectively.

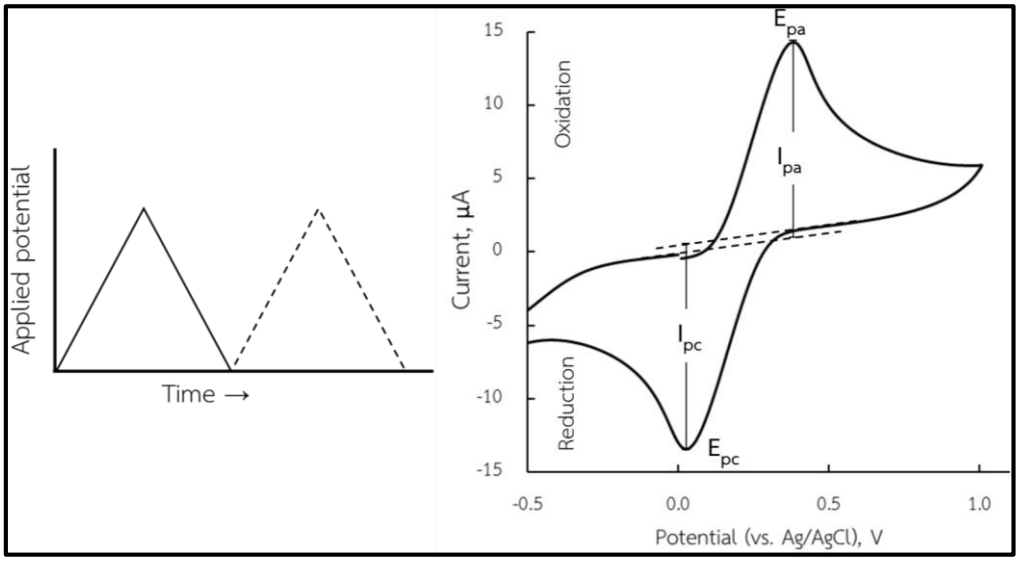

Figure 5. Cyclic voltammetric excitation signal (left) and cyclic voltammogram of a reversible reaction (right) [18].

For a reversible reaction, the ratio of i_{pa}/i_{pc} is approaching 1. This peak ratio can be impacted by chemical reaction coupled to the redox process. The formal potential for a reversible reaction is related to the peak potential (E_p) as follows:

$$E^0 = \frac{E_{pa} + E_{pc}}{2}$$

The peak current of reversible reaction is presented by Randles-Sevcik equation as shown below:

$$i_p = (2.69 \times 10^5) n^{3/2} A C D^{1/2} v^{1/2}$$

Where n is the number of transferred electron, A is the electrode surface area (cm^2), C is the concentration (mol cm^{-3}), D is the diffusion coefficient (cm^2 s^{-1}), and v is the scan rate (mV s^{-1}). From the Randles-Sevcik equation, the peak current is proportional to the square root of the scan rate.

For an irreversible reaction; when the rate of mass transport increases, the reverse peak becomes disappeared. Generally, a shift of the peak potential with a scan rate can occur for the irreversible process.

1.2.3 Open Circuit Potential (OCP) measurement

Open Circuit Potential (OCP) is a type of electrochemical technique for investigating various electrochemical processes by measuring the voltage without application of any potential or current to the system. It can be measured by determining a voltage difference between working electrode immersed in medium solution and a suitable reference electrode. The signal is a function of voltage against the measurement time. The magnitude and sign of OCP depend on the composition of working electrode itself, as well as on the temperature, and hydrodynamic of the electrolyte. These parameters and the type of reference electrode should be noted when the signal is recorded.

The OCP measuring instruments should be capable of accurately measuring small voltages without drawing an appreciable current, such as potentiometric circuit, a high-impedance voltmeter, or an electrometer. If the voltmeter is used, care must be taken to properly denote polarities.

Because of its simplicity, OCP can be used either in laboratories or in field. Moreover, it can be applied to simplified and miniaturized electrochemical systems for using in clinical diagnosis of diseases. [9].

Most electrochemical methods such as amperometry and voltammetry were considered as a prime candidate for the development of potable smart immunosensors. However, there are still some external requirements, including a voltage supply source from a suitable instrument and a skillful person to act as an operator. The scanning of potential during voltammetric measurement makes the whole system complicated in design and operation. Moreover, with the conventional three-electrode systems used in voltammetry and amperometry, many substrates can undergo redox reactions during the application of a voltage, which will cause great interference, especially in biological samples. At this point of view, we have interest in OCP as a new detection principle. Moreover, among of electrochemical techniques, OCP measurement has been regarded as a simple, efficient, and suitable tool for qualitative analysis using biochemically modified electrode and electrochemical system [19, 20]. Therefore, OCP can be applied to simplify and miniaturize electrochemical systems for using either in laboratories or in the field for clinical diagnosis [11]. Several advantages in the miniaturized reference electrodes include short-term stability, chemical inertness, easy manufacturing, and low cost [10]. Therefore, OCP is selected to use as detection technique in this research.

1.2.4 Electrode

The electrochemical cell, where the voltammetric experiment is performed comprised of a working electrode, a reference electrode and a counter electrode. Usually, the electrode provides the interface between solid phase and electrolyte which charge can be transferred. At the suitable applied potential, the reduction or oxidation of analytes occur at the surface of electrode and the current is generated.

1.2.4.1 Working electrode (WE)

The working electrode is the electrode at which the interesting reaction of target analytes occur. The reaction that occurred at the working electrode can be referred to as either anodic or cathodic. The applied potential of working electrode was varied in a specific value with the variations in the concentration of target analyte. The electrode performance seriously depends on the material of the electrode. The ideal working electrode should give a high signal-to-noise ratio of the interesting analytes, a reproducible electrode surface, a wide potential window, high electrical conductivity, low cost, low toxicity and availability.

1.2.4.1.1 Screen printed electrode (SPCE)

New technology for fabrication of disposable electrochemical platform is screen-printed method. This technology has advantages of design flexibility, process automation, good reproducibility, a wide choice of materials. The construction of SPCEs for the development of disposable sensors includes a series of basic stages, namely selection of the screen, selection and preparation of the inks, selection of the substrate and the printing, drying and curing stages. Compared to other technologies that are available for manufacturing electrodes, such as thin-film, thick-film electrodes, SPCEs are ease of fabrication, simplicity, portability, low-cost, small size and mass production capabilities. SPCEs have been successfully utilized for the analysis of environmental pollutants such as organic compounds, heavy metals and gas pollutants [21, 22].

For electrochemical immunosensor, it requires labelling of either antigen or antibody with electroactive species. Electrochemical immunosensors combine the specificity inherent to antigen–antibody interactions with the high sensitivity of electrochemical transduction [23]. Most of the reported using electrochemical immunosensors are based on the immobilization of antibodies onto a working electrode surface of SPCE.

A novel screen-printed carbon electrode (SPCEs) on sheets of vegetable parchment has been developed by M. Yan and coworkers [24]. They constructed immonosensor using

graphene nanosheets (GS) and horseradish peroxidase (HRP)-labeled signal antibody functionalized with gold nanoparticles (HRP-Ab_2/AuNPs). GS and AuNPs were used to increase the conductivity and stability of the immunosensor and amplify the electrochemical signal on the sandwich immuno-complexes modified SPCEs. With this developed sensor, highly sensitivity was observed toward the detection of prostate specific antigen (PSA), which shows considerable significance in early screening and clinical diagnosis of prostate cancer. Moreover, this immunosensor showed a wide linear range over 6 orders of magnitude with the minimum value down to 2 pg mL^{-1}. A year later, W. Dou et al. [25] have proposed 4-channel screen-printed carbon electrode for simultaneous detection of *Escherichia coli* O157:H7 and *Enterobacter sakazakii*. To enhance the sensor's sensitivity, multi-walled carbon nanotubes (MWCNTs)/ sodium algenate (SA)/ carboxymethyl chitosan (CMC) composited film was coated on surface of working electrode. MWCNT in biopolymer composite acted as electron-conduction pathway and promoted the electrical communication. Horseradish peroxidases (HRP) labeled antibodies of two bacteria were immobilize on different working electrode of the same SPCE respectively. Using proposed sensor, The LODs of 4.57 x 10^4 cfu mL^{-1} and 3.27×10^3 cfu mL^{-1} were observed for *E.sakazakii* and *E.coli* detection, respectively. Recently, a disposable electrochemical immunosensor strip for the detection of the Japanese encephalitis virus (JEV) has been reported by S. F. Chin and authors [26]. The assay is based on the use of a screen printed carbon electrode (SPCE) modified with carbon nanoparticles (CNPs). The deposition of CNPs can enhance the electron transfer kinetics and current intensity. Using electrochemical impedance spectroscopy (EIS), the LOD of JEV detection was found to be 2 ng mL^{-1}. This proposed sensor shows a cost-effective alternative to conventional diagnostic tests for JEV. In the same year, S. D. Tallapragada et al. [27] proposed an immunosensor for the detection of Human Epidermal Growth Factor Receptor-2 (HER2) based on SPCE using sandwich format. In this work, they show the simple use of unmodified SPCEs for the detection of HER2 antigen using the sandwich ELISA protocol. They found that the amperometric current increased linearly when the concentration of HER2 is increased in the range of 5–20 ng mL^{-1}, 20–200 ng mL^{-1} with the detection limit of 4 ng mL^{-1}. The result shows compatible with the sandwich ELISA system and high sensitivity was observed toward the presence of HER2.

As mentioned above, SPCEs show an efficient alternative to the traditional methods of detection of biological analysis. Although some modification is needed to improve the sensitivity and selectivity, the versatility and low-cost of this SPCE is attractive for its continuous development.

1.2.4.1.2 Pyrolysis photoresist carbon electrode (PPCE)

A pyrolyzed photoresist film is an attractive alternative to other carbon electrodes for application in electroanalyses with advantages of simple and inexpensive fabrication process compared with glassy carbon. The fabrication of PPCE was simply done by pyrolysis of photoresists on silicon wafers at temperatures ranging from 600 to 1100°C. When compared to other carbon electrode surfaces, such as polished glassy carbon (GC), the surface of PPCE is smother (<0.5 nm rms). Additionally, the curing under less carbon oxidation atmosphere makes PPCE be relatively stable toward air oxidation due to a low oxygen/carbon atomic (O/C) ratio. A surface shows a low capacitance with the low background levels resulting from smoothness and low O/C ratio. The most attractive feature of PPCE is the ability to create sensitive carbon electrodes through lithographically patterning photoresist that opens up many useful possibilities for electrode design in various applications [28-31].

Most of researchers have used PPCE as detectors in microfluidic devices. Hebert et al. [29] have introduced PPCE in a PDMS−quartz hybrid microchip device. The utility of PPCE is demonstrated by the separation and detection of various neurotransmitters. For dopamine, this sensor showed very high sensitivity, with a LoD of 100 nM. Luntes' group [32] compared various electrode materials including PPCE, carbon fiber, Pd and carbon ink. Dopamine (DA), norepinephrine, and catechol (CAT) were tested using amperometric detection in microchip electrophoresis devices. They proved that PPCE provides the best sensitivity and lowest detection limit of 35 nM for DA. PPCE has also been used as an on-chip detector for the online measurement of cellular release. S. T. Larsen and coworkers [33] showed that PPCE can be used for amperometric detection of potassium-induced transmitter release from large groups of neuronal PC 12 cells. This research opens the way for the use of PPCE in microfabricated devices for neurochemical drug screening applications.

Although most of PPFC based research is focused on microfluidic devices, few research has reported the use of PPCE in elecro-immunosensor. J. A. Lee et al. [34] presented the use of PPCE as a working electrode of electrochemical impedance biosensor for aptamer-based thrombin detection. Thrombin aptamer was grafted onto the PPCE surface using carbodiimide

mediator. Electron-transfer resistance changes resulted by thrombin binding onto the carbon surface. Thrombin concentrations between 0.5 nM and 500 nM were detected.

From many applications as mention above, PPCEs are attractive material with many benefits such as miniaturization, integration, and low-cost fabrication in electrochemical biosensors. Especially, it can be microfabricated into sensor electrodes of various sizes and shapes with excellent reproducibility that show the possibility to use in single molecule counting application.

1.2.4.1.3 Metal nanoparticles (MNPs) label electrochemical immunosensor

Metal nanoparticles (MNPs) exhibit unique optical, electrical, thermal and catalytic properties. Therefore, they have attracted considerable interest and extremely suitable for designing new and improved sensing devices, especially electrochemical sensors and biosensors. MNPs have some chemical behaviors similar to small molecules and can be used as specific electrochemical label. Generally, MNPs are applied to many fields involving food analysis, environmental analysis, information technologies, industry, biological medicine, and biosensors [35]. The basic functions of MNPs in electrochemical field are immobilization of biomolecules, catalysis of electrochemical reactions, enhancement of electron transfer, and labeling biomolecules. For labeling biomolecules, such as antigens and antibodies, MNPs play an important role in the development of biosensors. Biomolecules labeled with MNPs can maintain their bioactivity and interact with their counterparts. Moreover, the amount or concentration of analytes can be directly determined from those MNPs using electrochemical techniques [36].

- Gold nanoparticles (AuNPs)

Gold nanoparticles (AuNPs) are the most frequently used among all the metal nanoparticle. Its inherent advantages, including easy preparation, excellent biocompatibility, conductivity, high surface-to-volume ratio and surface free energy, and catalytic properties make AuNPs suitable candidates for use as amplifiers on electrode surfaces to enhance the electron transfer between redox centers in proteins, and as catalysts to increase electrochemical reactions. Especially, the biocompatibility of AuNPs is highly advantageous, enabling the incorporation of biomolecules such as enzymes and proteins into electrochemical systems. Compared to enzymes/protein, AuNPs show better long-term stability and are more easily prepared. Moreover, AuNPs enabled the incorporation of biomolecules such as enzymes and proteins into electrochemical systems. The ability of AuNPs to provide stable environments for

the immobilization of biomolecules has led to many developments in the design of biosensors. Therefore, AuNPs are often used as label for detecting antigen in electrochemical immunoassay [37, 38].

The literatures have become abundant with AuNPs-based biosensors for detection of antigens. Idegami and co-aurthors [8] developed sensitive immunosensor for the detection of pregnancy marker, human chorionic gonadotropin hormone (hCG), using sandwich-type immunoassay. The direct electrical detection of Au nanoparticles, which labeled on secondary antibodies, was measured to determine the concentration of hCG in samples. Using differential pulse voltammetry, a detection limit of 36 pg mL^{-1} hCG was observed. A year later, D. Tang and co-workers [39] have developed a new signal amplification strategy based on thionine (TH)-doped magnetic gold nanospheres as labels and horseradish peroxidase (HRP) as enhancer. The developed sensor promise to improve the sensitivity and detection limit of the immunoassay for carcinoembryonic antigen (CEA). The electrochemical signal is amplified both by magnetic bionanosphere labels and by the bound HRP on the magnetic bionanospheres toward the catalytic reduction of H_2O_2. The noise is reduced by employing the carbon fiber microelectrode (CFME) electrode and the hydrophilic immunosensing layer. The developed immunoassay could be increased LoD to 0.01 ng mL^{-1}. Li et al. [40] fabricated a new electrochemical immunoassay for the detection of Hepatitis B surface antigen (HBsAg) using nanogold-codified horseradish peroxidase-HBsAb conjugates as secondary antibodies. This developed system provided the detection limit of 0.1 ng mL^{-1}. Then a new electrochemical immunoassay protocol for sensitive detection of α-fetoprotein (AFP, as a model) is designed by J. Tang and co-workers [41]. Carbon nanoparticles (CNPs)-functionalized biomimetic interface was used as immunosensing probe and labeled secondary antibody with irregular-shaped gold nanoparticles (ISNGs)-labeled horseradish peroxidase-anti-AFP conjugates (HRP-anti-AFP-ISNG). The electrochemical immunosensor using developed sensor exhibited high bioelectrocatalytic response toward enzyme substrate with LoD of 10 pg mL^{-1} toward AFP. N. X. Viet et al. [42] developed a new sensitive gold-linked electrochemical immunoassay (GLEIA) for the detection of the pregnancy marker human chorionic gonadotropin (hCG). AuNPs were used to label the antibody immunocomplex on the single-walled carbon nanotube (SWCNT) microelectrodes. The concentration of hCG showed a linear relationship with the current intensity obtained from differential pulse voltammetry measurements with a limit of detection (LOD) of 2.4 pg mL^{-1} hCG. Recently, B. Kavosi and co-authors [43] presented a triple signal amplification strategy for ultrasensitive immunosensing of prostate-specific

antigen (PSA) tumor marker based on graphene-chitosan as platform and polyamidoamine dendrimer-encapsulated gold nanoparticles-enzyme linked aptamer as a synergetic signal amplification label. In the sandwich format, electrocatalytic reduction of H_2O_2 in the presence of enzymatically oxidized thionine was measured. Using electrochemical impedance spectroscopy (EIS), detection limit of 5 pg ml^{-1} was observed.

As illustrative examples given, AuNPs play an important role in the biosensing process and the mechanism of AuNPs can be used to improve the analytical performances.

- Platinum nanoparticles (PtNPs)

Platinum nanoparticles (PtNPs) are especially interesting in catalysis, as platinum is one of the most important materials used in industrial catalysts such as the contact process for producing sulfuric acid. It is also used as a catalyst for cracking oil, in fuel cells and in catalytic converters for cars. PtNPs has a substantially higher effectiveness because of the increased specific surface area. The preparation of PtNPs are synthesized in a similar fashion to AuNPs and silver nanoparticles (AgNPs). Because PtNPs is more expensive and less biocompatible than AuNPs, therefore it is less frequently used in bioanalytical fields. However, in biosensor, PtNPs were used as signal amplifier due to the excellent electrical conductivity and high catalytic activity. Moreover, the application of PtNPs can improve the immobilizing amount of antibody and the sensitivity of the proposed electrochemical immunosensor via the interaction of Pt-NH_2 [36, 37].

Although the literatures of PtNPs based biosensor are not as popular as AuNPs based biosensor, many researchers still used PtNPs for detecting antigens. J. Zhang and coworkers [44] have used platinum catalyzing a hydrogen evolution reaction as enhancement strategy for prostate-specific antigen (PSA) immunosensor. A gold electrode was utilized to bond with PSA capture antibodies via covalent bonding. After that, a secondary platinum nanoparticle-labeled detection antibody was used to complete the sandwich immunosensor. Using proposed platinum enhancement strategy, LoD of 1 fg mL^{-1} was achieved. Then an ultrasensitive multiplexed immunoassay method was developed using mesoporous platinum nanoparticles (M-Pt NPs) as nonenzymatic labels [45]. M-Pt NPs were prepared using ultrasonic method and labeled on the secondary antibody (Ab_2) as signal amplification. After the sandwich-type immunoreactions, the M-Pt-Ab_2 was bound to immunosensor surface. The electro-reduction of H_2O_2 reaction was catalyzed, which produced detectable signals. Using breast cancer related panel of tumor markers as model analytes, the LoDs of 0.002 U mL^{-1}, 0.001 U mL^{-1} and 7.0

pg mL^{-1} for CA125, CA153 and CEA were observed, respectively. Later, Y. Li et al. [46] designed a sensitive and facile electrochemical immunosensor for ultrasensitive detection of hepatitis B surface antigen (HBsAg) using platinum nanoparticle decorated amino silane functionalized montmorillonite (Pt–NH_2–MMT). Pt–NH_2–MMT showed high electrocatalytic activity toward the reduction of hydrogen peroxide. Under optimal conditions, the immunosensor provided a LoD of 2.0×10^{-4} ng mL^{-1}. Recently, Li Liu and coauthors [47] presented the development of quantitative monitoring of AFP. An incorporated signal amplification strategy of platinum nanoparticles anchored on cobalt oxide/graphene nanosheets (PtNPs/Co_3O_4/graphene) was proposed by acting as the label of secondary antibodies to achieve ultrasensitive sandwich-type electrochemical immunosensor. Under optimal conditions, this electrochemical immunosensor exhibited a low detection limit of 0.029 pg mL^{-1} for AFP.

In writing the literatures, we can conclude that MNPs have an important role to play in the field of biosensor application and continues to expand in the future.

1.2.4.2 Reference electrode (RE)

Reference electrode is an electrode having known electrode potential that remain constant at specific temperature and is independent of the concentration or composition of the analyte solution. This electrode acts as reference point along the potential axis by which the oxidizing or reducing power of the working electrode is evaluated. Moreover, the ideal reference electrode should be simple to fabricate and to use practically. The commonly used reference electrode is silver/silver chloride reference electrode because of simplicity, inexpensiveness, stability, and low toxicity.

1.2.4.3 Counter electrode (CE)

Counter electrode normally used to minimize errors from the cell resistance while controlling the potential of working electrode. This kind of electrode is generally made of a chemically inert conducting material with immense electrode surface area. Platinum wire or graphite rods are the most widely counter electrode in the electrochemical analysis.

1.3 Single molecule detection (SMD)

To increase understanding of disease processes and progression, new therapeutic method for earlier diagnosis that target different mechanisms of action are required. Essential to acquiring this understanding is the ability to differentiate between healthy and disease states.

Biomarkers are an important indicator for presence the stage of disease [48]. Many important research areas in chemical analysis, biomedical research, and clinical diagnostics have been a focus on the development of sensitive methods for detection and identification of target biomolecules. Single molecule detection (SMD) are developed for measurement of small changes at low concentrations in small volumes that can provide sensitive, accurate, reproducible, and rapid measurements. SMD has ability to detect single molecules and represents the ultimate level of sensitivity in analytical chemistry [49].

The conventional detection method for SMD is based on optical methods. Either absorbance or fluorescence is used as optical based method for analysis. Fluorescence is more sensitive because each fluorophore emits thousands are amplified to perhaps a million photons before it is photobleached. With both optical based method, the more of the absorbing or fluorescing species present, the higher the absorbance or fluorescence signal. [50]. Jin et al. developed a sensitive single-molecule imaging method with adsorption equilibrium. The adsorption equilibrium of protein was achieved between solution and glass substrate. Then, fluorescence images of protein molecules in an evanescent wave field were taken by total internal reflection fluorescence microscopy (TIRFM). Finally, the number of fluorescent spots corresponding to the protein molecules in the images was counted [51]. Later, they also used TIRFM for detection of anti-human IgG concentration. In this work, the strong biotin–streptavidin affinity, the target molecules were labeled with streptavidin-coated quantum dots as fluorescent probe. Then, images of fluorescent spots were obtained in the evanescent wave field [52]. Moreover, the same authors presented quantifying the antibody immobilzed on a surface using quantum dots and epi-fluorescence microscopy. Quantum dots were formed complexes with surface-immobilized antibody molecules and acted as fluorescent probes. The single-molecule fluorescence detection was performed using epi-fluorescence microscopy as the tool [49]. Duffy and co-workers developed a highly sensitive immunoassay, called digital ELISA. The single molecule detection is performed based on the detection of single enzyme-linked immunocomplexes on beads that are sealed in femtoliter well arrays. This digital ELISA was applied for detection of prostate-specific antigen (PSA) with high efficiency and sensitivity [53, 54]. In this context, it was found that optical method is the most popular method for using as detector in SMD. However, the drawback of optical method is performed with general bulky instrument that not suitable for point of care analysis [1]. Hence, miniaturization of diagnostic devices without affecting their sensitivity or limit of detection is highly desirable. Among the various immunosensors developed, electrochemical immunosensors have become the

predominant analytical technique for the quantitative detection of biomolecules. An effective strategy for electrochemical single molecule detection is to isolate each biomolecule into small electrode, one at a time. Therefore, simultaneous and parallel analyses of single biomolecule complexes, many electrode within each array are required.

1.4 Electron beam lithography (EBL) [55-58]

To fabricate micro-nano scale electrode, we are interested in the use of electron beam lithography (EBL) system. EBL is one of fabrication tool that allow to create patterns at micro-nanostructures on wide variety of materials. EBL is the operation of scanning a focused electron beam to draw a desired pattern on surface covered with an electron-sensitive film called a resist. The desired pattern is created based on the chemical modification of polymer resist film by electron irradiation. EBL is closely similar to SEM. The main difference is that the electron beam of EBL is scanned onto sample according to pattern coming from the pattern generator, while the electron beam of SEM is raster scanned over the sample to collect secondary electrons in order to get an image. EBL system consists of 3 main parts including:

(i) Chamber

Chamber is maintained in high vacuum by suitable set of pump. The sample is normally loaded into main chamber, and are typically placed on an interferometic stage for accurate positioning on sample.

(ii) Electron source

Electrons are emitted from a conducting material. Thermionic sources are emitted the electrons by heating material to the point where the electrons have enough energy to overcome the work function barrier. Field emission sources are emitted the electrons by applying an electric field sufficiently strong that they tunnel though the barrier. Three key factors of source are the virtual source size, its brightness (in $A/cm^2/rad$), and the energy

(iii) Column

Column is maintained in high vacuum by suitable set of pump. EBL column typically contains of all the electron optical element consisting lenses, a blanket for tuning the beam on/off, a mechanism for deflecting the beam, correcting astigmatism in the beam, defining the beam, and aligning the beam in the center of column, and an electron detector for focusing and locating marks on the sample.

The main advantages of EBL technique are

- High resolution up to 20 nm (photolithography~50 nm)
- Flexible technique with variety of material
- Print complex patterns directly on substrate
- Elimination of diffraction problem

According to many advantaged of EBL, it is selected to achieve the fabrication of micro-nano electrode array in this research.

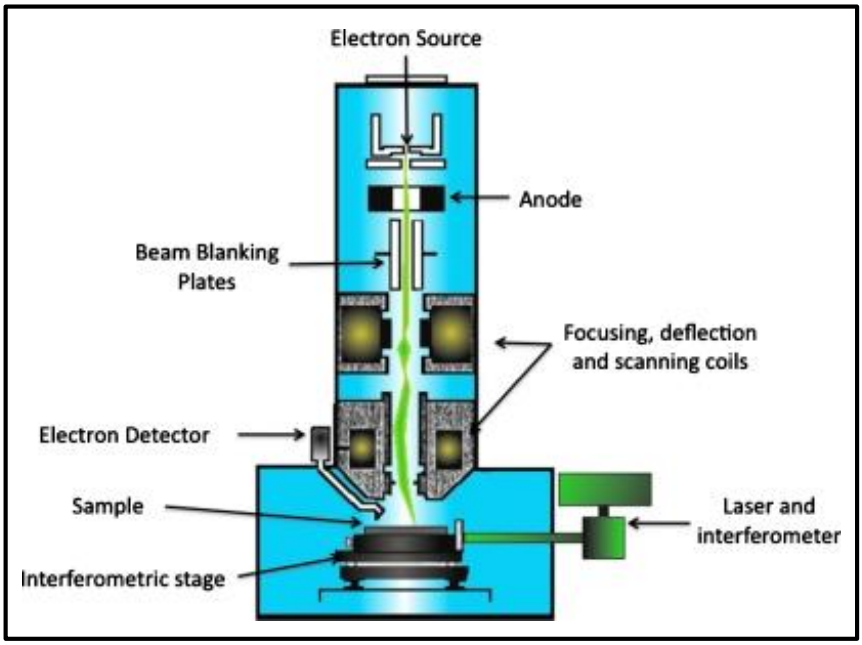

Figure 6. A typical EBL system, consisting of a chamber, an electron gun, a column containing all the electron optics needed to focus, scan, and turn on or turn off the electron beam [55].

1.5 Plasma dry etching process [59-61]

Dry etching refers to the removal of material in plasmas or etchant gasses. The reaction takes place by utilizing high kinetic energy of particle beam, chemical reaction or a combination of both. Processes are controlled by RF power, pressure, time, and gas selection to drive a reaction. Plasma dry etching can generally divide to three types including:

(1) Physical etching

Physical dry etching requires high energy particles such as ion, electron, or photon to etch off the atoms of substrate. When the atoms on the surface of substrate are hit by the high energy particles, the material evaporates and leaves from the surface. There is no chemical reaction taking place. Only the material at unmasked will be removed.

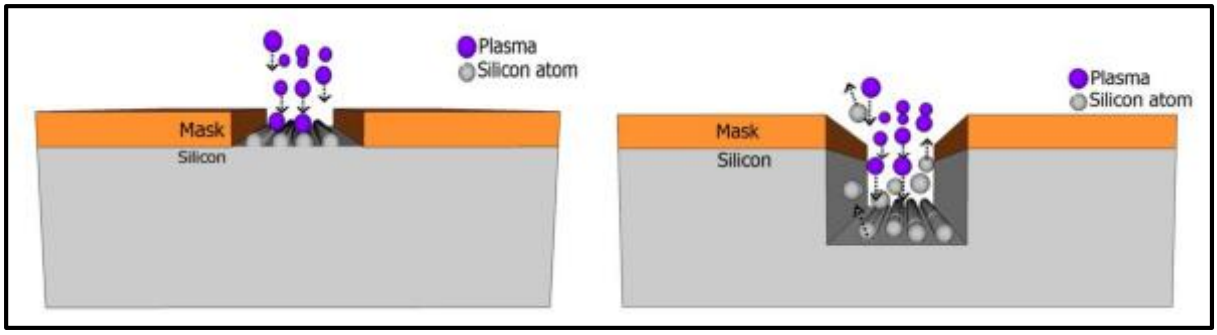

Figure 7. Scheme of physical etching process. (i) The plasma atoms hitting the surface. (ii) The silicon atoms being evaporated off from the surface [62].

(2) Chemical etching

Chemical dry etching or vapor phase etching does not use liquid chemicals or etchants. When etchant gases attack on the surface of substrate, the chemical reaction takes place. Normally, the chemical dry etching process is isotropic and displays high selectivity. Using anisotropic dry etching, the directional nature of dry etching, undercutting can be avoided. Therefore it shows the higher ability to etch with finer resolution and higher aspect ratio than isotropic etching. Some of the ions that are used in chemical dry etching is tetrafluoromethane (CH_4), sulfur hexafluoride (SF_6), nitrogen trifluoride (NF_3), chlorine gas (Cl_2), or fluorine (F_2)

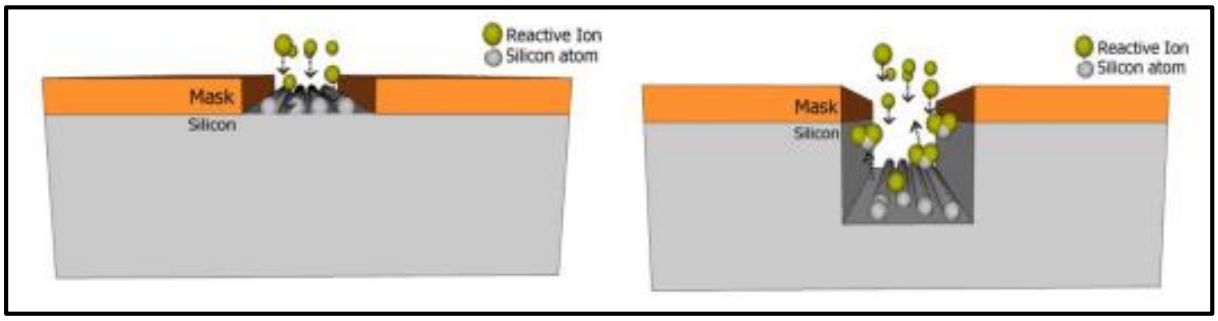

Figure 8. Scheme of chemical etching process. (i) The reactive ion interacts with the silicon atom. (ii) The reactive ion bondswith the silicon atom then chemically remove the silicon atoms from the surface [62].

(3) Reactive ion etching (RIE)

RIE uses both physical and chemical mechanisms to obtain higher resolution. This process is one of the most diverse and most widely used processes in industry and research. This process is much faster because it involves both physical and chemical interactions. The dissociation of the etchant molecules into more reactive species is supported by the high energy collision from the ionization. In RIE process, cations are produced from reactive gases such as

CF_4 and O_2, which are accelerated with high energy to substrate and chemically react with the surface.

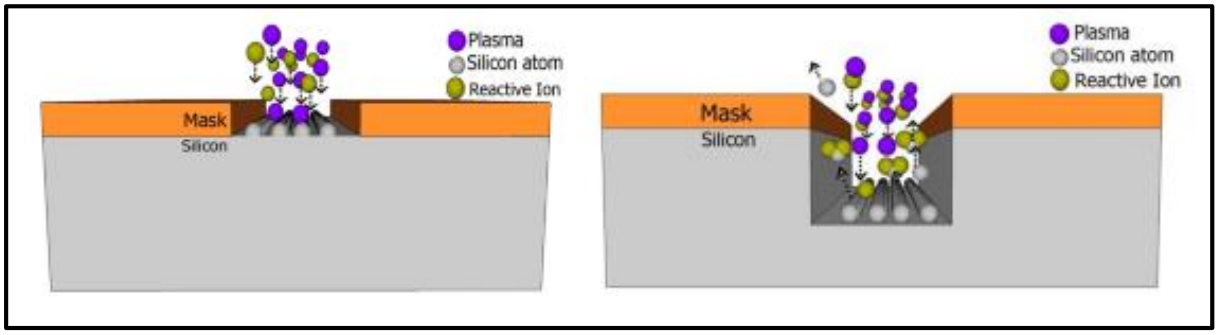

Figure 9. Scheme of RIE process. This process involves both physical and chemical reactions to etch off the silicon [62].

The advantages of plasma dry etching compared to traditional wet etching are following:

- Less sensitive to change of atmospheric such as temperature, pressure, and time
- Most of etchant gases are not toxic
- Waste products are mostly gaseous which are released into atmosphere
- Minimal amount of raw materials consumed
- Less undercutting
- Ease of automation
- High resolution and cleanliness

As mentioned above, dry etching process is attracted to use in micro-nano fabrication in this research.

1.6 Protein biomarkers [63, 64]

Biomarkers are a measurable indicator of a specific biological state, particularly one relevant to the risk of contraction, the presence or the stage of disease. The protein domain is likely the most directly and ubiquitously affected in disease. Protein biomarkers hold special promise for a wide range of clinical and biomedical applications as following;

- Disease screening / early detection
- Diagnosis
- Prognosis
- Disease activity monitoring

- Targeting molecular therapeutics
- Assessing therapeutic response
- Defining molecular taxonomies of patients and diseases
- Surrogate endpoints in early-phase drug trials

The quantitative analysis of protein biomarkers are commonly and easily obtained from biological fluids such as urine and serum. It offers the opportunity to improve the quality and safety of patient care with more accurate diagnoses and non-invasive manner as well as providing a potential towards more individually targeted treatment. The most importance to achieve progress in biomarker detection assay is the development of assay with high sensitivity and selectivity. In this thesis, human chorionic gonadotropin (hCG) is used as a model analyte.

1.6.1 Human chorionic gonadotropin (hCG)

Human chorionic gonadotropin (hCG) is a carbohydtrate hormone that was used as a target molecule in this work. The hCG is heterodimeric glycoprotein hormone consisted of 237 amino acid. hCG has two dissimilar α and β subunits that noncovalently linked by charge interactions. Both subunits required for the biological activity of the hormone. For α subunit, the molecular weight is approximately 18,000 daltons. This subunit is essentially identical to the alpha subunit of the pituitary glycoprotein hormones such as follicle-stimulating hormone (FSH), luteinizing hormone (LH), and thyroid-stimulating hormone (TSH). For β subunit, it has a molecular weight of approximately 30,000 daltons. The β subunit provides biological and immunological specificity to the entire hCG. The hCG is produced by trophoblast cells of placenta, trophoblast cells in gestational trophoblastic diseases, virtually all trophoblastic tumors and most germ cell tumors of the gonads. The amount of hCG is proportional to the amount of trophoblast cells. Therefore, the determinations of hCG are necessary and very important for detection of pregnancy, prenatal screening, or diagnosis and monitoring of cancer patients.[65-67].

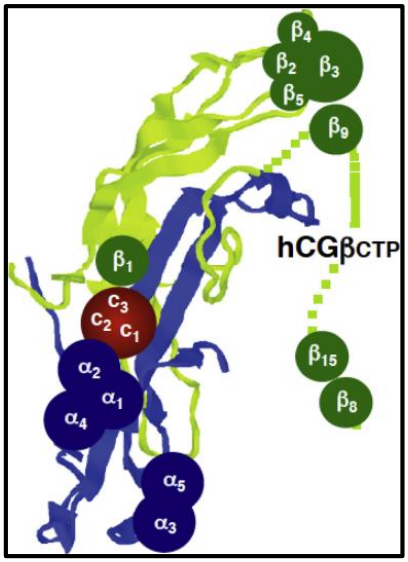

Figure 10. A 3-D model of hCG [67]

1.6.2 hCG levels in clinical application

- Monitoring of pregnancy [68, 69]

Either hCG or hCG together with hCG-β can be used for monitoring of pregnancy. Normally, woman produces 25 milli-international units per milliliter (mIU/mL) of hCG 10 days after the conception. The general hCG levels doubles every 2 to 3 days after the conception. The hormone is released in the first few weeks of pregnancy. The concentration of hCG rises rapidly, frequently exceeding 100 mIU/ml by the first missed menstrual period. Between 8 to 10 weeks of pregnancy, hCG rises to extremely high levels where approximately 30,000–200,000 mIU/ml (approximately 30 to200 nM) of hCG are released. The hCG levels chart during pregnancy is shown in table 1.

Table 1. The hCG levels in weeks from the last normal menstrual (LMP) period [69]

LMP period	**hCG levels**
3 weeks LMP	5 – 50 mIU/mL
4 weeks LMP	5 – 426 mIU/mL
5 weeks LMP	18 – 7,340 mIU/mL
6 weeks LMP	1,080 – 56,500 mIU/mL
7-8 weeks LMP	7, 650 – 229,000 mIU/mL
9-12 weeks LMP	25,700 – 288,000 mIU/mL

LMP period	hCG levels
13-16 weeks LMP	13,300 – 254,000 mIU/mL
17-24 weeks LMP	4,060 – 165,400 mIU/mL
25-40 weeks LMP	3,640 – 117,000 mIU/mL
Women who are not pregnant	<5.0 mIU/mL
Women after menopause	9.5 mIU/mL

For nonpregnant women and men, hCG and hCG-β in serum occur at low concentrations. In menstruating women, the upper reference limit is 3 mIU/mL, but it increases up to 6 mIU/mL during the menopause and increase up to 9.5 mIU/mL after menopause. In men, upper reference limit for men under 50 years of age is 1 mIU/mL while it is 2 mIU/mL in older men. However, chemotherapy can induce the gonadal dysfunction leading an increase of hCG concentration. This condition is not interpreted as a sign of tumor relapse. The condition can be identified on the basis of very high LH and FSH concentrations.

- Tumor markers [70-73]

In trophoblastic tumors, both hCG and hCG-β are produced, but the concentrations of hCG-β are typically lower than concentration of hCG. Aggressive tumor associated a high proportion of hCG β. A molar concentration of hCG-β exceeding 5% has been associated with malignant trophoblastic disease while the concentration is lower in benign molar disease and in pregnancy [16]. Normally, the separated screening of hCG and hCG-β is peformed for trophoblastic tumors determination. However, the assay of hCG-β is not widely utilized. Therefore, the assays for diagnosis of cancer recognize hCG and hCG-β together are generally recommended to be used.

For testicular germ cell tumors, Seminomas and non-seminomatous germ cell tumors of the testis (NSGCT) are the two main types of testicular germ cell tumors. About 50–70% of NSGTCs produce hCG, alpha fetoprotein (AFP) or both. In the other hand, 15–30% of seminomas produce only hCG. Therefore, hCG-β is a important marker for screening of testicular germ cell tumors especially for seminomas type.

In nontrophoblastic cancers, hCG-β is also important for screening because it is the only form that can be detected in serum of these patients. In patients with nontrophoblastic cancer, the concentrations of hCG-β are usually only moderately high. Therefore, it causes the

limited use of assays for measurement of hCG and hCG-β together. The specific assays for harmless hCG are not useful for determination of nontrophoblastic cancers.

1.7 Enzyme-linked Immunosorbent Assays (ELISAs) [74-76]

The immunoassays basically identify a label that is measured the amount of antigen or antibody which is present in a sample. The molecule that is used to label antigen or antibody, should retain a high signal efficiency while it incorporates into antigen or antibody. The most common labels are as followed:

- Radioisotopes
- Enzymes
- Chemiluminescence
- Fluorescence
- Bioluminescence
- Metal nanoparticles

In clinical application field, enzyme-linked immunosorbent assays (ELISAs) is biochemical test that mainly used in immunology to measure the presence of antigens or antibodies in sample. ELISA combines the specificity of antibodies with the sensitivity of simple enzyme assays, using an easily-assayed enzyme coupled with antibodies or antigens. There are two main variations on this method including (i) test of antigens by recognizing with antibody and (ii) test of antibody by recognizing with antigen. ELISA has been used as diagnostic tool for investigating the diseases. Generally, ELISA consists of 5 step following:

(1) Antigens (Ag) was coated or immoblized to a solid surface called ELISA plate such as 96-wells plastic plate.
(2) All of unbound sites were block to avoid false positive results.
(3) Primary antibodies (Ab) were added to the ELISA plate.
(4) Secondary antibodies, which conjugated with enzyme, were added.
(5) The product of reaction of a substrate with the enzyme was produced and then detected with suitable techniques.

ELISA can be classified based on the binding structure between the antibody and antigen into 4 types .

(i) Direct-ELISA

Direct ELISA is used only one set of antigens and one set of antibodies to react. The antigens are coated on the ELISA plate. Then, the antibodies, which labeld with enzyme, are react with antigens at ELISA plate. Finally, the substarts are added to test an enzyme linked antibody that attached with antigens. The disadvantages of direct ELISA are time-consuming and inflexible due to individual label of primary antibody, and lower sensitivity due to less amplified in direct ELISA.

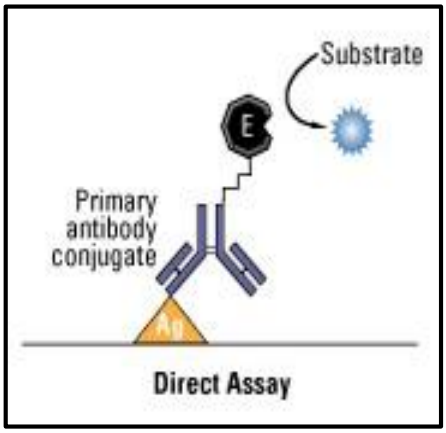

Figure 11. Schemetric of direct ELISA [77]

(ii) Indirect ELISA

For indirect ELISA, it has a difference to the direct ELISA in that one more additional antibody is added in the reaction. Almost of the procedure is the same as direct ELISA. But in this case, the primary antibody is not labeled. The secondary antibody with enzyme linked , directed at the first antibody, is added. This requirement is due to some patients antigen of disease-causing agent may not be present but a corresponding antibody is available in the patient sample. This corresponding antibody can be detected instead of patients antigen.

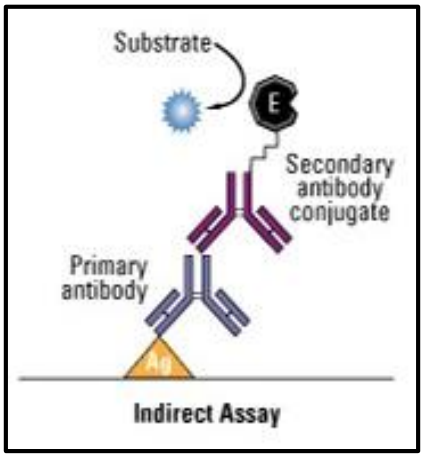

Figure 12. Schemetric of indirect ELISA [77]

(iii) Competitive ELISA

The third type of ELISA is the competition assay. The key of competitive ELISA is the process of competitive reaction between the sample antigen and antigen bound to the ELISA plate with the primary antibody. First, ELISA plate is coated with the sample antigen. Then, prepared antibody–antigen complexes by incubating the primary antibody with the sample antigen. The resulting antibody–antigen complexes are added to ELISA plate. After incubation period, any unbound antibody is washed off. In this step, the more antigen in the sample, the less antibody will be able to bind to the antigen in the ELISA plate, hence "competition." Then the secondary antibody that is specific to the primary antibody and conjugated with an enzyme is added followed by a substrate to produce a detection signal. The advntages of competitive ELISA are high specificity, since two antibodies are used the antigen/analyte is specifically captured and detectect.

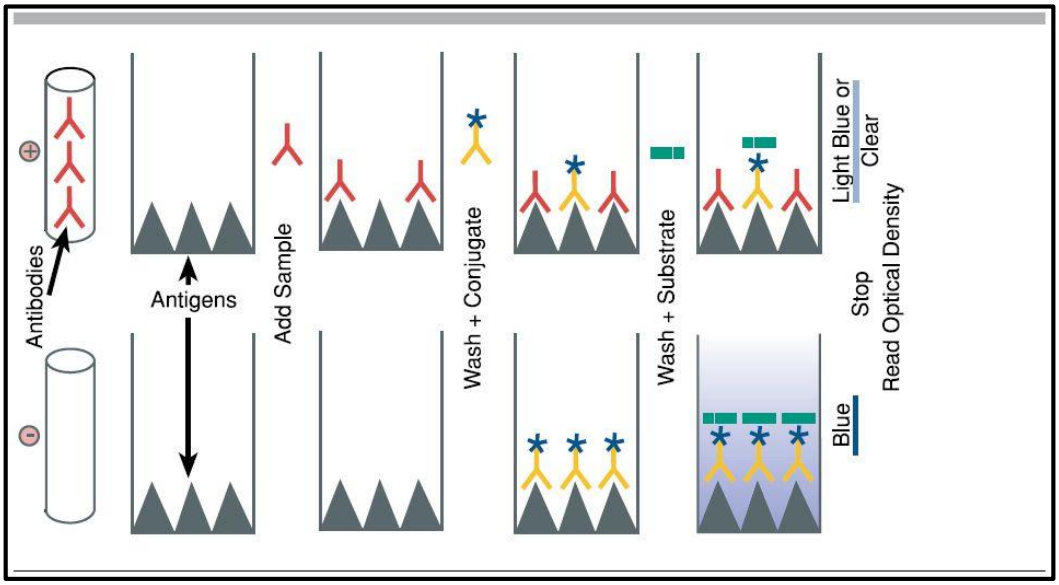

Figure 13. Schemetric of competitive ELISA [78]

(iv) Sandwich ELISA

Sandwich ELISA is also an indirect type of ELISA. Sandwich ELISA is highly efficient in sample antigen detection. Moreover, many commercial ELISA pair sets are built on this sanwich ELISA. The only difference in this ELISA principle is between two antibodies and antigen presenting like a sandwich. For sanwich ELISA procedure, that antibody is captured on a plate followed by adding a mixture of sample and any antigen present binds to capture antibody. Then detecting antibody is added, and binds to antigen. After that enzyme-linked secondary antibody is added, and binds to detecting antibody. Finally, substrate is added and is converted by enzyme to detectable form. The advantages of sanwich ELISA are high

specificity, suitable for complex samples, flexibility, and sensitivity. Recently, sandwich ELISA is commonly used in clinical diagnosis tool, especially home pregnancy test.

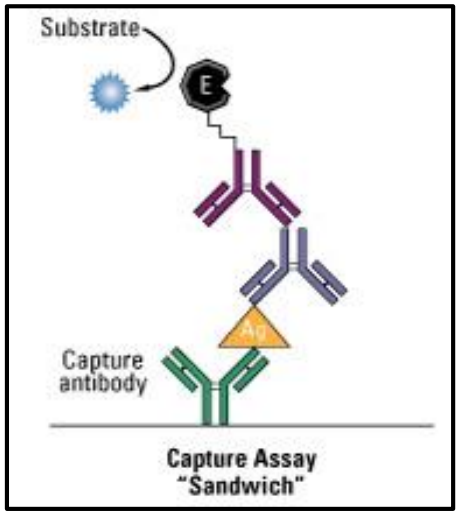

Figure 14. Schemetric of sandwich ELISA [77]

1.8 Objective of the thesis

The aims of this work are to develop a novel electrochemical method for simple and highly-sensitive detection of protein biomarkers for isolation and counting of single molecule. To achieve this aim, OCP method is chosen to simplify the detection procedure. Eventually, this system could be applied to a simplified and miniaturized diagnostic system for the development of single molecule detection. We expect this device to be an effective device for the clinical diagnostic.

1.9 Scope of the thesis

The development of ELISA for electrochemical detection of protein biomarker in this research consists of two parts. The first part is the development and simplification of OCP based electrochemical technique for protein biomarker detection. The second one is fabrication of micro-nano electrode and application to single molecule isolating and counting.

For the first part, we developed and simplified the detection procedure based on OCP technique. AuNPs and PtNPs were used as electrochemical label to test the ability and efficiency for protein biomarker detection. hCG was chosen as the model antigen of sandwich-type immunoassay because the information of its behavior and epitopes for the binding of two antibodies were well-documented.

In the second part, the key is to establish suitable materials and processes for fabricating nano-micro electrode array. We aim at fabricating an array of nano-sized working electrodes by electron beam lithography technique for single molecule analysis.

Chapter II

GOLD NANOPARTICLES LABELED ELECTROCHEMICAL IMMUNOASSAY USING OCP FOR PROTEIN BIOMARKER DETECTION

2.1 Introduction

In this chapter, we developed a new electrochemical detection method based on antigen-antibody reaction using OCP technique for highly sensitive detection of human chorionic gonadotropin hormone (hCG). AuNPs were selected to use as label for the electrochemical detection. The direct electrical signal of AuNPs resulted from electron transfer process between the AuNPs and the electrode was measured using OCP without application of neither potential nor current to the system. A series of sandwich-type immunoreactions, consisting of hCG antigen and AuNPs-labeled hCG antibody, were prepared on a screen-printed carbon electrode (SPCE) and pyrolysis photoresist carbon film elelctrode (PPCE). After preparation of sandwich-type immunosystem, a space between the AuNPs and electrode surface exists due to the formation of immunocomplexes that may hinder electron transfer process and cause unsuccessful detection of AuNPs at the secondary antibody. In order to overcome this issue, pre-oxidation and reduction processes were applied to the system to cancel/clear the gap. As a result, the detection of AuNPs at secondary antibody was significantly improved. The detection of hCG using SPCE and PPCE electrode was also demonstrated. For the optimization of preoxidation and reduction processes, the applied potential and time period were studied. Using SPCE, It was found that the preoxidation potential of 1.2 V for 60 s and reduction potential of -0.3 V for 30 s provided the highest potential change. Using PPCE, the optimal conditions were preoxidation potential of 1.2 V for 30 s and reduction potential of -0.4 V for 30 s. The OCP signals were proportional to the amount of AuNPs at electrode surface that related to hCG concentration. Using the optimal condition, detection limit was improved to be 0.016 and 0.011 ng/mL for SPCE and PPCE, respectively. The proposed system shows high electrochemical sensitivity for hCG detection using AuNPs-labeled immunocomplex. Moreover, this developed system could be applied to a simplified and miniaturized the detection system for using in clinical diagnosis.

2.2 Experimental

2.2.1 Chemicals and materials

All chemicals and materials used in these experiments are listed in Table 2.

Table 2. List of chemicals and materials including their suppliers

Chemicals/materials and reagents	Suppliers
Monoclonal anti-hCG α-subunit of follicle-stimulating hormone (Mab-FSH), 5.1 mg/mL	Medix Biochemica, Finland
Monoclonal anti-hCG (Mab-hCG), 5.4 mg/mL	Medix Biochemica, Finland
Human chorionic gonadotropin (hCG), 1 mg/mL	Sigma-Aldrich, Japan
Gold colloidal solution with 40 nm diameter	BBI solution, UK
Bovine serum albumin (BSA), 1% and 10% (v/v)	Sigma-Aldrich, Japan
Hydrochloric acid (HCl), 37% w/w	Wako Pure Chemical Industries, Japan
di-Sodium hydrogen phosphate (Na_2HPO_4), 99% w/w	Wako Pure Chemical Industries, Japan
Sodium dihydrogen phosphate (NaH_2PO_4), 99% w/w	Wako Pure Chemical Industries, Japan
Polyethylene glycol 20,000 (PEG)	Wako Pure Chemical Industries, Japan
Potassium dihydrogen phosphate (KH_2PO_4), 99% w/w	Wako Pure Chemical Industries, Japan
Sodium Hydroxide (NaOH), 99% w/w	Wako Pure Chemical Industries, Japan
Sodium azide (NaN_3)	Wako Pure Chemical Industries, Japan
Sodium chloride (NaCl), 99.5% w/w	Nacalai tesque, Japan
OAP	Tokyo Ohka Kogyo Co., Ltd., Japan
AZ5214E	AZ Electronic Materials, Japan
Ag/AgCl ink for reference electrode	ALS Co., Ltd, Japan

2.2.2 Instruments and equipment

All instruments and equipment are listed in Table 3.

Table 3. List of all instruments and equipment including their suppliers

Instruments and equipment	Suppliers
Potentiostat	Metrohm Autolab, Netherlands
Screen-printed carbon electrode (SPCE)	Bio Device Technology Ltd., Japan
SiO_2 100 nm/ p^+-Si	KST World Corp., Japan
pH meter	Horiba, Japan
Analytical balance	Mettler Toledo, Japan
Scanning electron microscope (SEM) model S-4500	Hitachi, Japan
Mili Q system	Barnstead Milli Q-purification system
Autopipette	Eppendrof, Germany
Vortex	IKA, Japan
Centrifuge	CS Bio Co., USA
Sonicator	AS ONE, Japan
Furnace	ASH, Japan
Plasma asher PDC210	Yamato scientific Co., Ltd., Japan
Spin coater	Mikasa, Japan

2.2.3 Preparation of chemical solution

2.2.3.1 Phosphate buffer solution pH 7.4

50 mM of phosphate buffer solution was prepared by dissolving 0.134 g of potassium dihydrogen phosphate (KH_2PO_4) and 0.570 g of di-sodium hydrogen phosphate (Na_2HPO_4) in Mili-Q water to final volume of 100 mL. The solution was then precisely adjusted to the desired pH (pH 7.4) with ortho-phosphoric acid and sodium hydroxide (NaOH).

2.2.4 Procedure

2.2.4.1 Fabrication of pyrolysis photoresist carbon electrode (PPCE)

In this study, the SiO_2 (100 nm)/p^+-Si was used as a substrate. Prior to use, the substrate was thoroughly rinsed by acetone and DI water, followed by a soft-bake at 150 ^oC. Remained organic substances were removed by using O_2 plasma ashing (O2 30 sccm, RF power 15 W for 3 min). To create carbon film, AZ5214E photoresist was used as a carbon source. First, OAP was spin-coated on the substrate at 3000 rpm for 30 s, and baked at 110 ^oC for 3 min as an adhesion-promoting agent between the substrate and the photoresist. After that, AZ5214E was spin coated at 6000 rpm for 60 s, and baked at 90 ^oC for 10 min. Two coatings were used to obtain the desired thickness of PPCE, which is around 600 nm. The pyrolysis was performed in a furnace with a quartz tube flushed by forming gas (95%N_2 + 5%H_2,) for 15 min at room temperature. Under continuous gas flow, the temperature was increased from room temperature to 700 °C with a heating rate of 10 ^oC/min, then held at 700 °C for 1 h, and finally cooled down to room temperature. The set-up of pyrolysis system was shown in Figure 15.

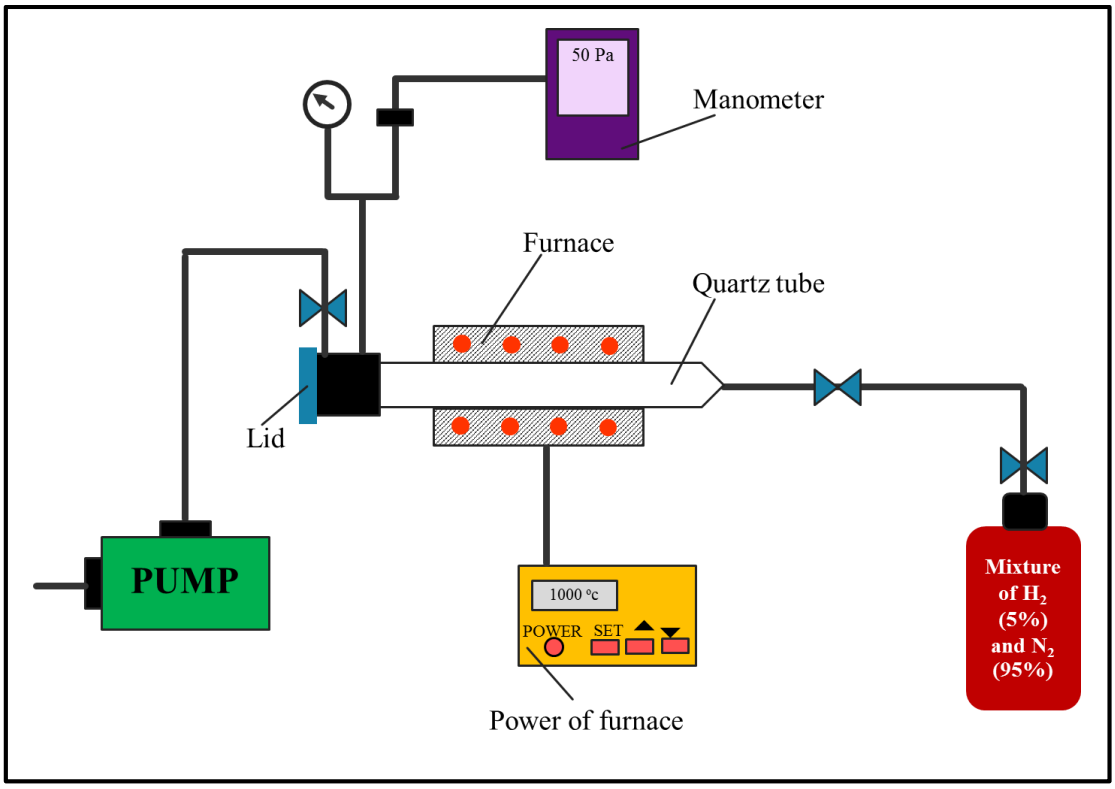

Figure 15. Scheme of pyrolysis system's set-up

2.2.4.2 Preparation of primary monoclonal antibody onto working electrode surface (Mab-FSH-immobilized immunosensor)

The immobilization of the primary monoclonal antibody onto the carbon electrode surface was shown in Figure 16. 2 µL of 100 µg/mL of Mab-FSH solution in 50 mM phosphate buffer (pH 7.4) was dropped onto working electrode surface and incubated at 4^{o}C for 12 hr. Then the electrode was rinsed with PBS to remove excess antibodies. For the elimination of non-specific adsorption, 2µL of the 1% BSA blocking solution was incubated on the working electrode surface at 4^{o}C for 12 hr. A sufficiently strong adsorption of BSA was obtained when incubated overnight. The incubation of BSA was performed in controlled temperature to prevent the denaturation of BSA during the process. As a result, the uncoated part of electrode surface was adsorbed by BSA that helped to prevent the further adsorption of biological interferences. Finally, the electrode was rinsed with PBS and kept at 4 ^{o}C until use.

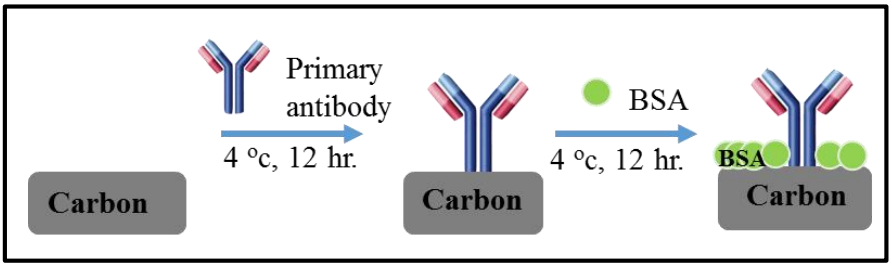

Figure 16. Schematic illustration of the preparation of primary monoclonal antibody onto working electrode surface

2.2.4.3 Preparation of AuNPs-labeled hCG antibody (Au-Mab-hCG)

200 µL of 50µg/mL of Mab-hCG solution in 5 mM KH_2PO_4, pH 7.5 was mixed with 1.8 mL of 1% AuNPs solution, and kept at room temperature for 10 min. Then, 100 µL of 1% PEG in 50 mM KH_2PO_4 (pH 7.5) was added, followed by 10% BSA in 50 mM KH_2PO_4 (pH 7.5) and incubated for 5 min to block the uncoated surface of AuNPs. After immobilization and blocking processes, AuNPs-conjugated Mab-hCG (Au-Mab-hCG) was collected by centrifugation at 8000 g, 4^{o}C for 15 min. Au-Mab-hCGs were suspended in 2 mL of the preservation solution (1% BSA, 0.05% PEG 2000, 0.1% NaN_3 and 150 mM NaCl in 20 mM Tris-HCl buffer, pH 8.2), and collected again using centrifuge at the same condition. For the stock solution, Au-Mab-hCGs were suspended in 200 µL of preservation solution.

2.2.4.4 Immobilization of hCG antigens and Au-Mab-hCG onto Mab-FSH-immobilized immunosensor

Different concentrations of hCG sample solutions in the range of 0 to 10 ng/mL were prepared by diluting the stock of 1 mg/mL of hCG in 1% BSA in 50 mM PBS pH 7.4. These sample solutions were dropped onto the Mab-FSH-immobilized immunosensors and incubated for 30 min at room temperature, followed by thoroughly rinsing with the PBS buffer. After that, 2 µL of Au-Mab-hCG solution was applied to the immunosensor surface and incubated at the same condition as described above, and washed out by the PBS buffer to remove unbound Au-Mab-hCG. Finally, a direct redox-reaction was performed and generated charges were detected using OCP measurement. The procedure was shown in Figure 17.

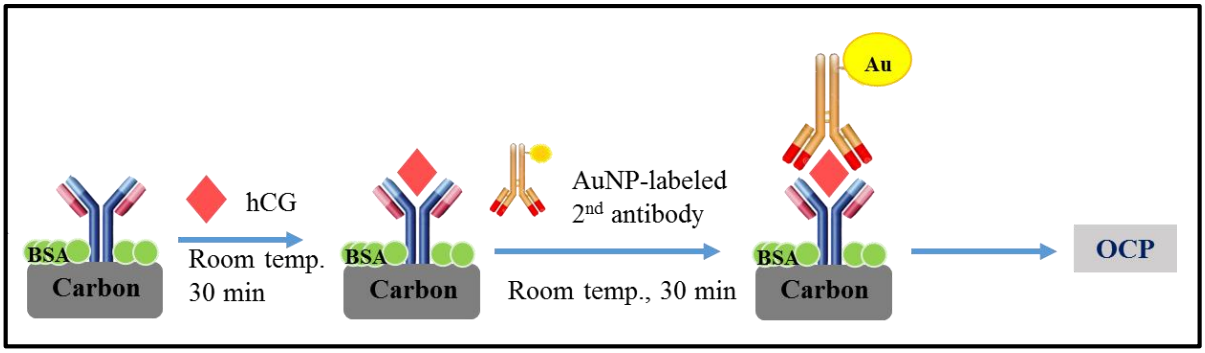

Figure 17. Schematic illustration of the immobilization of hCG antigens and Au-Mab-hCG onto Mab-FSH-immobilized immunosensor (enlarge character size in figure)

2.2.4.5 Electrochemical system

For the electrochemical detection, OCP method was used as detection technique because of its simplicity and miniaturized ability. The detection procedure was performed using a potentionstat system. First, the direct redox reaction was performed using 0.1 M HCl solution which covered the three-electrode zone of the SPCE at room temperature. (Figure 18a). For PPCE, the set up for OCP detection was shown in Figure 18b using Ag/AgCl as reference electrode. A preoxidation process was applied at a constant potential of 1.2 V for 60 s, then waited for 4 min. After that a reduction process was applied at a constant potential of -0.3 V for 30 s, immediately followed by OCP measurement for 5 min.

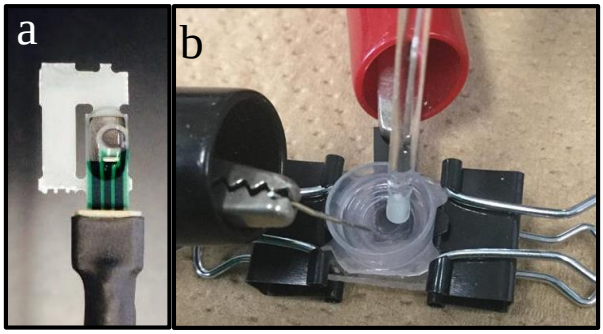

Figure 18. A photograph of the sandwich-type immunosensor covering with 0.1 M HCl solution on SPCE (a), and PPCE (b).

2.3 Results and discussion

2.3.1 SPCE based working electrode for AuNPs labeled electrochemical immunoassay using OCP

2.3.1.1 Surface morphology of sandwich-type immunosensor labeled with AuNPs

Surface morphologies of the AuNPs-labeled immunocomplexes, consisting of primary Mab, hCG, and AuNPs-labeled secondary Mab, were evaluated by the scanning electron microscopy (SEM) as shown in Figure 19. Different hCG concentrations ranged between 0 and 10 ng/mL were investigated. The AuNPs were clearly observed at the electrode surface at the hCG concentration of 10 ng/mL which confirmed that AuNPs-labeled secondary Mab was successfully immobilized on the immnosensor. The size of AuNPs was approximately 40 nm in diameter, which is consistent to the originally gold colloidal solution.

a

b

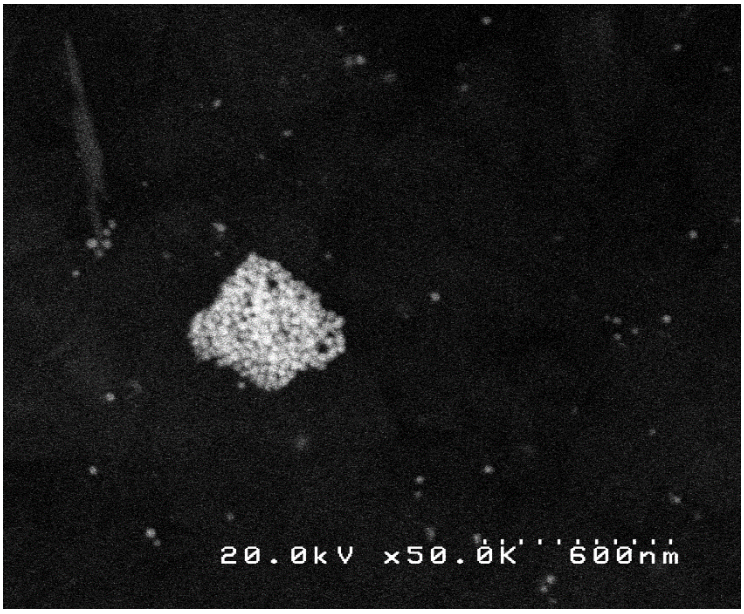

Figure 19. SEM image of AuNPs-labeled immunocomplexes immobilized on SPCE surface at the concentration of hCG of 0 ng/mL (a), and 10 ng/mL (b).

2.3.1.2 The detection of hCG using OCP measurement of antigen-antibody complex label by AuNPs without preoxidation and reduction processes

The OCP method was used to measure the hCG concentration after preparing the sandwich-type immunosensor. The number of AuNPs at the secondary Mab was dependent on the hCG concentration and directly detected in 0.1 M HCl solution. The different amounts of AuNPs on electrode surface affected to the catalytic activities towards proton in the solution that result in the change of OCP signal. Figure 20 shows the OCP signal of AuNPs-labeled immunocomplexes immobilized on SPCE at different concentrations of hCG. As a result, the OCP signal was slightly changed upon the concentrations of hCG. A possible reason would be the poor electrocatalysis of proton in the acid solution by AuNPs. The immunocomplexes, consisting of primary Mab, hCG, and AuNPs-labeled secondary Mab, made a space between AuNPs and electrode surface that did not facilitate electron transfer of poor electrocatalytic process. Another reason could be due to the detection process. The AuNPs-labeled secondary Mab was released from immunocomplex to the 0.1 M HCl test solution. AuNPs in the solution could not induce the change of OCP signal as shown in Figure 21. Therefore, the catalytic activity of AuNPs was lost. The use OCP measurement was not successful for the detection of different amounts of AuNPs at the secondary antibody.

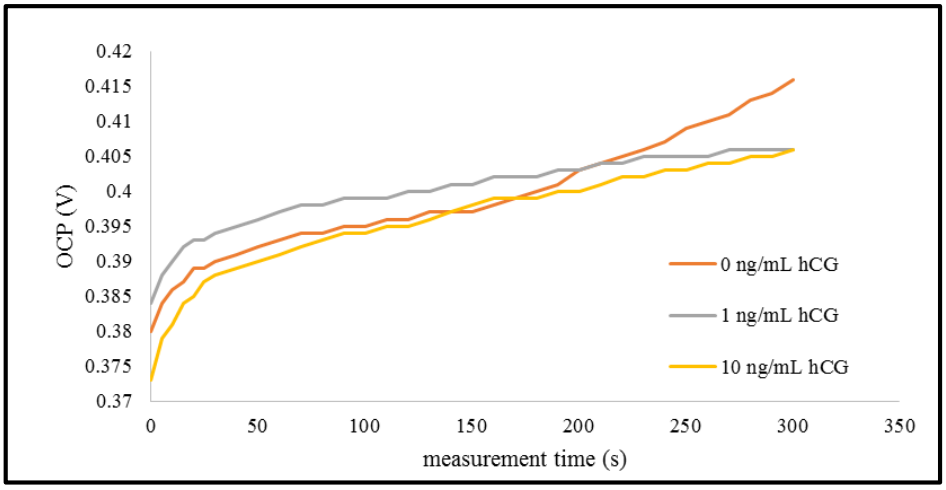

Figure 20. The OCP signal of AuNPs-labeled immunocomplexes immobilized on SPCE

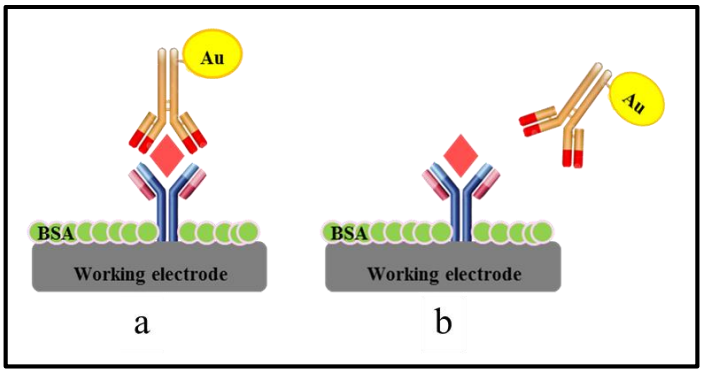

Figure 21. The schematic AuNPs-labeled immunocomplexes immobilized on SPCE (a) and the releasing of AuNPs-labeled secondary Mab in 0.1 M HCl (b).

2.3.1.3 The detection of hCG using OCP measurement of antigen-antibody complex label by AuNPs with preoxidation and reduction processes on SPCE

From previous result, OCP signal was hardly changed due to the poor electrocatalytic of proton on AuNPs at electrode surface. To solve this problem, the preoxidation and reduction processes were applied in the detection procedure to obtain the direct attachment of AuNPs at electrode surface, followed by electrical detection using OCP as shown in Figure 22. The direct attachment of AuNPs on electrode surface facilitated the electron transfer and affected to the OCP signal. For the preoxidation step, AuNPs at secondary electrode was oxidized to Au (III) ion in the 0.1 M HCl solution by applying a constant positive potential. After waiting for diffusion for few minutes, the reduction process was applied to reduce Au (III) ion to AuNPs at electrode surface. The reactions were shown below:

Preoxidation process: $Au^0 + 4Cl^- \rightarrow AuCl_4^- + 3e^-$

Reduction process: $AuCl_4^- + 3e^- \rightarrow Au^0 + 4Cl^-$

The OCP measurement was immediately performed after the reduction process. The OCP measurements of different concentrations of hCG were shown in Figure 23. The concentration of hCG detected was related to the amount of AuNPs at the electrode surface after the reduction. As a result, it was found that OCP signal increased when the concentration of hCG was increased. When the electrocatalysis reduction of proton occurred at the surface of AuNPs, the overall reduction current on the AuNPs together with that on the working electrode becomes larger than the overall oxidation current. To maintain the OCP condition, the OCP shifts positively to produce a zero net current. Therefore, this procedure was successful for differentiating different hCG concentrations. Figure 24 shows OCP signals at different concentrations of hCG with and without the preoxidation and reduction processes. Obvious signal changes suggested that our proposed procedure is essentially effective.

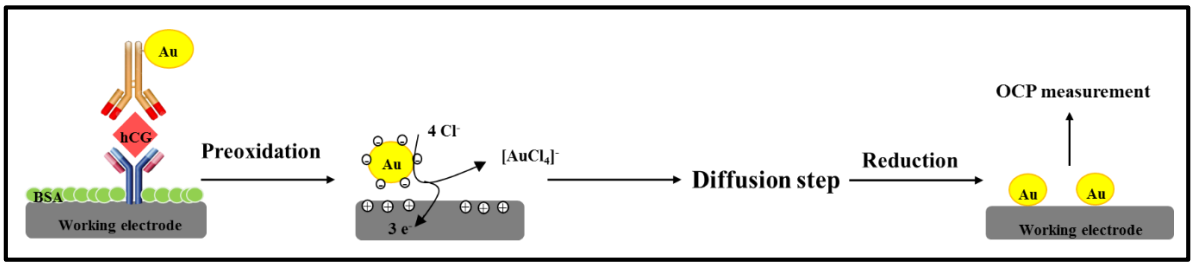

Figure 22. The detection procedure with preoxidation and reduction processes

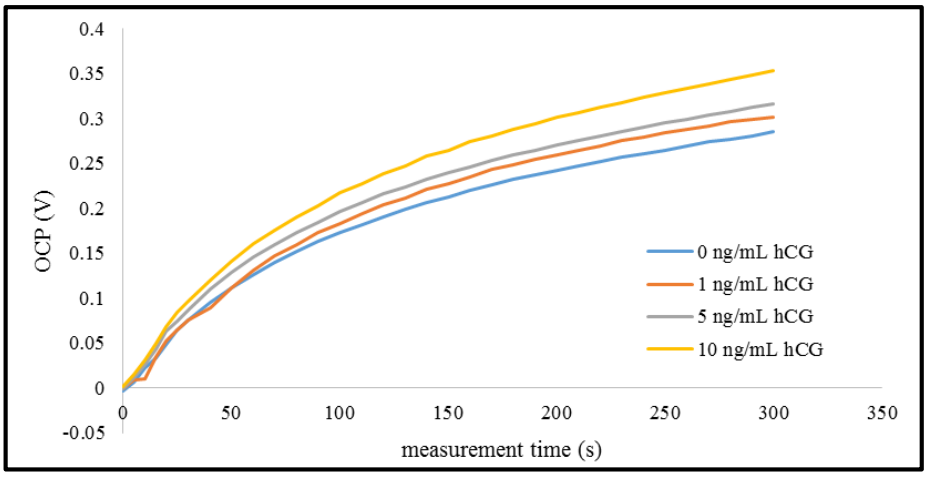

Figure 23. The OCP signal of AuNPs-labeled immunocomplexes immobilized on SPCE after applied preoxidation and reduction processes.

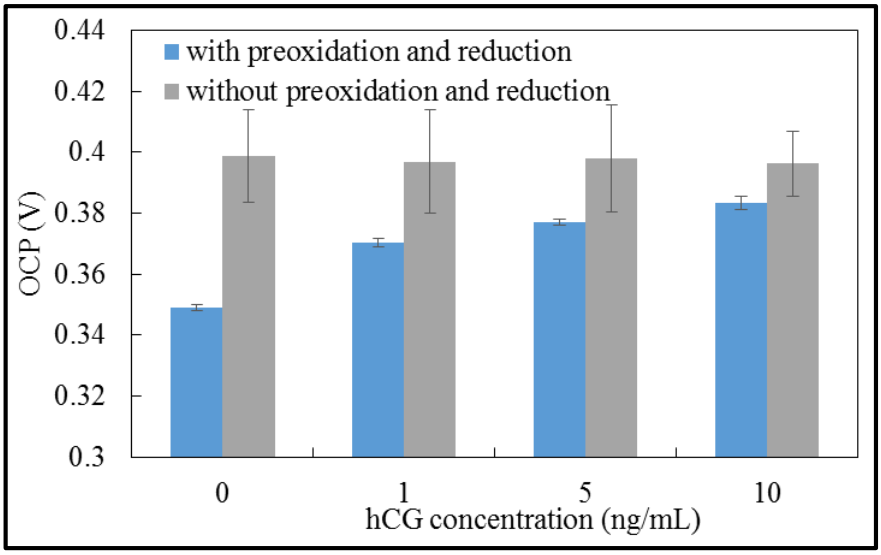

Figure 24. The comparison of OCP signal between with (blue) and without (gray) preoxidation and reduction processes.

(1) Surface morphology of immunocomplex on SPCE surface

The AuNPs-labeled immunocomplexs immobilized on the surface of immunosensor after the detection procedure were confirmed step by step using SEM images as shown in Fig. 25. AuNPs- labeled secondary Mab were observed at the electrode surface with particle size of 40 nm which corresponds to that of the original gold particle in colloid solution (Fig. 20a). After applying preoxidation process, the AuNPs at electrode disappeared as seen from SEM image (Fig. 25b). This is because during the preoxidation process, AuNPs at the secondary Mab were oxidized to Au (III) ions. Figure 20c showed electrode surface after applied reduction process at -0.2 V for 30s. The reduction of Au (III) ions in the solution was occurred that generated AuNPs on electrode surface. The size and number of AuNPs were dependent on the reduction potential and time. Under the reduction potential of -0.2 V for 30 s, the smaller particle size around 30-40 nm in diameter was observed. From Fig. 25c, it was confirmed that Au (III) ions in the solution were reduced to AuNPs which remained on the electrode surface. Therefore, the applied preoxidation and reduction processes successfully produced the AuNPs attached on electrode surface, which is essentially needed for OCP measurement.

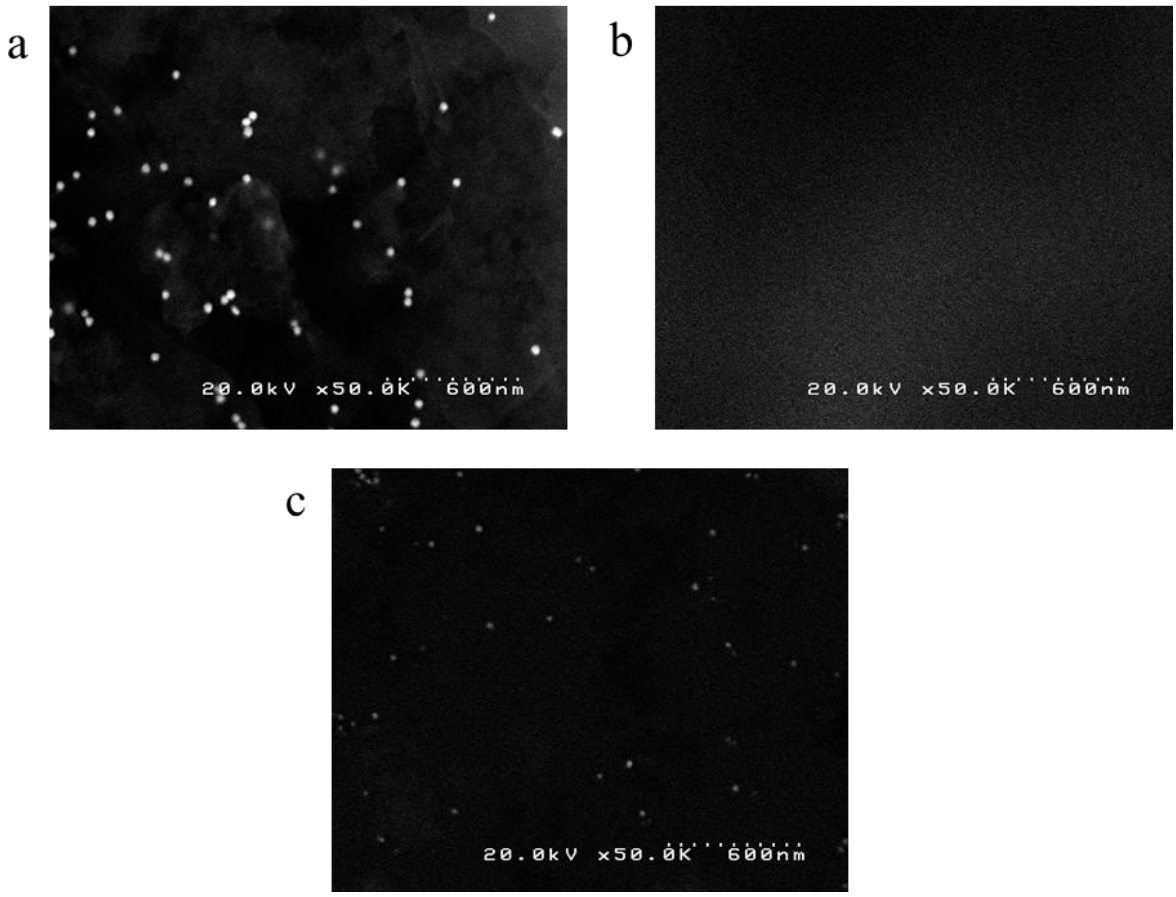

Figure 25. The SEM images of electrode surface of AuNPs-labeled immunocomplexes immobilized on SPCE surface (a), after preoxidation (b), and after reduction (c) at the concentration of hCG of 10 ng/mL.

(2) The optimization of detection procedure

The detection procedure consists of three processes including preoxidation process, diffusion step, and reduction process. The parameters of these processes were studied because these factors can effect to the analytical results. These data was plotted as a function of studied parameters. After that, the net OCP signal after background subtraction was studied, and difference of signal-to-blank (S-B) was plotted corresponding to the studied parametes.

(i) Preoxidation process

The preoxidation process was conducted for the oxidation of AuNPs at secondary antibody to Au (III) ion form in the solution by applying constant potential. Preoxidation condition was studied while fixed the time of diffusion step at 4 min and reduction potential at -0.4 V for 30 s. The preoxidation potential of 1.1 V was the minimum potential that facilitate the oxidation reaction of AuNPs. At the preoxidation higher than 1.2 V, the background signal

was high that can prevent the signal of AuNPs. Therefore, the preoxidation potential and preoxidation time were optimized in the range of 1.1 to 1.2 V, and 0 to 90 s, respectively. The preoxidation potentials significantly affected oxidation of AuNPs and the OCP signal as well as the background signal. After background subtraction, it was found that the OCP increased when the preoxidation potential increased up to 1.2 V for 60 s. (Figure 26). Therefore, the preoxidation potential of 1.2 V, and preoxidation time of 60 s were used as the optimal preoxidation condition.

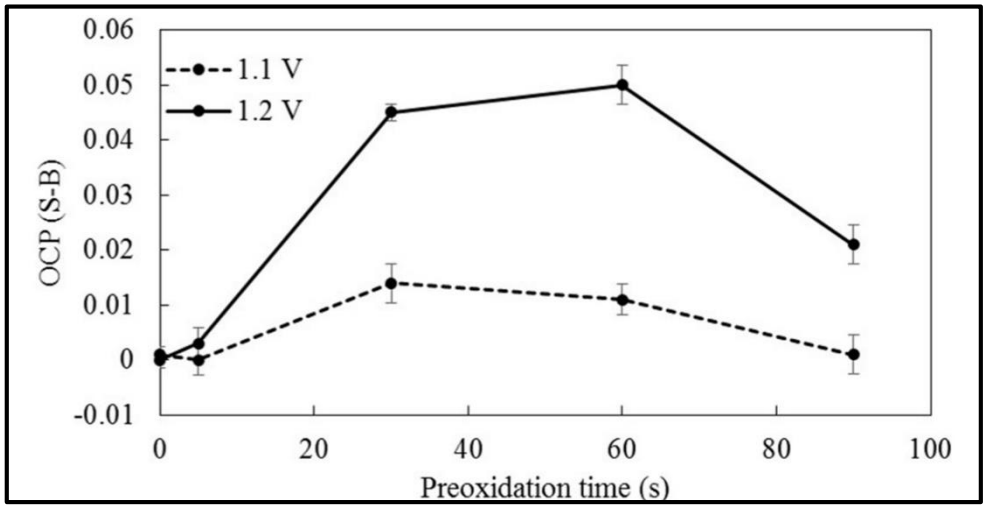

Fig. 26 Effect of preoxidation process with waiting time of 4 min and reduction potential of -0.4 V for 30 s after background subtraction (S-B) at hCG concentration of 10 ng/mL. Data are shown as the mean ± SD derived from three replicates

(ii) Diffusion process

In the preoxidation process, not only Au (III) ion was oxidized but oxygen from water in the solution was also oxidized and then reduced along with Au (III) ion in the reduction process that caused the high background signal. Diffusion process was the waiting process without applying any potential or current to the system after preoxidation process to allow the ions diffused out of electrode surface for decreasing the background signal. The diffusion time was studied in the range of 0 to 300 s at preoxidation potential of 1.2 V for 60 s, and reduction potential of -0.2 V for 30 s. The OCP signal decreased when diffusion time was increased. The decrease of OCP signal by diffusion time was attributed to the diffusion of Au (III) from electrode surface to the solution, which affected to the amount of AuNPs after the reduction process. The less diffusion time, the amount of Au (III) ion at electrode surface was raised resulting in the reduction of Au (III) ion. On the other hand, at long diffusion time, Au (III) ion was significantly diffused out of electrode surface, therefore the reduction of Au (III) ion was

less occurred. However, at short diffusion time of 0 to 60 s, not only the concentration of Au (III) ion but that of oxygen in the solution at electrode surface is also high. Oxygen can be reduced in the reduction process and provided a high background signal that hid the OCP signal from AuNPs. The reactions were shown below:

Preoxidation process: $Au^0 + 4Cl^- \rightarrow AuCl_4^- + 3e^-$

$H_2O \rightarrow O_2 + 4H^+ + 4e^-$

Reduction process: $AuCl_4^- + 3e^- \rightarrow Au^0 + 4Cl^-$

$O_2 + 4H^+ + 4e^- \rightarrow H_2O$

After background subtraction, the highest OCP signal was obtained at the diffusion time of 240 s as shown in Fig. 27. Therefore, the diffusion time of 240 s was used as the optimal diffusion condition.

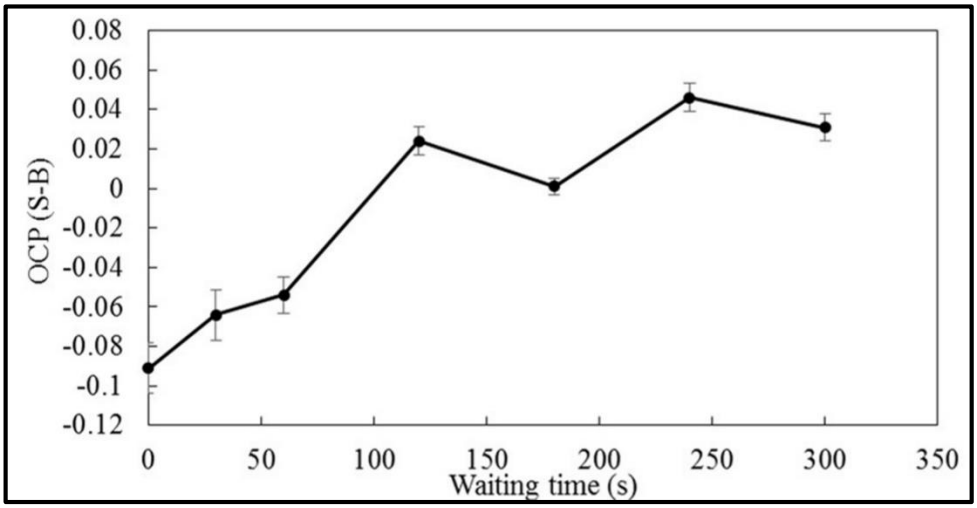

Fig. 27 Effect of diffusion process with preoxidation potential of 1.2 V for 60 s and reduction potential of -0.2 V for 30 safter background subtraction (S-B) at hCG concentration of 10 ng/mL. Data are shown as the mean ± SD derived from three replicates

(iii) Reduction process

For the reduction process, it was applied after the preoxidation and diffusion processes to reduce the Au (III) ions to AuNPs that directly attached on electrode surface. The reduction potential and time were studied in the range between -0.2 and -0.6 V, and 0 and 90 s, respectively. The OCP signal decreased when the reduction potential and reduction time were increased. After background subtraction, it was found that the maximum OCP signal was obtained at the reduction potential of -0.2 V and reduction time of 30 s (Figure 28).

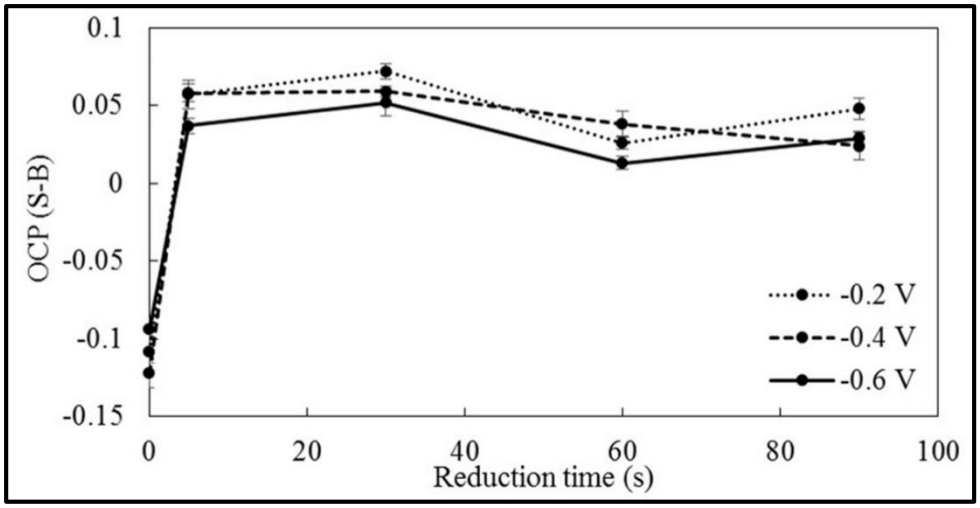

Fig. 28 Effect of reduction process with preoxidation potential of 1.2 V for 60 s and waiting time of 4 min after background subtraction (S-B) at hCG concentration of 10 ng/mL. Data are shown as the mean ± SD derived from three replicates

From the optimization of detection procedure, a summary of optimal condition is shown in Table 4. These conditions were used for the detection of hCG using AuNPs-labeled immunocomplexes immobilized on SPCE by OCP measurement.

Table 4. The optimal detection procedure

Parameters	Potential (V)	Time (s)
Preoxidation	1.2	60
Diffusion time	-	240
Reduction	-0.2	30

(3) Analytical performance

The analytical performance of this proposed system was studied. The calibration curve between the concentration of hCG and OCP signal was plotted. We found that the linearity range was expanded to be logarithm as shown in Fig. 29a. Therefore, the logarithm of hCG concentrations were plotted against the OCP signal as shown in Fig. 29b. Under the optimal condition, a wide linearity was observed in the range between 0.05 and 10 ng/mL. The limit of detection (LOD) and limit of quantification (LOQ) were calculated from 3 SD/S, where SD is the standard deviation of ten measurements (n=6) of blank solution, and S is the sensitivity of the method (slope of linearity at low concentration). Good linearity value with correlation coefficient (r^2) > 0.97 was obtained. LOD was 79 pg/mL. This LOD is sufficient to screen the

hCG concentration in pregnancy, marijuana use, hypogonadism (testicular failure), cirrhosis, inflammatory bowel disease, and duodenal ulcers [65]. In addition, when the performance of proposed electrochemical immunoassay was compared to the previous electrochemical immunoassay using differential pulse voltammetry (DPV) for the detection of hCG [8]. It was found that wider measurable range were obtained using the proposed electrode. Therefore, the proposed system offers high sensitivity, simplicity, and low cost.

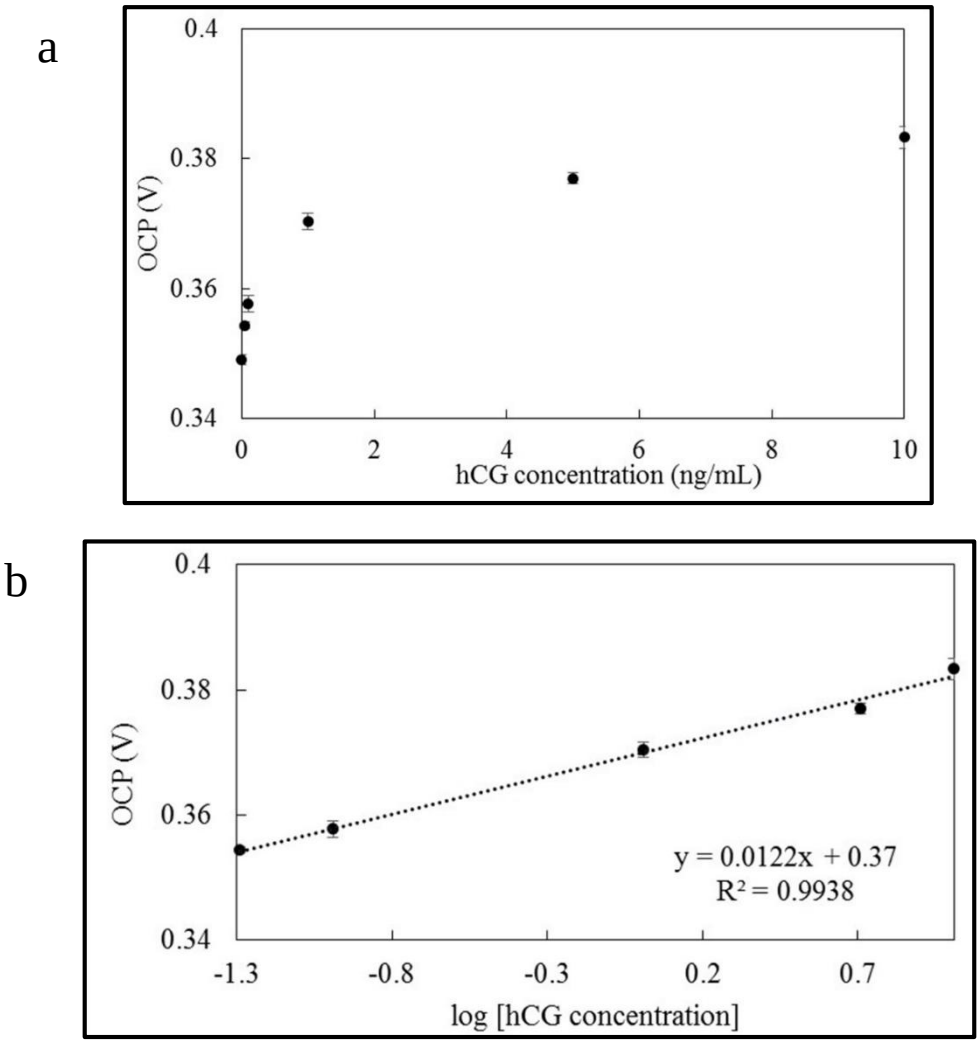

Figure 29. The calibration curve between the concentration of hCG and OCP signal (a), and between the logarithm concentration of hCG and OCP signal (b). Measurements were performed under the optimal conditions.

To verify the applicability of the proposed sensor, hCG in 5% human serum sample was analyzed. The standard addition method was used to investigate the practical applicability of the sensor. The concentrations of hCG were determined from the calibration curve. In the

standard addition, the estimated values were in good agreement with the added a concentration of hCG, and a recovery experiment was used to evaluate the accuracy of the sensor (Table 5). The RSDs and recoveries were found in the ranges of 10.5–11.2% and 94.2–100.9%, respectively. The LoD of hCG detection in 5% human serum was 0.26 ng/mL. Thus, the results clearly indicates the ability to measure hCG in real biological samples.

Table 5. Determination of hCG in 5% human serum in 50 mM PBS (n = 3).

Added (ng mL^{-1})	**Detected (ng mL^{-1})**	**RSD (%)**	**Recovery (%)**
1	0.94±0.10	10.5	94.2
3	2.92±0.31	10.5	97.5
5	4.84±0.54	11.2	96.8
7	7.06±0.79	11.2	100.8
9	9.08±0.96	10.5	100.9

2.3.2 PPCE based working electrode for AuNPs labeled electrochemical immunoassay using OCP

2.3.2.1 Surface morphology of PPCE

As mentioned above, the detection of hCG using AuNPs based OCP method with preoxidation and reduction processes was successful on SPCE. Therefore, we are interested to find other carbon materials that can be detected hCG concentration and have the possibility to pattern and fabricate in micro-nano scale. Pyrolysis photoresist carbon film electrode (PPCE) is an attractive alternative to other carbon electrodes because of its advantages such as simple and inexpensive fabrication process. The most attractive of PPCE is the ability to create sensitive carbon electrodes through lithographically patterning photoresist that opens up many useful possibilities for electrode design in various application. The fabrication of PPCE was simple prepared by pyrolysis of photoresists on silicon wafers at temperatures of 700°C. The thickness of fabricated PPCE was observed round 600 nm. The smoothness of fabricated PPCE was compared to SPCE as shown in AFM (Figure 30). We observed that the smoother surface of PPCE was observed compared to SPCE, and RMSs of both surface were found to be 0.70 nm for PPCE and 25.14 nm of SPCE.

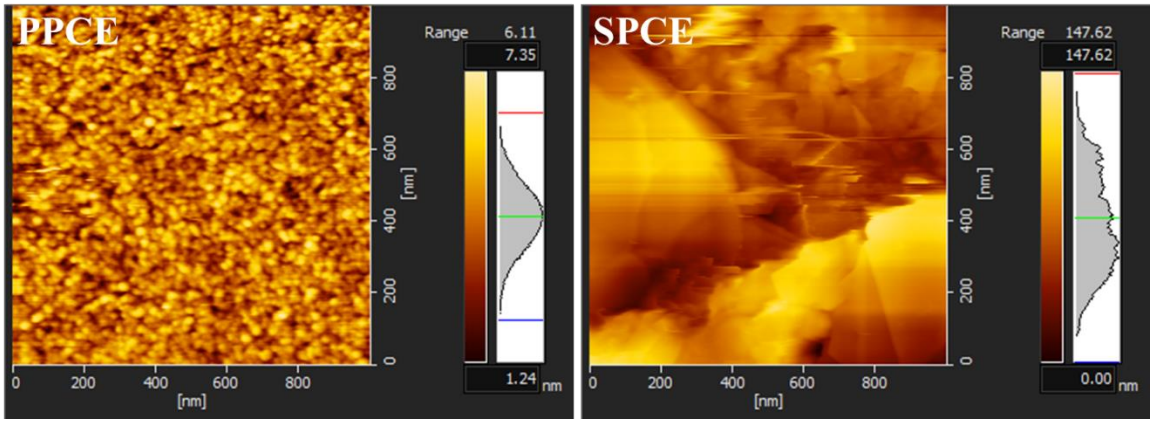

Figure 30. AFM images of PPCE and SPCE surface

2.3.2.2 The detection of hCG using OCP measurement of antigen-antibody complex label by AuNPs with preoxidation and reduction processes on PPCE

(1) Surface morphology of immunocomplex on PPCE surface

After fabricated of PPCE, the immobilization of immunocomplex was prepared using the same procedure as SPCE. The AuNPs-labeled immunocomplexs immobilized on the PPCE surface of immunosensor after the detection procedure were confirmed step by step using SEM images as shown in Fig. 31. AuNPs- labeled secondary Mab were observed at the electrode surface with particle size of 40 nm which corresponds to that of the original gold particle in colloid solution (Fig. 31a). After applying preoxidation process, the AuNPs at electrode disappeared as seen from SEM image (Fig. 31b). This is because during the preoxidation process, AuNPs at the secondary Mab were oxidized to Au (III) ions. Figure 31c showed electrode surface after applied reduction process at -0.2 V for 30s. The reduction of Au (III) ions in the solution was occurred that generated AuNPs on electrode surface. The size and number of AuNPs were dependent on the reduction potential and time. The particle size was found around 30-40 nm in diameter. From Fig. 31c, it was confirmed that Au (III) ions in the solution were reduced to AuNPs which remained on the electrode surface. Therefore, the applied preoxidation and reduction processes successfully produced the AuNPs attached on electrode surface, which is essentially needed for OCP measurement.

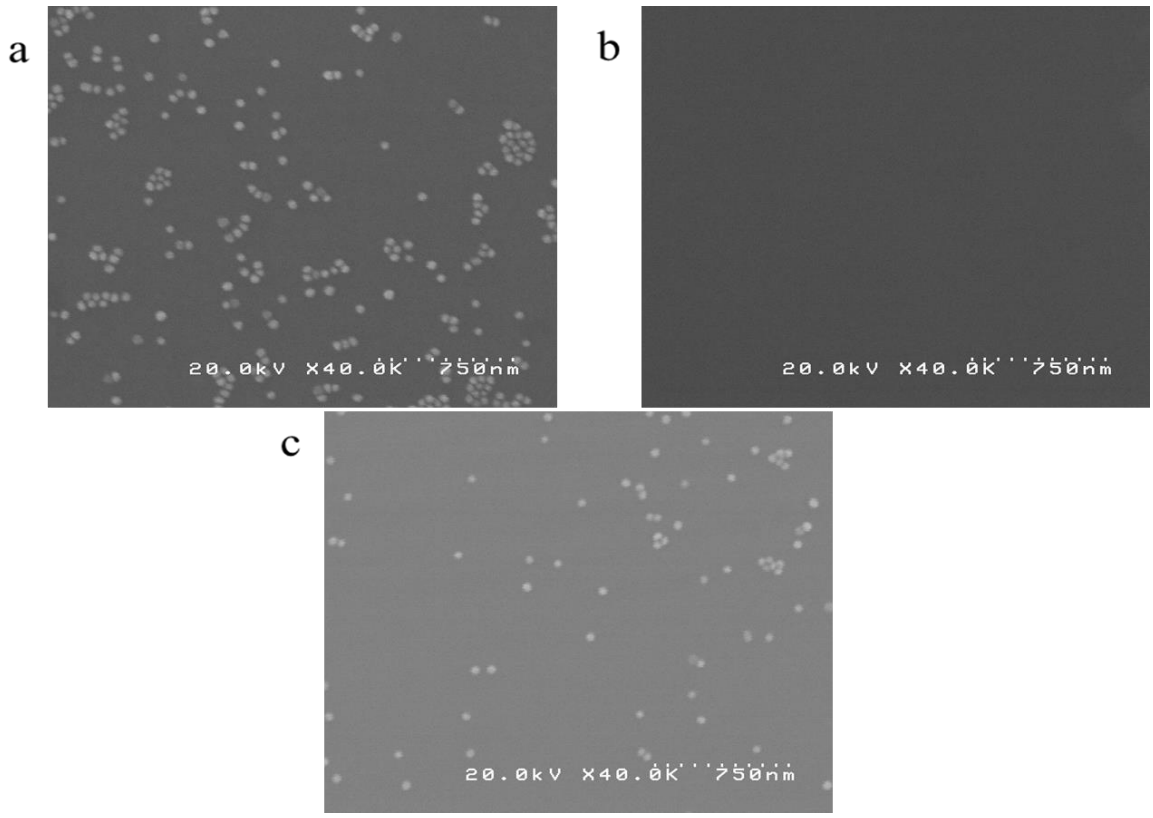

Figure 31. The SEM images of electrode surface of AuNPs-labeled immunocomplexes immobilized on PPCE surface (a), after preoxidation (b), and after reduction (c) at the concentration of hCG of 10 ng/mL.

(2) The optimization of detection procedure

Same as SPCE based detection, the detection procedure consists of three processes including preoxidation process, diffusion step, and reduction process. The parameters of these processes were studied. After that, the net OCP signal after background subtraction was studied, and difference of signal-to-blank (S-B) was plotted corresponding to the studied parametes.

(i) Preoxidation process

The preoxidation process was conducted for the oxidation of AuNPs at secondary antibody to Au (III) ion form in the solution by applying constant potential. Preoxidation potential was studied in the range of 1.1 and 1.2 V because 1.1 V was the minimum potential for oxidation reaction of AuNPs. At potential higher than 1.2 V, the background signal was high that prevent the signal of AuNPs. After background subtraction, it was found that the OCP increased when the preoxidation potential increased up to 1.2 V for 30

s. (Figure 32). Therefore, the preoxidation potential of 1.2 V, and preoxidation time of 30 s were used as the optimal preoxidation condition.

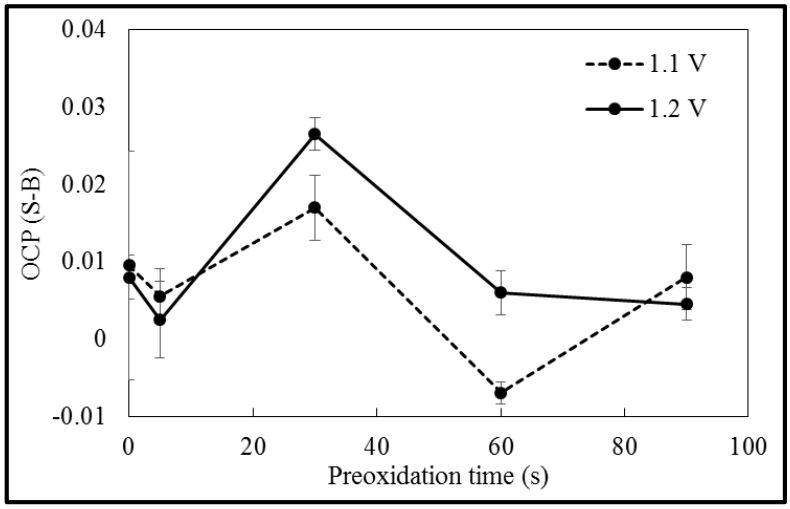

Fig. 32 Effect of preoxidation process with waiting time of 4 min and reduction potential of -0.2 V for 30 s after background subtraction (S-B) at hCG concentration of 10 ng/mL. Data are shown as the mean ± SD derived from three replicates

(ii) Diffusion process

Diffusion process was the waiting process without applying any potential or current to the system after preoxidation process to allow the ions diffused out of electrode surface for decreasing the background signal. In preoxidation process, not only Au (III) ion was oxidized but oxygen from water in the solution also was oxidized and it was reduced along with Au (III) ion in the reduction process that cause the high background signal. Thus, the diffusion step is necessary. The diffusion time was studied in the range of 0 to 300 s at preoxidation potential of 1.2 V for 30 s, and reduction potential of -0.2 V for 30 s. After background subtraction, the highest OCP signal was obtained at the diffusion time of 180 s as shown in Fig. 33. Therefore, the diffusion time of 180 s was used as the optimal diffusion condition.

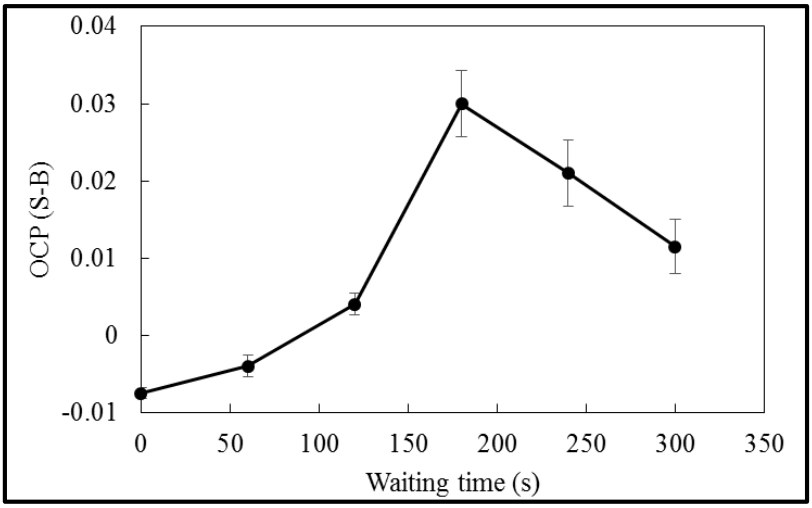

Fig. 33 Effect of diffusion process with preoxidation potential of 1.2 V for 30 s and reduction potential of -0.2 V for 30 s after background subtraction (S-B) at hCG concentration of 10 ng/mL. Data are shown as the mean ± SD derived from three replicates

(iii) Reduction process

The reduction process was applied after preoxidation and diffusion time to reduce the Au (III) ion to AuNPs, which directly attached on PPCE surface. The reduction potential and reduction time were studied in the range of -0.2 to -0.6 V, and 0 to 90 s, respectively. After background subtraction, it was found that the maximum OCP signal was obtained at reduction potential of -0.4 V and reduction time of 30 s (Figure 34).

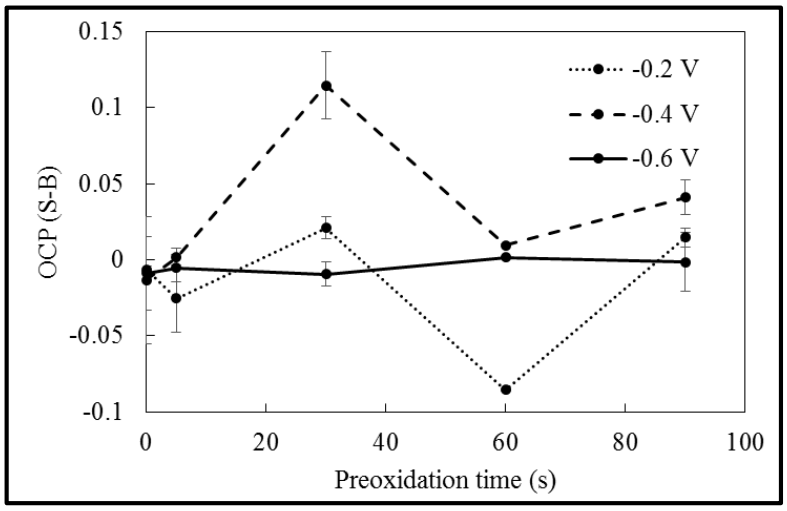

Fig. 34 Effect of reduction process with preoxidation potential of 1.2 V for 30 s and waiting time of 3 min after background subtraction (S-B) at hCG concentration of 10 ng/mL. Data are shown as the mean ± SD derived from three replicates

A summary of optimal condition is shown in Table 6. These conditions were used for the detection of hCG using AuNPs-labeled immunocomplexes immobilized on PPCE by OCP measurement.

Table 6. The optimal detection procedure

Parameters	Potential (V)	Time (s)
Preoxidation	1.2	30
Diffusion time	-	180
Reduction	-0.4	30

(3) Analytical performance

The analytical performance of proposed method on PPCE was studied under the optimal condition. The calibration curve between the concentration of hCG and OCP signal was plotted. We found that the linearity range was expanded to be logarithm as shown in Fig. 35. Therefore, the logarithm of hCG concentrations were plotted against the OCP signal. Under the optimal condition, the linearity was found in the range of 0.7 to 5 ng/mL. Good linearity value with correlation coefficient (r^2) > 0.99 was obtained. LOD was 0.1 ng/mL. Compared to SPCE based detection, the LOD was comparable. This LOD is sufficient to screen the hCG concentration in pregnancy, marijuana use, hypogonadism (testicular failure), cirrhosis, inflammatory bowel disease, and duodenal ulcers [65]. In addition, when the performance of proposed electrochemical immunoassay was compared to the previous electrochemical immunoassay using differential pulse voltammetry (DPV) for the detection of hCG [8]. It was found that lower LOD and wider measurable range were obtained using the proposed electrode. Therefore, the proposed system offers high sensitivity, simplicity, and low cost.

a

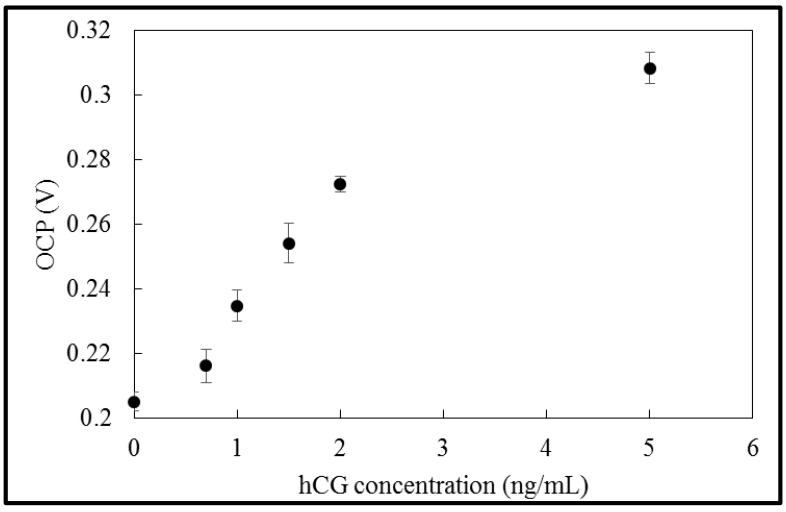

b

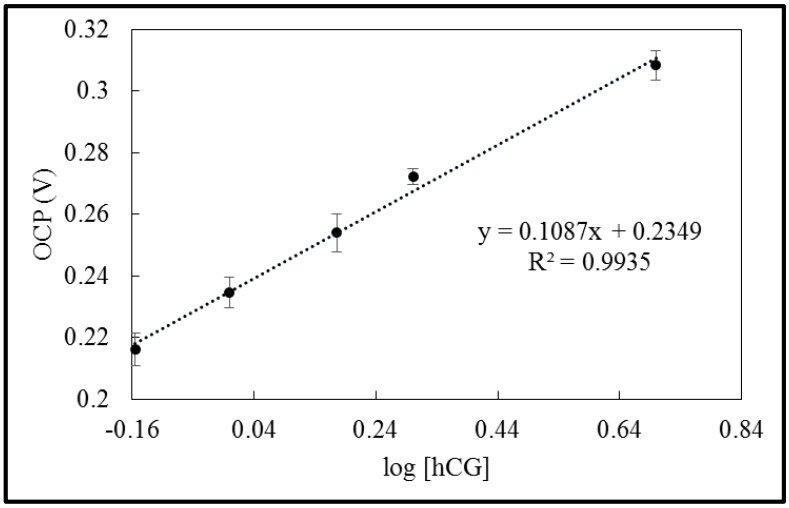

Figure 35. The calibration curve between the concentration of hCG and OCP signal (a), and between the logarithm concentration of hCG and OCP signal (b). Measurements were performed under the optimal conditions.

2.4 Conclusion

In this chapter, a novel electrochemical immunosystem, AuNPs labeled electrochemical immunoassay of hCG detection using OCP was successfully developed. For application of biomarker detection, the detection of hCG, pregnancy marker, was developed by direct electrical detection of AuNPs using OCP measurement. The immunocomplex was prepared on SPCE surface. The primary antibody was immobilized directly on SPCE and PPCE, and a series of sandwich-type immunoreactions, consisting of hCG antigen and AuNPs-labeled hCG antibody, were performed on a single electrode. After preparation of sandwich-type immunosystem, the preoxidation and reduction processes were applied, followed by electrical detection using OCP measurement. It was found that the peroxidation and reduction processes are essentially necessary for the OCP measurement. For the optimization of preoxidation, diffusion, and reduction processes, the applied potential and time period were studied. Using the optimal condition, detection limit was founded to be 0.079, and 0.1 ng/mL for SPCE and PPCE, respectively. The proposed system offers simplicity, uncomplicated, and low cost. Additionally, the proposed system shows high electrochemical sensitivity for hCG detection using AuNPs-labeled immunocomplex. Finally, this developed system could be applied to a simplified and miniaturized electrochemical system for using in clinical diagnosis.

Chapter III

SIMPLIFICATION OF OCP DETECTION USING PTNPS LABELED ELECTROCHEMICAL IMMUNOASSAY

3.1 Introduction

In this chapter, we aim to simplify OCP based measure to make the whole detection procedure less complicated and easier operation. We proposed a more simple immunoassay based on platinum nanoparticles (PtNPs) labeled antibody using OCP. In the chapter II, we have reported the immunoassay based on gold nanoparticles (AuNPs) labeled antibody with electrochemical pre-oxidation and reduction processes followed by OCP measurement. However, this method requires the application of both oxidation and reduction potentials to achieve detectable signal, which makes it not simplified as OCP method should be. The application of both preoxidation and reduction potential make the whole system complicated in detection procedure and design of micro-nano electrode for single molecule counting. To simplify OCP measurement, we are interested in the use of PtNPs in a hydrazine solution, solution of redox molecules. Because the reaction of interest, the oxidation of hydrazine, was good electrocatalyzed at the PtNPs [79], the new simple electrochemical immunoassay based on PtNPs was developed in this chapter. The detection of hCG was demonstrated by direct electrical detection of PtNPs in a hydrazine solution using OCP measurement without any application of external potential procedure. After preparation of sandwich-type immunosystem, hydrazine solution was dropped on electrosurface, followed by electrical detection using OCP immediately. The change of OCP signal was originated from electrocatalytic oxidation of the hydrazine on PtNPs. The potential was shifted to negative direction with increasing hCG concentration. It was found that the pH of 6.0 and hydrazine concentration of 1 mM provided the highest potential change. Under the optimal condition, a detection limit of 0.28 ng/mL and a linearity of 0-10 ng/mL were obtained. The PtNPs based method shows simpler electrochemical detection procedure than those obtained from AuNPs based method with an acceptable sensitivity and reproducibility. Moreover, it could be applied to a simplified and miniaturized diagnostic system with minimal user manipulation.

However, to apply in micro-nano fabrication, Au thin film and PPCE were tested. Unfortunately, the use of Au thin film for detection was unsuccessful because it required some linker that interfered the detection. Then, we used PPCE as working electrode because

it is one of carbon material similar to SPCE, and the immobilization can be easily performed using physical absorption without any linker. We found that using PPCE electrode, it was successful to distinguish the OCP signal in the presence and absence of hCG.

3.2 Experimental

3.2.1 Chemicals and materials

All chemicals and materials used in these experiments are listed in Table 7.

Table 7. List of chemicals and materials including their suppliers

Chemicals/materials and reagents	Suppliers
Platinum colloidal solution with 40 nm diameter	BBI solution, UK
Hydrazine monohydrate	Wako Pure Chemical Industries, Japan
Ag/AgCl ink for reference electrode	ALS Co., Ltd, Japan

3.2.2 Instruments and equipment

All instruments and equipment are listed in Table 8.

Table 8. List of all instruments and equipment including their suppliers

Instruments and equipment	Suppliers
Electron beam evaporator	ULVAC, Japan

3.2.3 Preparation of chemical solution

3.2.3.1 Hydrazine solution

Stock solution of 50 mM of hydrazine was prepared by dissolving 5 mg of hydrazine in phosphate buffer solution. Then diluted stock solution to desired concentration by phosphate buffer solution.

3.2.4 Procedure

3.2.4.1 Fabrication of pyrolysis photoresist carbon electrode (PPCE)

The fabrication of PPCE was similar as mentioned in Chapter 2.

3.2.4.2 Fabrication of Au thin film electrode

The fabrication of Au thin film electrode was performed on conductive Si substrate (p^+-Si) coated with 100 nm of SiO_2 using electron beam evaporator. The design of Au thin film electrode was shown in Figure 36 with working electrode's diameter of 2 mm. First, substrate was cleaned by sonicating in acetone for 5 min, followed by rinsing with DI water for 2 min, and drying on hot plate at 150 ^oC for 5 min. After that, the substrate was put into O_2 plasma asher to remove remained organic contaminations on surface. To deposit Au thin film, Ti was deposited on substrate at deposition rate of 0.01 nm/s with 5 nm of thickness to improve the adhesion between substrate and Au. Then, Au was deposited at thickness of 50 nm with deposition rate of 0.03 nm/s. Finally, conductive glue was applied to connect the wire and harden by baking at 90 ^oC for 10 min. The fabricated Au thin film electrode was ready to use.

Figure. 36. Scheme of Au thin film

3.2.4.3 Preparation of primary monoclonal antibody onto working electrode surface (Mab-FSH-immobilized immunosensor)

For SPCE and PPCE, the primary antibody can directly absorb on carbon based electrode via physical absorption, the treatment of surface was not necessary. In the other hand, primary antibody was immobilized on Au thin film electrode via a cysteamine self-assembled monolayer using glutaraldehyde as a cross-linker. Therefore, Au thin film surface was treated before immobilized primary antibody. 10 µL of 10 mM cysteamine was treated to surface of Au for overnight at room temperature. After rinsing with DI water, 10 µL of 15% glutaraldehyde was incubated on surface for 4 hr at room temperature, to introduce aldehyde residue which can bind amine residue of protein surface. Finally, Au thin film surface was ready to use for immobilizing of primary antibody in next step. In the case of PPCE, the immobilization of primary antibody can directly performed using physical absorption without cysteamine-glutaraldehyde ligand.

To immobilize primary antibody on treated Au thin film, SPCE and PPCE surfaces, the procedure was similar to chapter II. Briefly, 100 µg/mL of Mab-FSH solution was dropped onto working electrode surface and incubated at 4°c for 12 hr. Then the electrodes were rinsed with PBS to remove an excess antibodies. Then, the blocking solution of 1% BSA was incubated on the working electrode surface at 4°c for 12 hr. Finally, the electrodes were rinsed with PBS and kept at 4 °c until use.

3.2.4.4 Preparation of PtNPs-labeled hCG antibody (Pt-Mab-hCG)

200 µL of 50µg/mL of Mab-hCG solution in 5 mM KH_2PO_4, pH 7.5 was mixed with 1.8 mL of 1% PtNPs solution, and kept at room temperature for 10 min. Then, 100 µL of 1% PEG in 50 mM KH_2PO_4 (pH 7.5) was added, followed by 10% BSA in 50 mM KH_2PO_4 (pH 7.5) and incubated for 5 min to block the uncoated surface of PtNPs. After immobilization and blocking processes, PtNPs-conjugated Mab-hCG (Pt-Mab-hCG) was collected by centrifugation at 8000 g, 4°c for 15 min. Pt-Mab-hCGs were suspended in 2 mL of the preservation solution (1% BSA, 0.05% PEG 2000, 0.1% NaN_3 and 150 mM NaCl in 20 mM Tris-HCl buffer, pH 8.2), and collected again using centrifuge at the same condition. For the stock solution, Pt-Mab-hCGs were suspended in 200 µL of preservation solution.

3.2.4.5 Immobilization of hCG antigens and Pt-Mab-hCG onto Mab-FSH-immobilized immunosensor

Different concentrations of hCG sample solutions were prepared by diluting in 1% BSA in PBS. These sample solutions were introduced to the Mab-FSH-immobilized immunosensor at room temperature for 30 min, then rinsed with PBS. After that, Pt-Mab-hCG solution was applied to the surface and incubated at the same condition as described above, and rinsed with PBS. Finally, the direct redox reaction was performed and detected using OCP measurement. The procedure was shown in Figure 37.

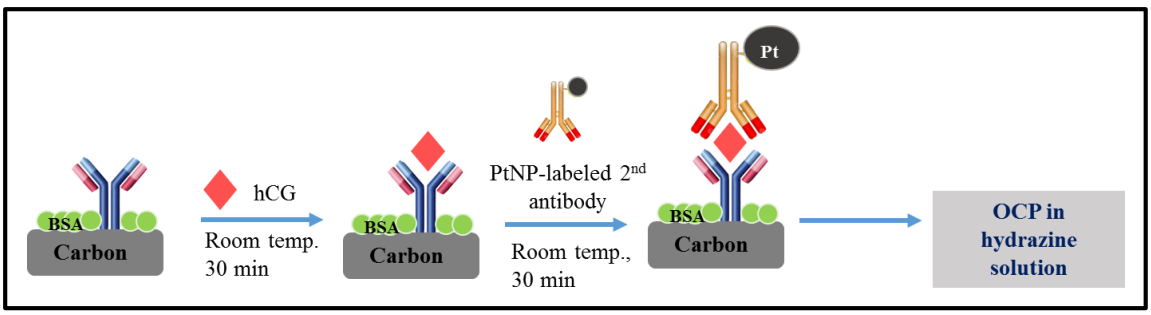

Figure 37. Schematic illustration of the immobilization of hCG antigens and Pt-Mab-hCG onto Mab-FSH-immobilized immunosensor

3.3 Results and discussion

3.3.1 SPCE based working electrode for PtNPs labeled electrochemical immunoassay using OCP

(1) Surface morphology of sandwich-type immunosensor labeled with PtNPs

Surface morphologies of the PtNPs-labeled immunocomplexes, consisting of primary Mab, hCG, and PtNPs-labeled secondary Mab, were evaluated by the scanning electron microscopy (SEM) as shown in Figure 38. Different hCG concentrations ranged between 0 and 10 ng/mL were investigated. The PtNPs were clearly observed at the electrode surface at the hCG concentration of 10 ng/mL which confirmed that PtNPs-labeled secondary Mab was successfully immobilized on the immnosensor. The size of PtNPs was approximately 40 nm in diameter, which is consistent to the originally platinum colloidal solution.

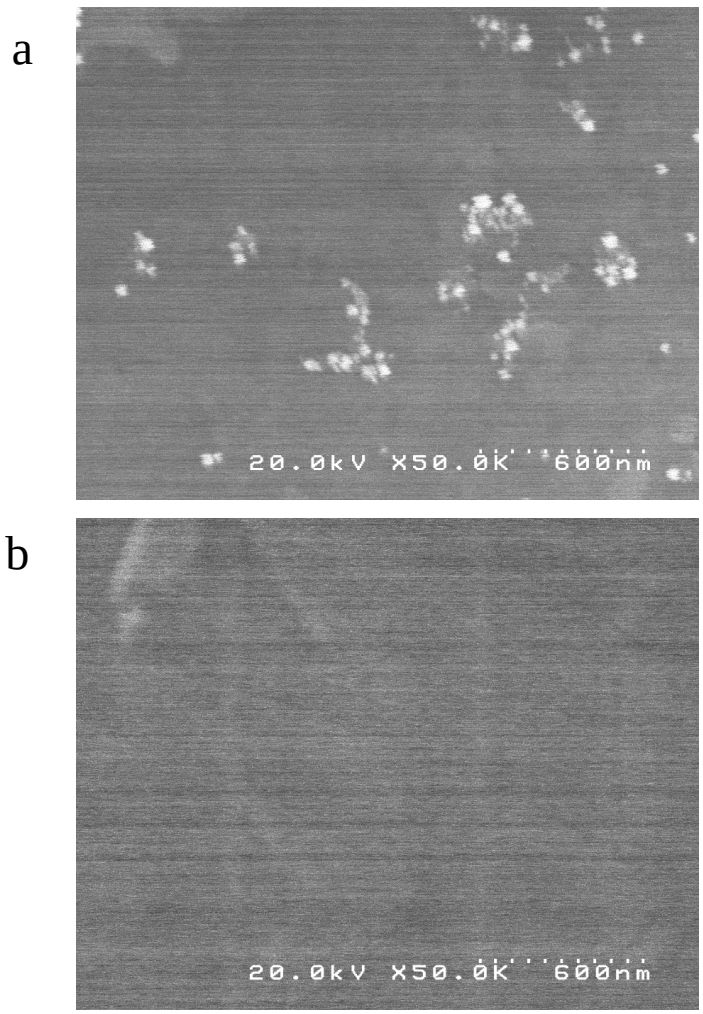

Figure 38. SEM image of PtNPs-labeled immunocomplexes immobilized on SPCE surface at the concentration of hCG of 0 ng/mL (a), and 10 ng/mL (b).

(2) The detection of hCG using OCP measurement of antigen-antibody complex label by PtNPs in hydrazine solution

The OCP was used to measure the hCG concentration after preparing the sandwich-type immunosensor. The number of PtNPs at secondary Mab was dependent on the hCG concentration and directly detected in 1 mM hydrazine solution. The different amounts of PtNPs on electrode surface affected to the catalytic activities towards the oxidation of hydrazine that result in the change of OCP signal as shown in Figure 39. The potential was shifted to negative direction with increasing of hCG concentration because of the PtNP electrocatalysis of hydrazine oxidation, the overall oxidation current on the PtNP together with that on the working electrode becomes larger than the overall reduction current. To maintain the OCP condition, the OCP shifts negatively to produce a zero net current. Figure 40 shows the OCP signal of PtNPs-labeled immunocomplexes immobilized on SPCE at different concentrations of hCG. From these results, the oxidation of hydrazine effectively occurred at Pt surface due to its good electrocatalytic activity. Accordingly, detection of hCG by the OCP can be simplified without any preoxidation and reduction steps, which are not affordable in case of AuNPs.

Figure 39. Schematic illustration of the electrocatalysis of hydrazine by PtNPs

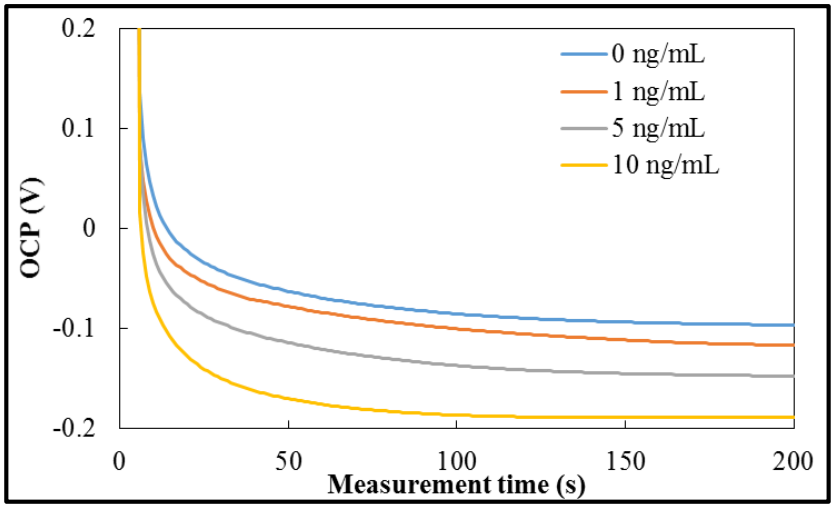

Figure 40. The OCP signal of PtNPs-labeled immunocomplexes immobilized on SPCE at different concentration of hCG.

(3) Optimization

For the detection, the pH of solution and concentration of hydrazine were studied because these factors can effect to the analytical results. These data was plotted as a function of studied parameters. After that, the net OCP signal after background subtraction was studied, and difference of signal-to-blank (S-B) was plotted corresponding to the studied parametes.

(i) Effect of pH of buffer solution

The influence of pH of phosphate solution was investigated from 5.5 to 8.0, because this range is along with pH range in human body, at hydrazine concentration of 1 mM to obtain the most appropriate medium for electrocatalytic oxidation of hydrazine. The OCP signals were significantly shifted to negative potential with the increase of pH in both presence and absence of PtNPs in the system as shown in Figure 41a. The more positive potential at lower pH was resulted from the protonated state of hydrazine (hydrazinium, $N_2H_5^+$) under low pH (pKa of hydrazine is 7.9). In the presence of PtNPs, the OCP was more rapidly shifted to negative potential than in the absence of PtNPs due to the electrocatalytic of oxidation of hydrazine at PtNPs surface. The net OCP signal as a function of pH after background subtraction was plotted as shown in figure 41b. As a result, the highest different OCP signal was observed at pH 6.0. Therefore, the phosphate solution pH 6.0 was used as optimal medium solution in further experiment.

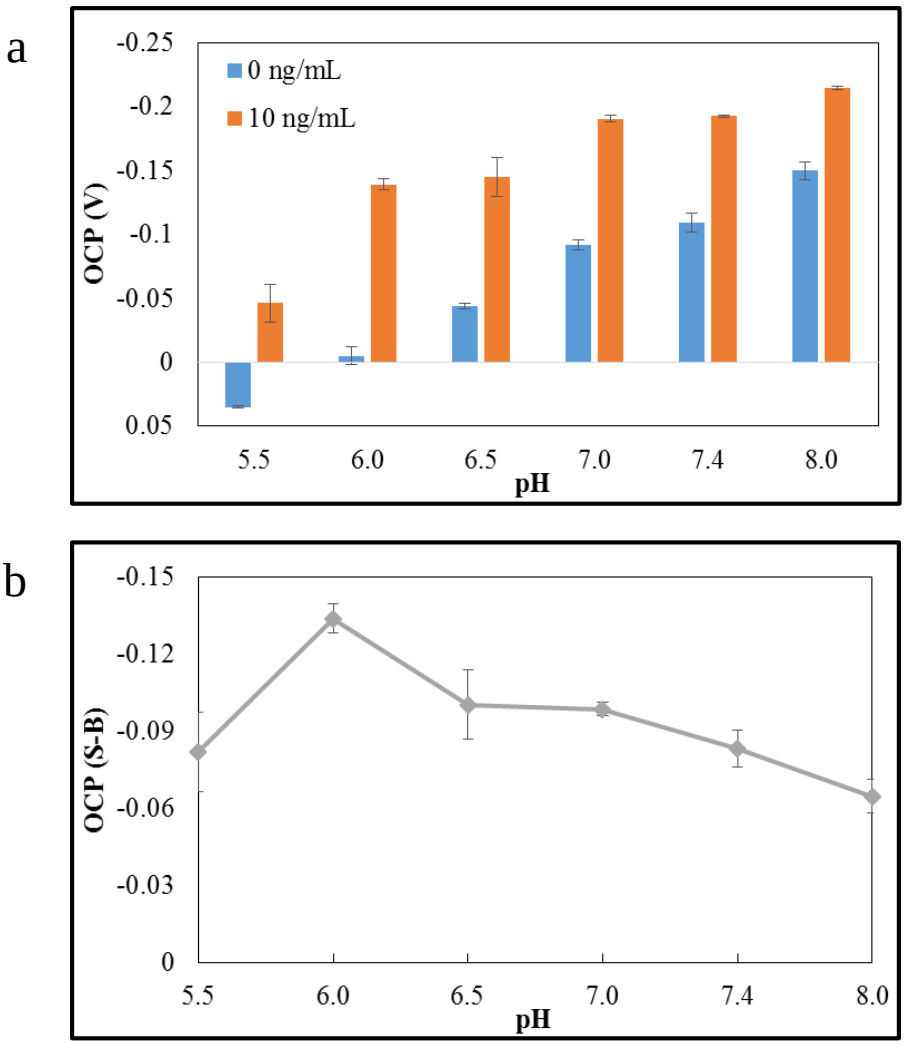

Figure 41. The effect of pH to OCP signal (a) of blank (0 ng/mL of hCG: blue) and 10 ng/mL of hCG (red), and the plot between pH and OCP signal after background subtraction (b) in 1 mM hydrazine solution

(ii) Concentration of hydrazine solution

Not only the change of pH but also concentration of hydrazine solution may affect to change of the OCP signal. The signal was shifted to negative potential with increase of hydrazine's concentration because of self-electrocatalytic oxidation of hydrazine at the surface of electrode. The OCP signal more significantly shifted in the presence of PtNPs than in the absence of PtNPs (Figure 42a). The dependence of OCP signal on the concentration of hydrazine after background subtraction was studied as shown in Figure 42b. At concentration of 1 mM, the highest OCP signal was observed. Accordingly, the concentration of 1 mM was chosen as optimal condition for further experiments.

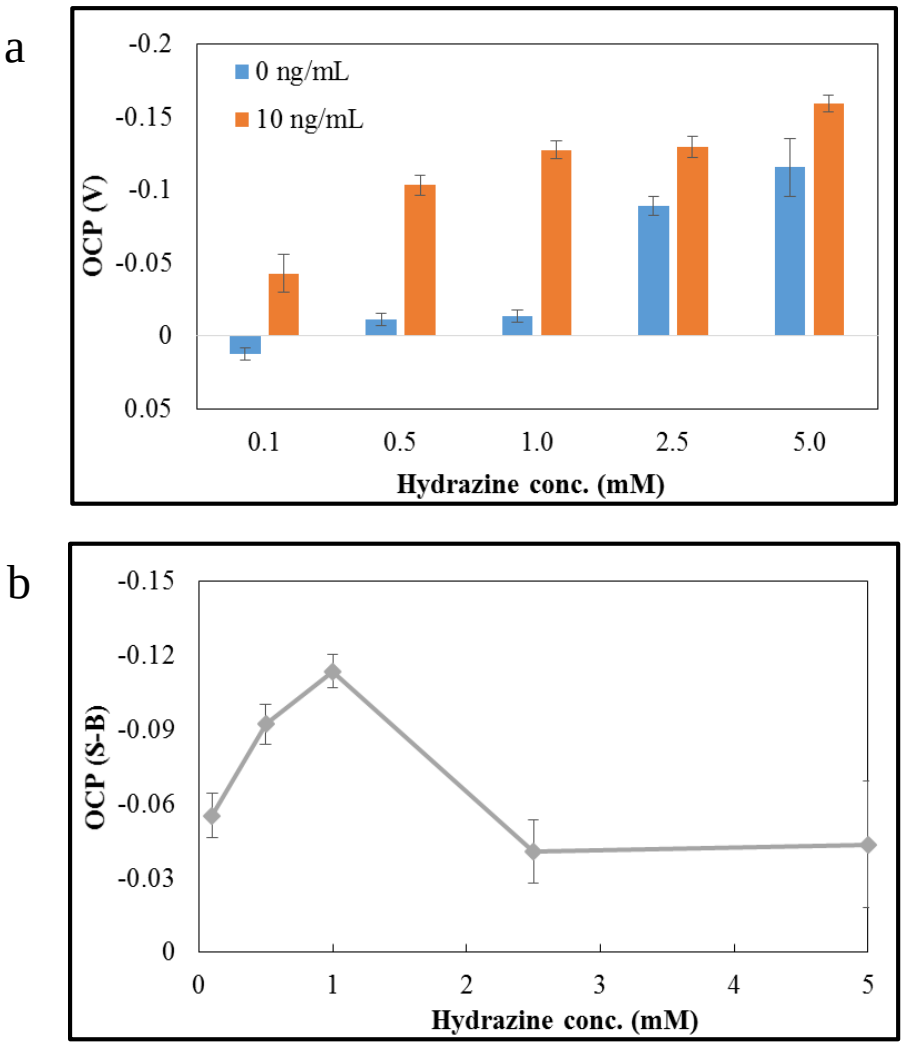

Figure 42. The effect of concentration of hydrazine to OCP signal (a) of blank (0 ng/mL of hCG: blue) and 10 ng/mL of hCG (red), and the plot between concentration of hydrazine and OCP signal after background subtraction (b).

From the optimization, optimal condition is summarized in Table 9. These conditions were used for the detection of hCG using PtNPs-labeled immunocomplexes immobilized on SPCE by OCP measurement.

Table 9. The optimal detection procedure

Parameters	Optimal
pH	6.0
Concentration of hydrazine	1 mM

(4) Analytical performance

The analytical performance of this proposed system was studied. The detection of hCG was performed under optimal condition. A calibration curve was constructed by plotting the OCP signal versus known concentrations of hCG. The linearity was observed in the range between 0 and 10 ng/mL with correlation coefficient (r^2) higher than 0.99 (Figure 43). The limit of detection (LOD) was calculated from from 3 S_{bl}/S, where S_{bl} is the standard deviation of blank measurement (*n=6*), and S is the sensitivity of the method (slope of linearity). The LOD was found to be 0.28 ng/mL (28 mIU/mL). According to the amount of hCG in pregnancy, marijuana use, hypogonadism (testicular failure), cirrhosis, inflammatory bowel disease, and duodenal ulcers, the obtained LOD is low enough to screen hCG concentration in clinical diagnosis applications [65]. Therefore, our proposed PtNPs based method shows simpler electrochemical detection procedure than those obtained from the AuNPs based method with an acceptable sensitivity and reproducibility. Moreover, it could be applied to a simplified and miniaturized diagnostic system with minimal user manipulation.

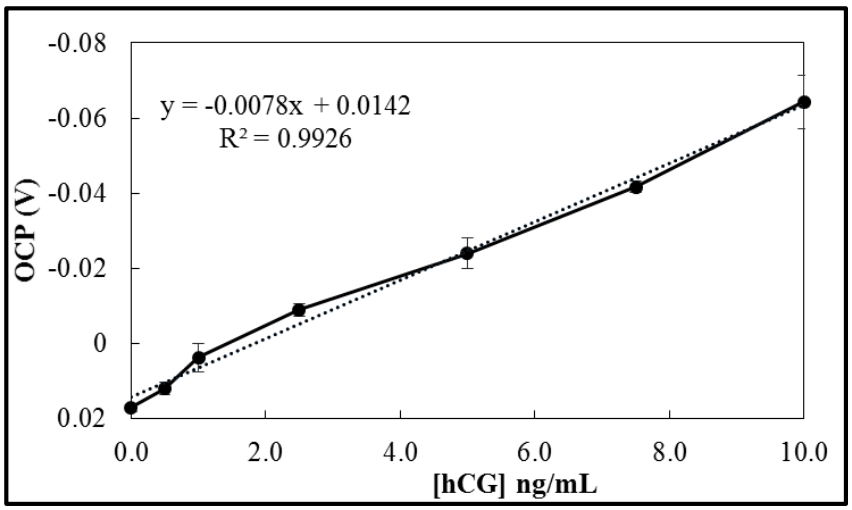

Figure 43. The calibration curve between the concentration of hCG and OCP signal under optimal condition

To verify the applicability of the proposed sensor, hCG in 5% human serum sample was analyzed. The standard addition method was used to investigate the practical applicability of the sensor. The concentrations of hCG were determined from the calibration curve. In the standard addition, the estimated values were in good agreement with the added a concentration of hCG, and a recovery experiment was used to evaluate the accuracy of the sensor (Table 10). The RSDs and recoveries were found in the ranges of 2.2–7.3% and

94.27.7–100.8%, respectively. The LoD of hCG detection in 5% human serum was 0.60 ng/mL. Thus, the results clearly indicates the ability to measure hCG in real biological samples.

Table 10. Determination of hCG in 5% human serum in 50 mM PBS (n = 3).

Added (ng mL^{-1})	**Detected (ng mL^{-1})**	**RSD (%)**	**Recovery (%)**
1	1.01±0.02	7.3	100.8
3	2.93±0.10	2.5	97.7
5	4.98±0.22	3.9	99.7
7	6.90±0.13	2.8	98.7
9	8.91±0.20	2.2	99.0

3.3.2 PPCE based working electrode for PtNPs labeled electrochemical immunoassay using OCP

As mentioned above, the detection of hCG using PtNPS based OCP method was successful on SPCE. Therefore, we are interested to find other carbon materials that can be detected hCG concentration and have the possibility to pattern and fabricate in micro-nano scale. PPCE is an attractive alternative to other carbon electrodes because of its advantages such as simple and inexpensive fabrication process. The most attractive of PPCE is the ability to create sensitive carbon electrodes through lithographically patterning photoresist that opens up many useful possibilities for electrode design in various application. After fabricated of PPCE, the immobilization of immunocomplex was prepared using the same procedure as SPCE. The immobilization of immunocomplex was investigated using SEM image. Figure 44 shows the SEM images of PtNPs on PPCE, it confirmed that PtNPs was successfully immobilized on electrode surface. Then, OCP measurement based on PtNPs was performed to confirm the ability for detection of hCG. Figure 45 shows relationship between OCP signal and concentration of hCG. As a result, although PtNPs based OCP detection of PPCE cannot show the different signal at various concentration of hCG but it was successful to distinguish the surface in the presence and absence of hCG (Figure 45). This success is provided the possibility to process the development for single molecule separation and counting. Therefore, PPCE was selected to use as material for fabricating the sensor in further experiment.

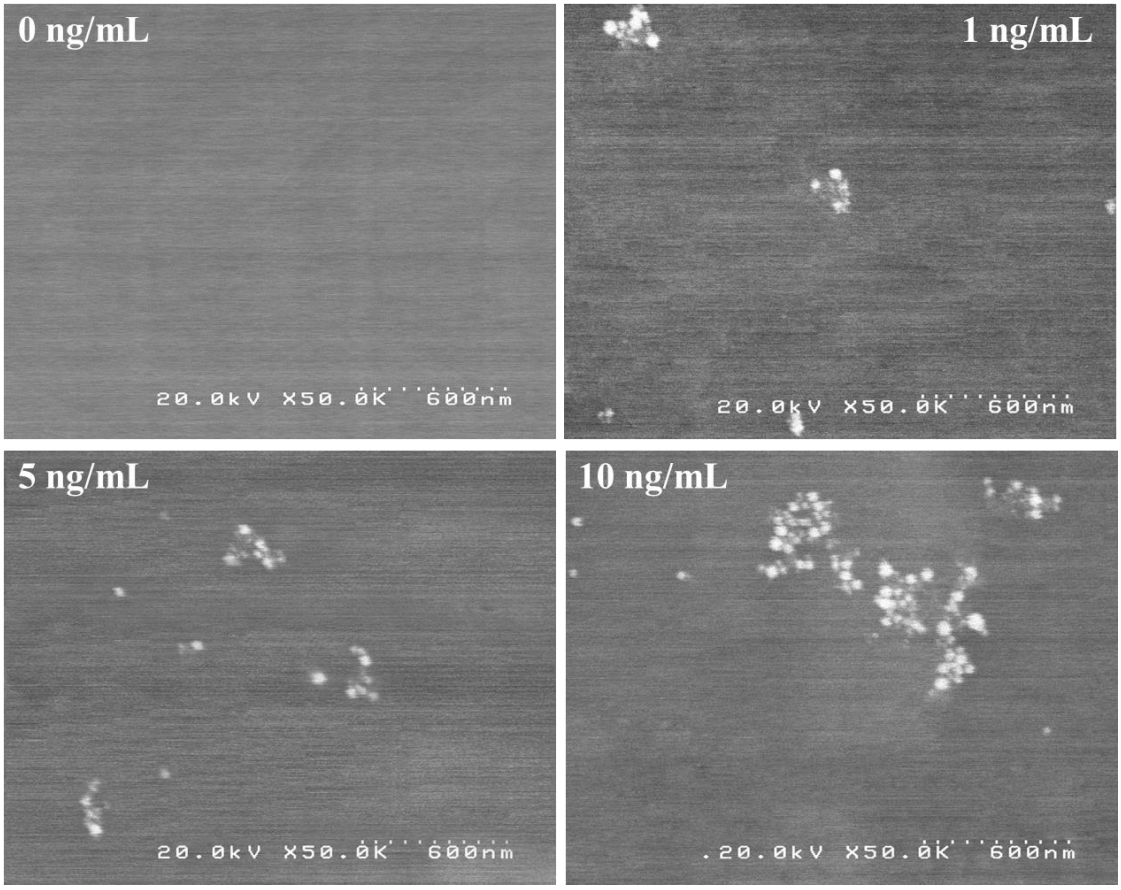

Figure. 44. SEM images of immobilization of PtNPs at PPCE at hCG concentration of 0, 1, 5, 10 ng/mL.

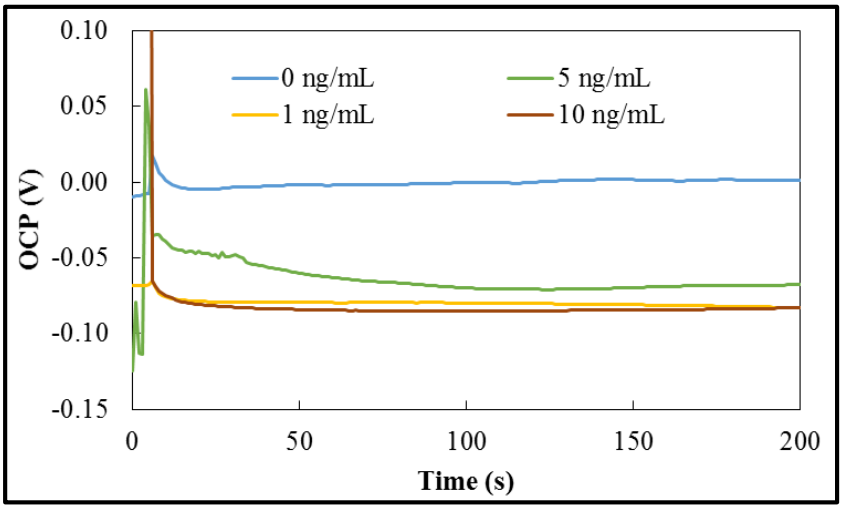

Figure. 45. OCP signal of PtNPs-labeled immunocomplexes immobilized on PPCE at different concentration of hCG.

3.3.3 Au thin film electrode based working electrode for PtNPs labeled electrochemical immunoassay using OCP

Only carbon based material but we also tried to apply our developed OCP method to detection hCG concentration on Au thin film electrode because Au thin film electrode has been used extensively in the construction of electrochemical sensor and can relatively easily be deposited by a thermal vacuum evaporation process. Moreover, Au thin film electrode has possibility to fabricate in micro-nano scale using a common technique in the preparation of thin metallic films. The primary antibody was immobilized on Au thin film surface via a cysteamine self-assembled monolayer using glutaraldehyde as a cross-linker. After added various concentration of hCG, followed by PtNPs labeled secondary antibody, SEM was used to studied the immobilization of PtNPs on Au thin film electrode surface. From SEM images in Figure 46, it confirmed that the immobilization of hCG and PtNPs was successful. Then, OCP behavior was studied to observe the relationship between hCG concentration and OCP signal in hydrazine solution. Figure 47 shows the plot between OCP signal and concentration of hCG at 0, 1, 5, and 10 ng/mL. It found that the OCP signal was randomly change and did not related to the concentration of hCG. Because the mixed OCP is defined by both the cathodic and anodic half-reaction currents, very small changes in these can result in appreciable changes in the potential. Thus, in this system, not only electrocatalytic oxidation of hydrazine on PtNPs occurred but other electroactive species as cysteamine-glutaraldehyde also existed at surface that can automatically provide some current itself to effect on OCP change. Figure 48 shows the OCP signal in 1mM hydrazine solution after immobilization of cysteamine, and glutaraldehyde step by step. It was found that the immobilization of glutaraldehyde significantly affected to the change of OCP signal. Glutaraldehyde was main interference on the OCP detection of PtNPs on secondary antibody. As a result, we can conclude that the PtNPs based detection of hCG using OCP method was unsuccessful on Au thin film electrode.

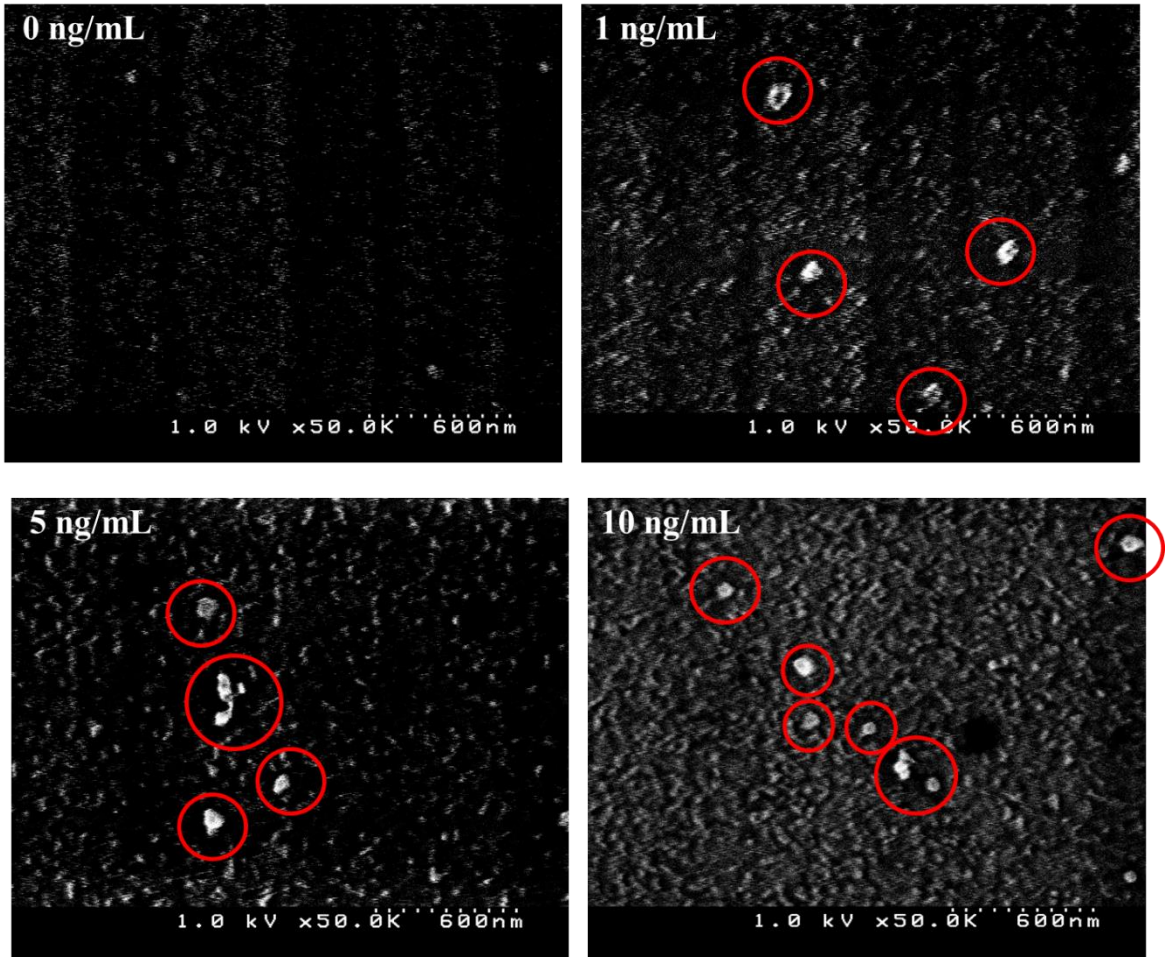

Figure. 46. SEM images of immobilization of PtNPs at Au thin film electrode at hCG concentration of 0, 1, 5, 10 ng/mL.

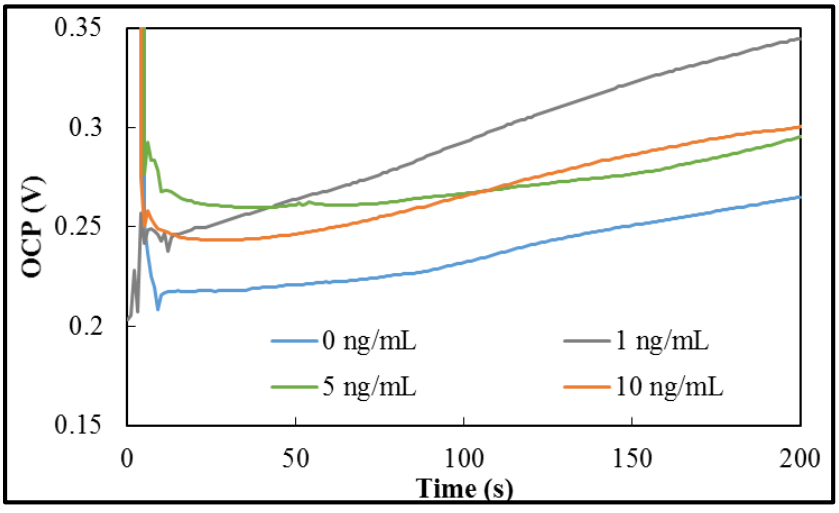

Figure. 47. OCP signal of PtNPs-labeled immunocomplexes immobilized on Au thin film electrode at different concentration of hCG.

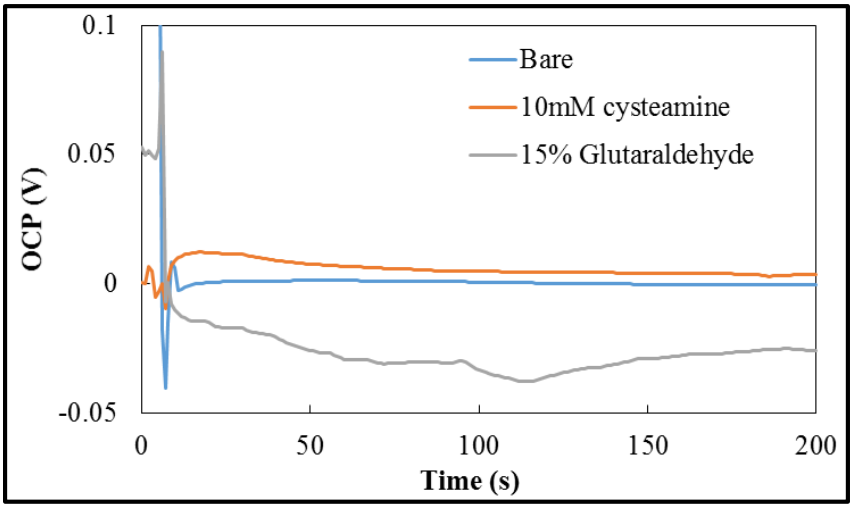

Figure 48. The effect of cysteamine, and glutaraldehyde on OCP signal in 1 mM hydrazine solution (in 50 mM PBS pH 7.4)

3.4 Conclusions

To simplify the OCP measurement of hCG, PtNPs based detection was successfully used instead of using AuNPs. The good electrocatalytic property of hydrazine on PtNPs surface can eliminate the complicated preoxidation and reduction processes during measurement. The change of signal was observed by direct electric detection by OCP method without any external power source. After preparation of immunocomplex, hydrazine solution was added to the sensor surface, immediately followed by OCP measurement. The negative shift of OCP signal was resulted from electrocatalytic oxidation of hydrazine on PtNPs surface. Throughout optimization using SPCE as working electrode, it was found that the pH of 6.0 and hydrazine concentration of 1 mM provided the highest potential change. Under the optimal condition, low detection limit of 0.28 ng/mL and wide linearity of 0-10 ng/mL were achieved. Therefore, our proposed PtNPs based detecion enabled a very simple procedure for detecting biomarker with acceptable sensitivity and reproducibility. Finally, this proposed system will be applied to develop method for single molecule detection in clinical diagnostic system.

To approach the application for single molecule detection, we have to find the suitable material which has ability to fabricate in micro-nano scale. First, we used Au thin film as electrode material because it is easily prepared using a thermal vacuum evaporation process. Unfortunately, the immobilization of antibody on Au surface required some linker that interfered the detection led to unsuccessful detection with OCP. Then, we interested in PPCE because primary antibody can directly absorb on surface via physical absorption

without any linker. We found that using PPCE electrode, it was successful to distinguish the OCP signal in the presence and absence of hCG. Therefore, PPCE was chosen as material to develop and fabricate micro-nano electrode for single molecule's application in next chapter.

Chapter IV

THE FABRICATION OF MICRO-NANO CARBON ELECTRODE

4.1 Introduction

According to chapter III, the simplification of the OCP measurement for hCG using PtNPs based detection, which circumvents the need of peroxidation and reduction processes before detection, was successfully. Recently, single-molecule detection techniques are widely used in the development of ultrasensitive biosensors. Duffy and coworkers [80] have developed an approach for detecting thousands of single protein molecules simultaneously using arrays of femtoliter-sized reaction chambers for isolating and detecting single enzyme molecules by fluorescence imaging. This research was sucessfully detected prostate-specific antigen (PSA) at concentrations as low as 14 fg/mL. A few year later, Noji et al. [81] present a novel device employing one million femtoliter droplets immobilized on a substrate for the quantitative detection of extremely low concentrations of streptavidin-β-galactosidase conjugate. They expected that digital counting using a large number of chambers would improve the LOD. The performance of their proposed digital counting device was demonstrated with a limit of detection (LOD) of 10 zM.

As mention above, although the single molecule counting uses optical detection is effective and high sensitive method, several drawbacks associated can suffer from this type of measurement. These include a requirement for generally bulky instrument and potential false signals arising from complex colored samples. In this context, we are interesting in the use of OCP technique as detector for counting single molecule. To our knowledge, there is no publication report about the use of electrochemical technique for the detection of single molecule. To apply proposed OCP method for isolating and counting single molecule, we focused on fabricating micro-nano sized carbon electrode array by electron beam lithography (EBL) technique. An effective strategy for single molecule detection is to isolate each biomolecule into small electrode, one at a time. Therefore, simultaneous and parallel analyses of single biomolecule complexes, many electrode within each array are required. We are planning to fabricate a hundred of working electrode array for trapping single molecule and detecting electrochemical signal. The size of electrode is nanometer scale according to the size of nanoparticle. The optimization of electrode size and shape will be discussed. This chapter shows the possibility to fabricate pyrolysis photoresist carbon film (PPCE) in micro-nano size. First, the immobilization density of PtNPs was conducted to

estimate the suitable electrode size. Then, the simple dot pattern was designed. Preliminarily, we considered to pattern the PPCE film by using EBL and dry-etching techniques. The negative EB resist pattern was performed on PPCE film on a SiO_2/Si substrate using an EBL system. Important EBL parameters such as dot size, pitch, electron beam current, and dose time were systematically studied to achieve the desired size of the pattern. After the EB resist patterning, a dry etching process was performed to fabricate micro-nano carbon dot patterns. However, by using this method EB resist pattern was faster etched than PPCE. Therefore EB resist could not be used as the mask to protect PPCE under the pattern that caused the nano-sized PPCE patterning was not very successful. Due to similarity in chemical structure of the AZ photoresist and the EB resist, it can be considered that pyrolysis of the EB resist film would also be able to apply for electrode. Therefore, I tried to directly pyrolyze the patterned EB resist to form electrode array. As a result, it was found that this method was successful to fabricate carbon dot in sub-micrometer scale.

4.2 Experimental

4.2.1 Chemicals and materials

All chemicals and materials used in these experiments are listed in Table 11.

Table 11. List of chemicals and materials including their suppliers

Chemicals/materials and reagents	Suppliers
SAL601 SR2	Shipley Co., Ltd., Japan

4.2.2 Instruments and equipment

All instruments and equipment are listed in Table 12.

Table 12. List of all instruments and equipment including their suppliers

Instruments and equipment	Suppliers
Digital microscope VH-2450	KEYENCE, Japan
Surface profiler P-15	KLA Tencor, Japan
Electron beam lithography, ELS-3700	ELIONIX INC., Japan
Inductively Coupled Plasma (ICP) Etching system RIE-101 iPH	Samco, Japan

4.2.3 Procedure

4.2.3.1 Fabrication of simple EB resist pattern on PPCE

After fabrication of PPCE film, the OAP solution was coated on the substrate using spin coating at 4000 rpm for 30 s, followed by baking on a hot plate at 110 ºC for 3 min. After that, the SAL601-SR2 negative EB resist, was coated at 4000 rpm for 60 s, and baked at 110 ºC for 1 min. Simple dot pattern array with various diameters ranged between 50 and 1000 nm were fabricated using EBL system at different beam currents and dose times. After EB exposure, the sample was post baked at 100 ºC for 5 min, and developed in MF319 for 5 min, followed by de-ionized water risning for 3 min to remove unexposed area. Finally, the patterns of EB resist were investigated using digital microscope and SEM.

4.2.3.2 Fabrication of micro-nano pattern of PPCE

To isolate individual PPCE, a dry etching process was applied after EB resist patterned. Firstly, the etching rates of PPCE and SAL601 SR2 resist were studied under various etching conditions including O_2, and mixture of O_2 and Ar. The etching behaviors of PPCE and exposed SAL601-SR2 were investigated on SiO_2 100 nm/p^+-Si substrate. After that, the suitable dry etching condition was chosen and performed on SAL601 SR2 patterned on PPCE. Finally, SEM was used to observe the fabricated micro-nano PPCE. Figure 49 shows a schematic fabrication process of the PPCE in micro-nano scale.

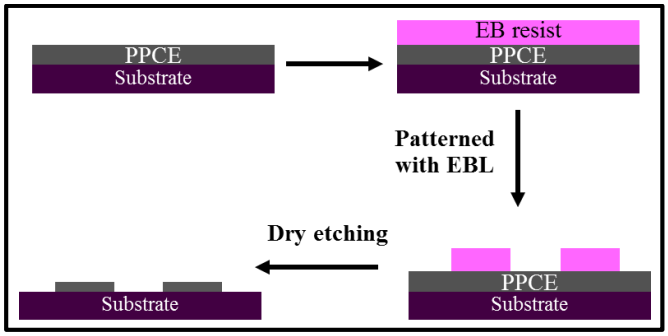

Figure 49. Scheme of fabrication process of PPCE in micro-nano scale

4.3 Results and discussion

4.3.1 Estimation of electrode size

To consider the electrode size of PPCE, the density of immobilized PtNPs was studied using SEM and image J. The high concentration of 100 ng/mL of hCG was used to approach the saturated immobilization. After that the Pt particle density was estimated. Figure 50 shows the immobilization of PtNPs at 100 ng/mL of hCG's concentration at

different magnification, the number of particles were counted using image J program. The particle density was found to be 113.4 particles/μm^2 (n = 10) that means 1 particle uses area for immobilization of 8818 nm^2. Using typical formula for area of a circle, the suitable diameter of an electrode was approximately 100 nm. However, in the clinical application, such high concentration is not necessary to be detected because it needs to detect protein biomarker at low concentration. Considering to analytical performance using PtNPs based OCP detection on SPCE, the number of PtNPs was linearly with concentration of hCG. The highest concentration in linear range is 10 ng/mL. Using this concentration, the particle density was found to be 11.3 particles/μm^2. The electrode size was estimated approximately to be 300 nm in diameter. Therefore, the electrode size of 300 nm is small enough to use in single molecule isolating and counting application.

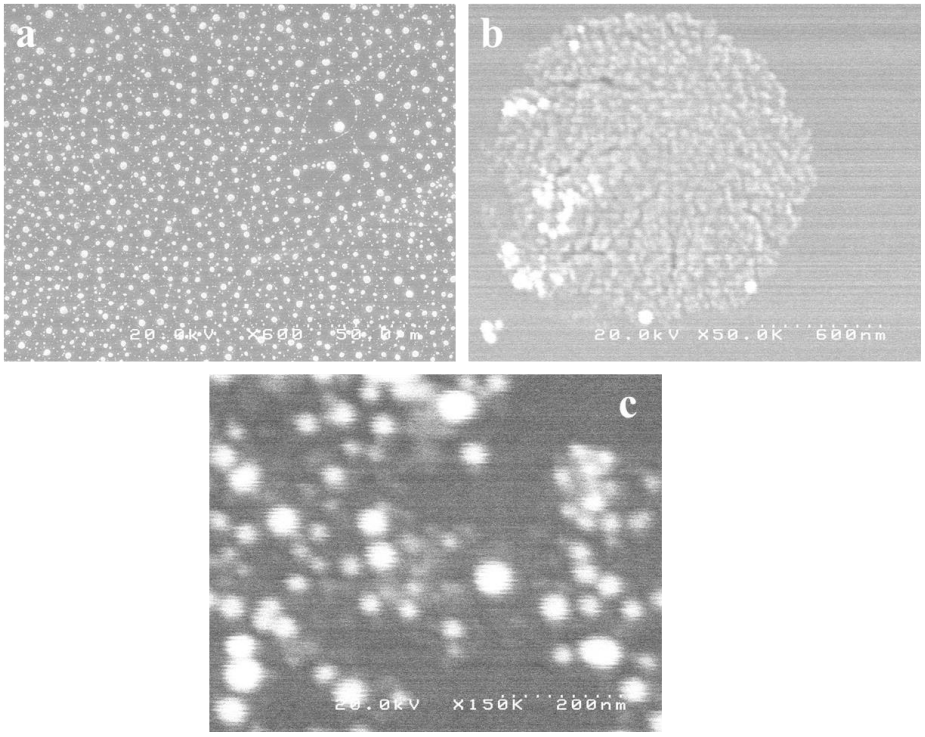

Figure 50. SEM of immobilized PtNPs at concentration of hCG of 100 ng/mL with magnification of ×600 (a), ×50.0K (b), and ×150K (c)

4.3.2 Study of EBL condition

Different diameters of dots were designed to study the possibility to make small pattern. Various diameters of 100, 200, 500, and 1000 nm with different pitches were studied. For EBL system, the effects of beam current and dose time were investigated because these factors affect to uniformity and size of desired pattern. Figure 51, 52, and 53 present the optical microscope images of the resist patterns after exposed with EBL at beam

currents of 300 pA, 1 nA, and 2 nA, respectively. The results showed that dot patterns of 1 μm, 500 nm, and 200 nm in diameter was clearly observed when the spot size larger than 1 nA. On the other hand, at spot size of 300 pA, the dot size smaller than 500 nm could not be observed. From these observations, we can conclude that the resist pattern larger than 200 nm in diameter was successfully created on PPCE substrate.

In order to evaluate smaller dot pattern (below 200 nm), SEM characterization was performed. The exact size after exposure and pattern's uniformity were studied. Figure 54 and 55 show the SEM images of dot patterns with 100 nm in diameter at the beam currents of 1 nA and 2 nA, respectively. From SEM image, the smallest pitches, of which dot patterns did not connect, was 400 nm and 600 nm for the beam currents of 1 nA and 2 nA, respectively. Then, the precise size of obtained dot was estimated using image J program. Table 11 shows the summary of exact dot diameter and uniformity at designated dot size of 100 nm diameter. It was found that the dot size increased with the increase of dose time and beam current. As well known that the dose time is the time during which the electron beam is irradiated to each dot (μs/dot). When increasing the dose time, the amount of energy deposited per unit area will be increased that makes the dot the bigger in size. Considering to the beam current, it is defined as how many electrons are impinging on the sample each second. Its value affects to obtainable resolution. Therefore, high beam current tends to be poorer resolution than small current one. Based on both size and uniformity of patterns after exposure as shown in table 13, the spot size of 1 nA and dose time of 0.6 μs/dot were selected as optimal EBL condition for patterning PPCE.

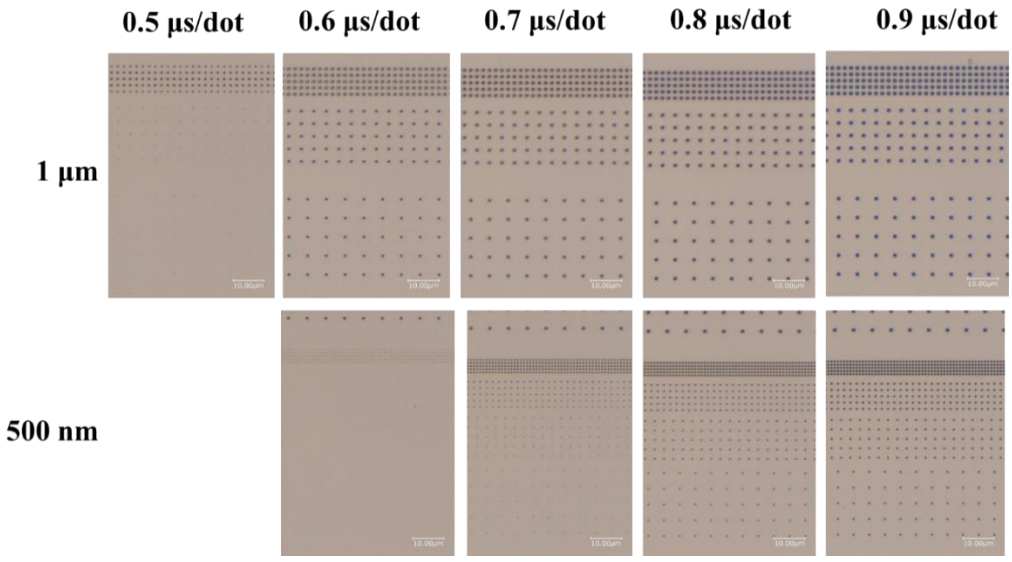

Figure 51. Image of obtained pattern at spot size of 300 pA

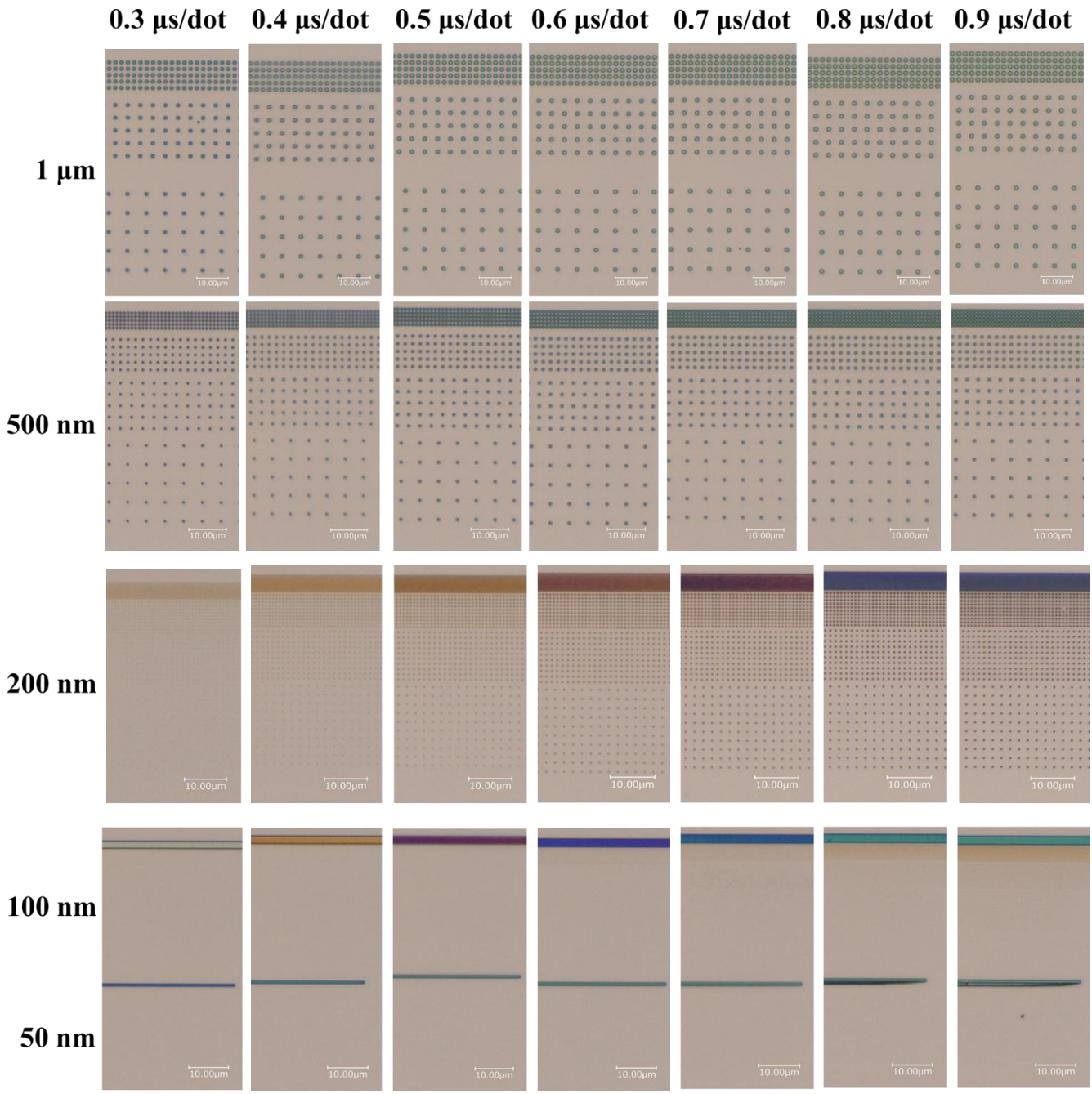

Figure 52. Image of obtained pattern at spot size of 1 nA

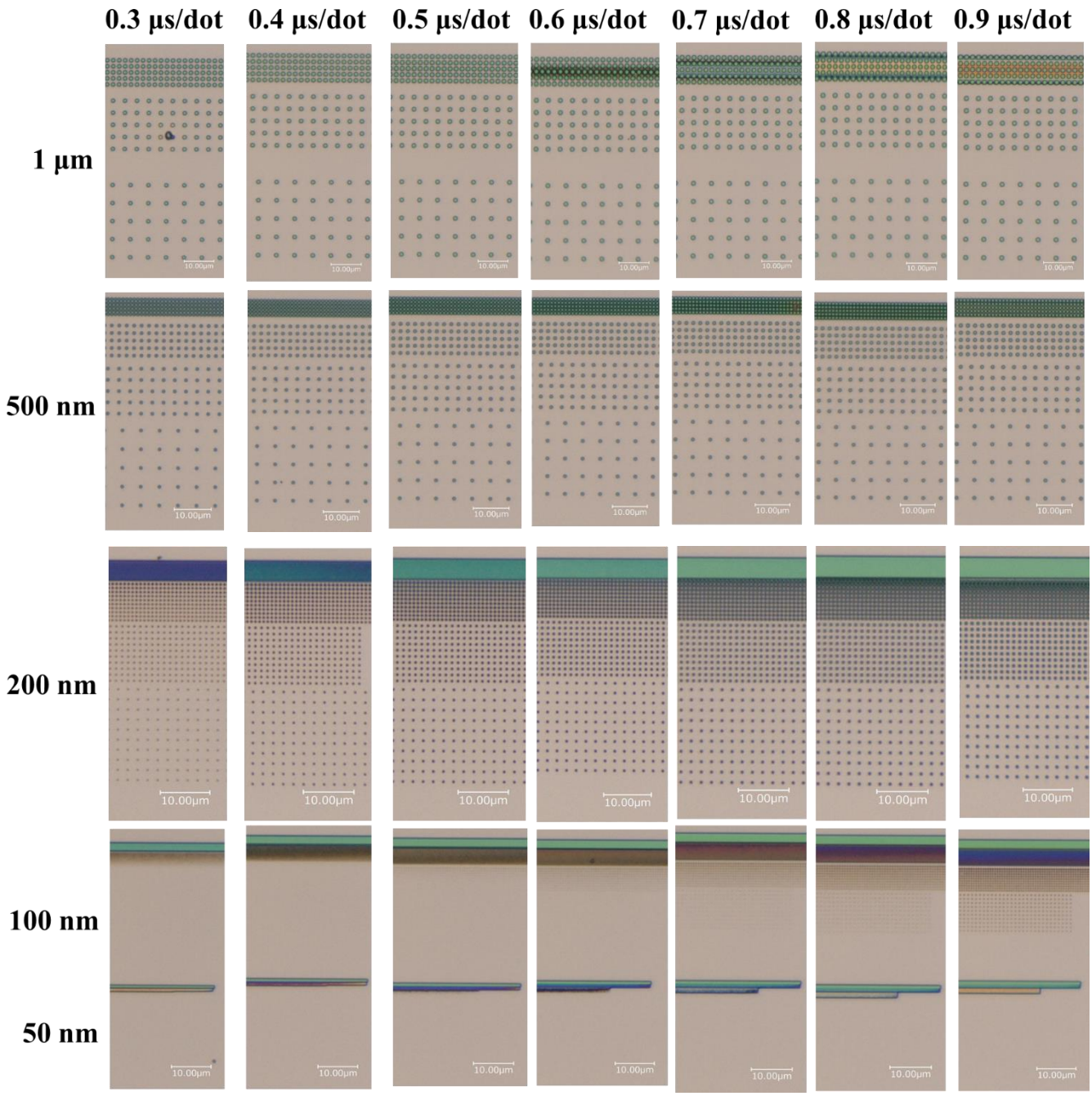

Figure 53. Image of obtained pattern at spot size of 2 nA

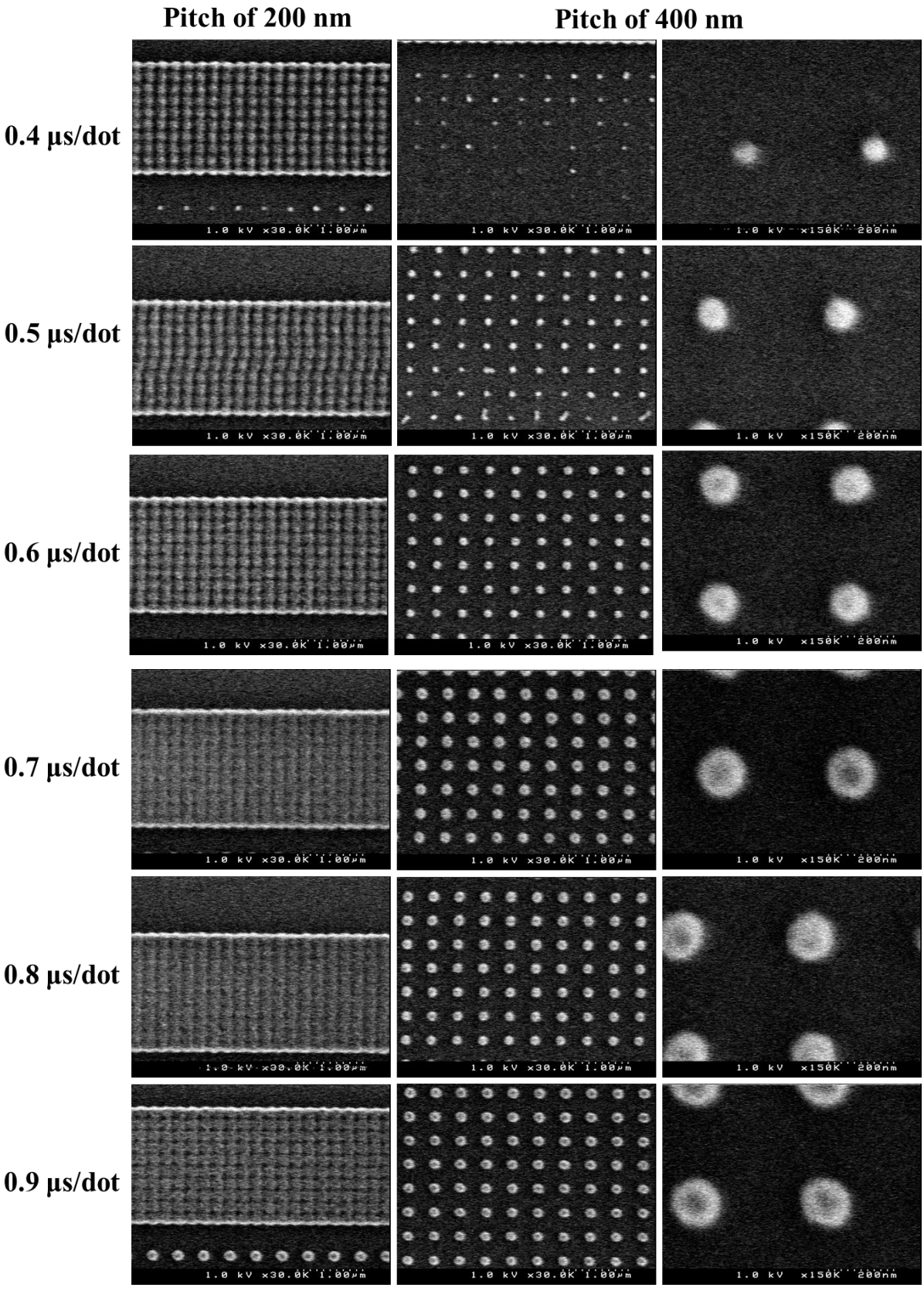

Figure 54. SEM images of 100 nm of diameter of dot size at spot size 1 nA.

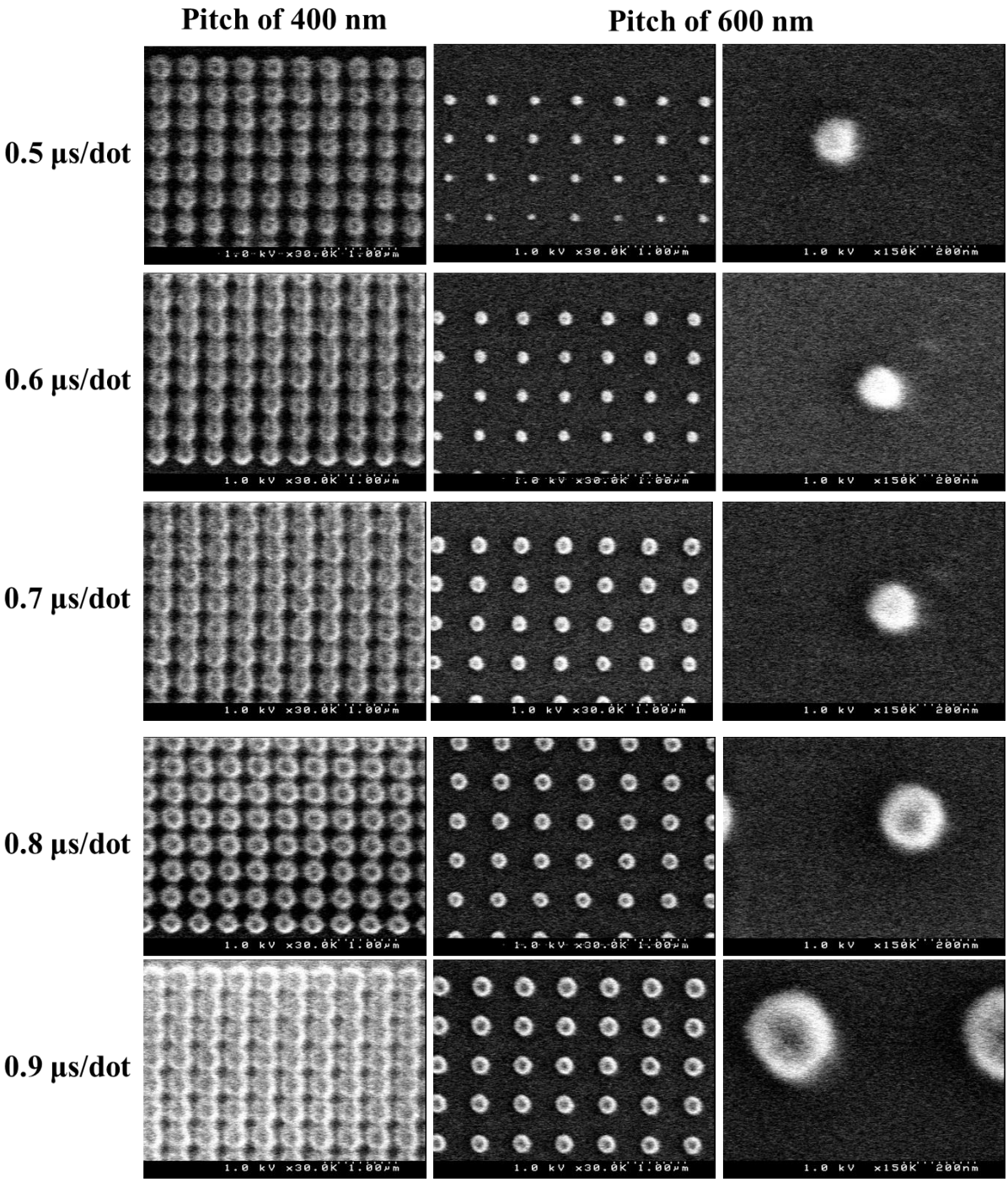

Figure 55. SEM images of 100 nm of diameter of dot size at spot size 2 nA.

Table 13. The summary of exactly dot diameter and uniformity at designed dot size of 100 nm diameter.

Spot size / Dose time (μs/dot)	1 nA		2 nA	
	Obtained diameter (nm)	**Uniformity**	**Obtained diameter (nm)**	**Uniformity**
0.4	74.25	×	-	-
0.5	101.3	Δ	130	Δ
0.6	122.3	○	138.3	○
0.7	148.4	○	148.6	○
0.8	150	○	184.6	○
0.9	153.3	○	246.4	○

* ×, Δ, and ○ mean non-uniform, rarely uniform, and uniform, respectively.

4.3.3 Study dry etching behavior of PPCE and SAL601-SR2 resist

To fabricate electrode array in micro-nano scale, the etching rates of PPCE and SAL601 SR2 resist were studied under various etching conditions including different gases such as O_2, and mixture of O_2 and Ar. The etching rates of PPCE and exposed SAL601-SR2 film deposited on SiO_2 100 nm/p^+-Si substrates were investigated. For the SAL601-SR2, the simple square pattern was created to use for studying dry etching process. The etching rate of individual material was calculated using a slope of a plot between etching thickness and time. Figure 56 shows the relationship between etching thickness of PPCE and SAL601-SR2 and time at O_2/Ar gas ratios of 20/0, 18/2, 16/4, 14/6, and 18/2 sccm. It was found that the etching rate of SAL601-SR2 was slightly faster than that of PPCE, and the etching rate of both substances increased when the amount of Ar was increased. We proposed that O_2 is reactive gas, it chemically etched PPCE by turning it into ash. Then, ash was removed though the vacuum pump. On the other hand, Ar is non-reactive gas, the main etching mechanism when using Ar gas is physical bombardment. Thus, when Ar was added to etching gas, not only chemical etching but physical etching also occurred causing the increase of etching rate. The summary of etching rate at different conditions is shown in table 14. We selected to use only O_2 to fabricate micro-nano PPCE in dry etching process, because this condition provided the smallest different etching rate between PPCE and SAL601-SR2.

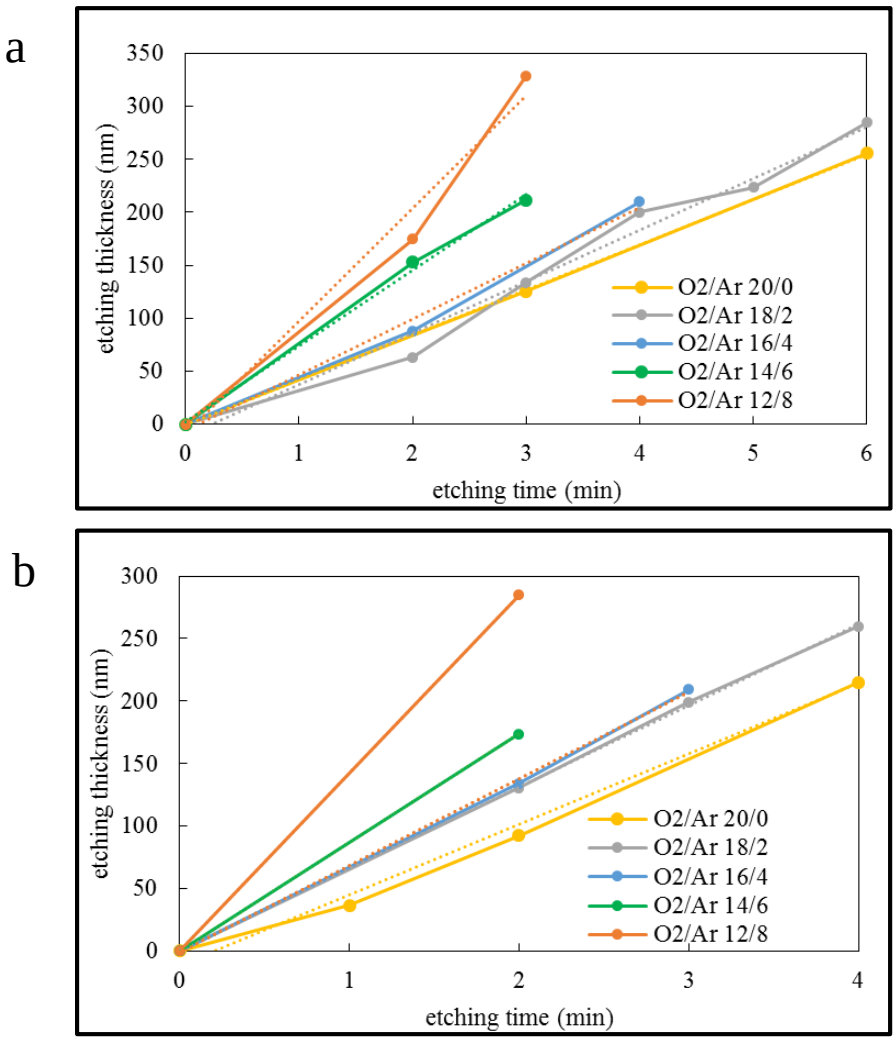

Figure 56. The plot between etching of PPCE (a), and SAL601-SR2 (b) versus time at different dry etching condition with RF power of 100 W and bias power of 20 W.

Table. 14. The summary of etching rate of SAL601SR2 and PPCE

O_2/Ar (sccm)	Etching rate (nm/min)	
	SAL601-SR2	PPCE
20/0	56.36	42.58
18/2	65.28	48.71
16/4	69.41	52.52
14/6	86.91	71.44
12/8	142.56	106.53

4.3.4 Fabrication of micro-nano PPCE

Dry etching of patterned PPCE was performed under 20 sccm of O_2, RF power of 100 W, and RF bias power of 20 W. The etching time was calculated using dry etching rate of PPCE related to initial thickness of PPCE before dry etching. Figure 57 shows the pattern before and after dry etching. Before dry etching process, it was clearly observed the dot pattern of SAL601-SR2 on PPCE. However, after dry etching process, the SAL resist was completely removed and the remained PPCE patterns under the resist pattern were not uniform as a discontinuous film. Moreover, PPCE also remained at the non-patterning area. Consequently, the fabrication of micro-nano PPCE was not successful by this method. Considering to dry etching rate and thickness of resist and PPCE, the thicknesses were 250 nm for resist pattern and 590 nm for PPCE. When performing the dry etching process, the resist was etched out faster than PPCE. Thus, the resist pattern could not act as a mask to protect the PPCE film from dry etching process by O_2 leading to non-uniform structure as shown in figure 57. Therefore, the fabrication of PPCE in nano scale was unsuccessful.

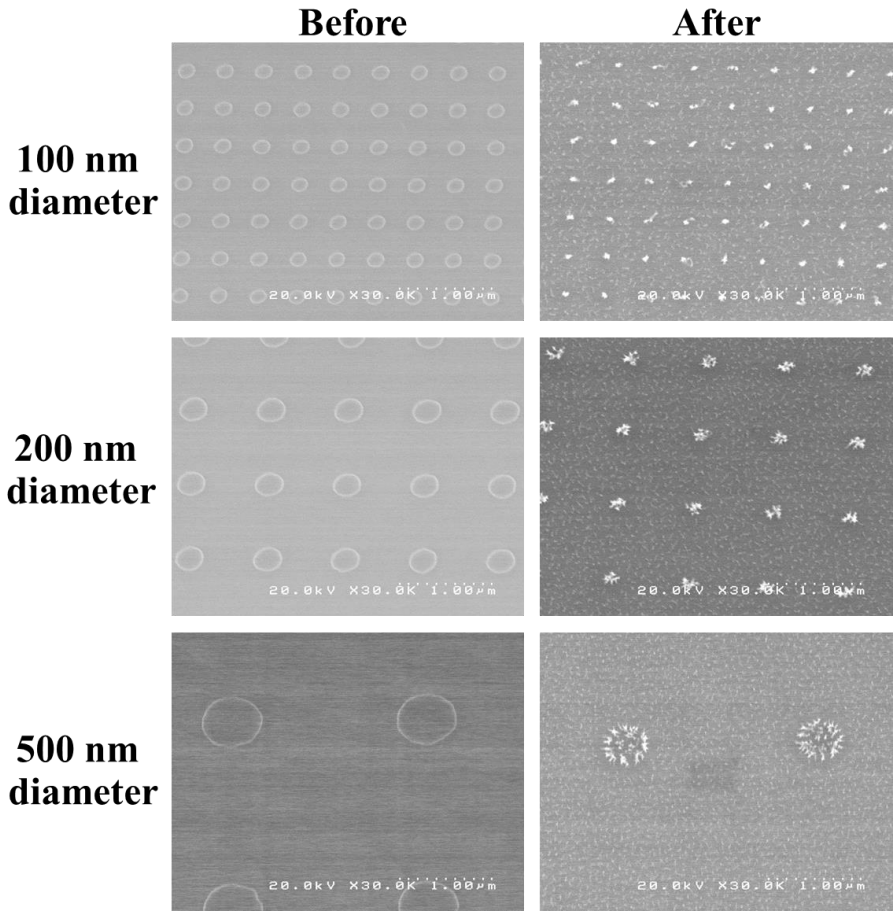

Figure 57. The obtained pattern before and after dry etching at beam current of 1 nA and dose time of 0.6 μs/dot.

4.3.5 Pyrolysis SAL601-SR2

Because of unsuccessful dry etching process, we try to find other procedure to make micro-nano carbon dot. SAL601-SR2 is the negative electron beam resist which consists of novolak polymer, a melamine resin as crosslinker, and a bromic triazine as an acid generator. In the case of AZ5214E photo resist, the main components are novolak polymer, and photosensitive of diazonaphthoquinone. Considering to component in both resist, they contain similar main component of novolak resin. Therefore, we are interested in fabricating micro-nano carbon dot by directly pyrolyze SAL601-SR2. The pyrolysis of SAL601-SR2 has been proposed in reference [82]. First, OAP was used to coat on substrate before coating resist to increase adhesion between substrate and resist. Then SAL601-SR2 was coated with thickness of about 250 nm on cleaned SiO_2/Si substate. After that, sample was pyrolyzed under the mixture of 5% H_2 and 95% N_2 atmosphere at 700 ^oC for 1 hr. Finally, the surface morphology and resistivity of obtained substrate were investigated. Figure 58 shows surface morphology of pyrolyzed SAL601 film, the RMS was found to be 0.37 nm. Pyrolyzed SAL601-SR2 provided a smoother surface than those provided from SPCE and PPCE. The sheet resistance of pyrolyzed SAL601 film was found to be 127.2 kΩ/sq, compared to SPCE (115.4 Ω/sq) and PPCE (253.6 Ω/sq), the sheet resistance of pyrolyzed SAL601 film was much higher. It means the conductivity of this film was not good. To improve the conductivity, we tried to increase pyrolysis temperature. At pyrolysis temperature of 850 ^oC, the sheet resistance of SAL601-SR2 film was decreased to be 5.5 kΩ/sq, about 25 times lower. Therefore, the increasing of pyrolysis temperature can significantly improve conductivity of pyrolyzed SAL601 film. Based on this result, we consider that the pyrolyzed SAL601 film would be used as an alternative material to fabricate micro-nano carbon dot.

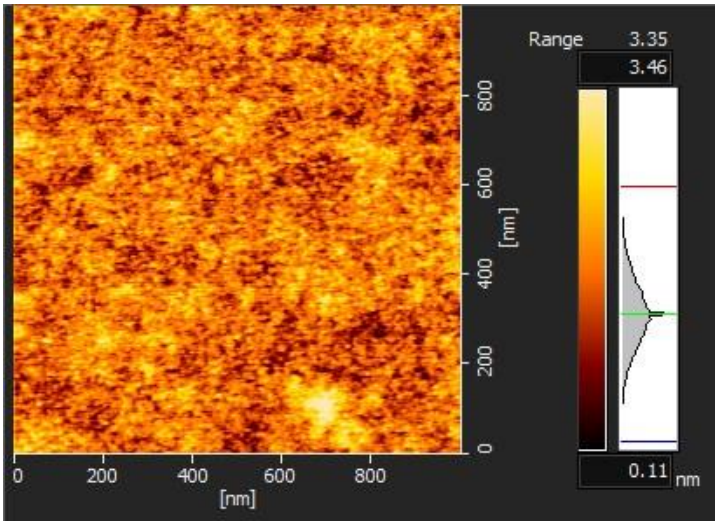

Figure 58. AFM images of SPCE, PPCE, and pyrolyzed SAL601-SR2 film

4.3.6 Fabrication of micro-nano carbon dot on pyrolzed SAL601-SR2 film

After preparation of pyrolzed SAL601-SR2 film, the patterns of different of dot's diameter at different dose times were studied. The thickness of SAL601-SR2 before pyrolysis was found to be 250 nm. Figure 59 shows the SAL601-SR2 pattern with a beam current of 1 nA at different dose times. It was found that the dot's diameter over 200 nm was successfully fabrication. For 100 nm of dot's diameter, the pattern was observed when dose time was higher than 0.7 μs/dot and uniform dot was observed at dose time high than 0.8 μs/dot. After pyrolysis at 700 ^{o}C for 1 hr, the thickness was decreased to 50 nm which was 20% of the initial SAL601 thickness. Figure 60 shows the pattern of pyrolzed SAL601-SR2 film, it was found that the pattern was expanded by pyrolysis. The expansion about 2 times from original size was observed. Temperature is the average kinetic (or movement) energy of the molecules in a substance. We believed that the rise of temperature caused kinetic energy of molecules increased, the molecules start vibrating or moving, and take up more space causing a large pattern after pyrolysis. Table 15 shows a summary of size of pattern before and after pyrolysis. It shows that this method is able to fabricate carbon dot with the smallest of 186 nm in diameter. Currently, the proposed method was successful in the sub-micrometer fabrication and could realize the desired dot's size of 300 nm.

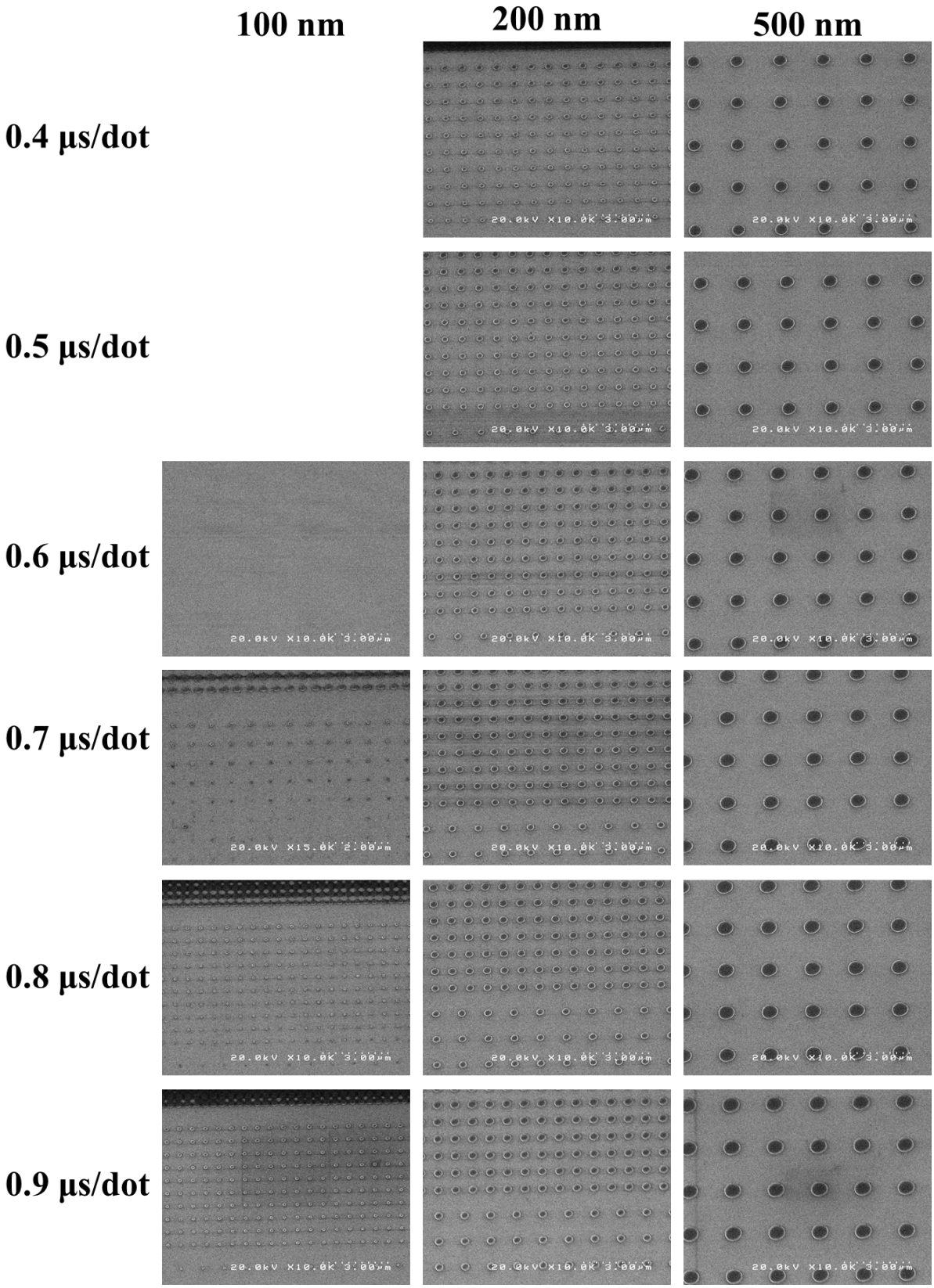

Figure 59. The resist pattern before pyrolysis at beam current of 1 nA

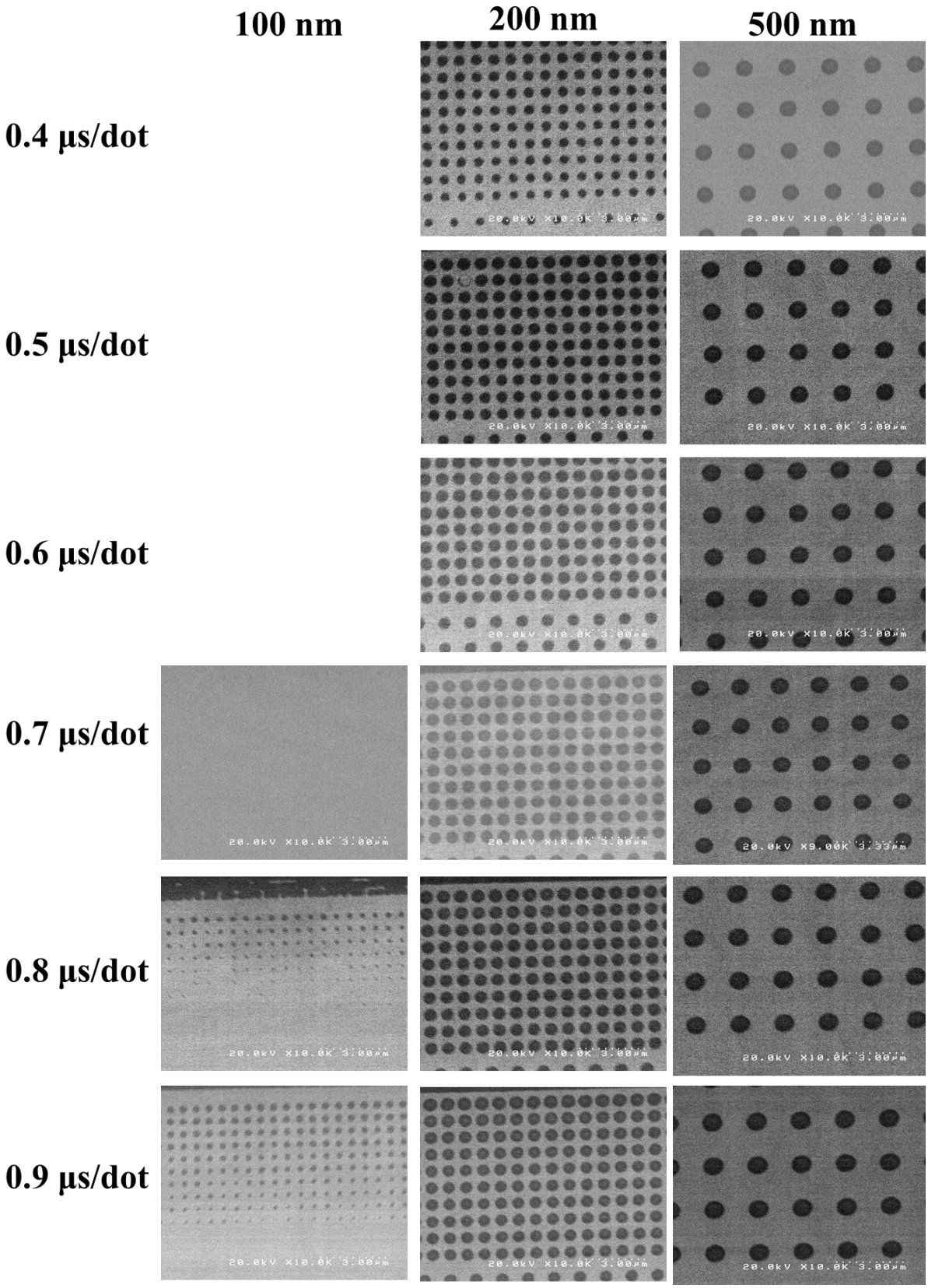

Figure 60. The patterned SAL601-SR2 film after pyrolysis at 700 ºC for 1 hr.

Table. 15. Summary of the size of obtained pattern before and after pyrolysis

Size of dot / Dose time (µs/dot)	100 nm diameter		200 nm diameter	
	Before pyrolysis	**After pyrolysis**	**Before pyrolysis**	**After pyrolysis**
0.4	-	-	227.8	428.6
0.5	-	-	226.2	533.8
0.6	-	-	260.6	585.0
0.7	-	-	287.2	579.0
0.8	99.2	186.0	306.0	574.2
0.9	132	312.0	351.2	553.0

4.4 Conclusion

The fabrication of micro- nano sized carbon dot array was studied. First, the size of electrode was estimated from the immobilization density of PtNPs on PPCE. Then, PPCE in nano scale was fabricated by patterning SAL601-SR2 negative resist covered on PPCE with EBL, followed by dry etching process. Because the etching rate of resist was faster than the etching rate of PPCE, the obtained pattern was not successful. Therefore, we tried to find the alternative method to approach the aim. We are interested in the pyrolysis of SAL601-SR2 because both AZ5214E and SAL601-SR2 contains novolak resin as the main component, it may have a possibility to pyrolyze and turn to carbon film. SAL601-SR2 was patterned on SiO_2/Si substrate, followed by pattern using EBL system. Finally, the patterned substrate was pyrolyzed at 700 ^oC. This method succeeded in sub-micrometer fabrication of carbon dot with smallest size of 186 nm. This opens new opportunity for isolating and counting biomolecule.

Chapter V

CONCLUSION

4.1 Conclusion

In this work, novel metal nanoparticles labeled electrochemical immunoassay for hCG detection using OCP measurement was successfully developed. For AuNPs based OCP detection, the pre-oxidation, diffusion, and reduction processes were performed to the immunocomplex system in order to clear the gap between AuNPs and the electrode surface. The pre-oxidation and reduction processes were found to have significant effect on the sensitivity of the proposed system since they enabled catalytic activities of AuNPs. However, this method requires the application of both oxidation and reduction potentials to achieve detectable signal, which makes it not simplified as OCP method should be. Therefore, the more simple electrochemical immunoassay based on PtNPs was developed. The good electrocatalytic property of hydrazine on PtNPs surface can diminish the need of complicated preoxidation and reduction processes during measurement. The change of signal was observed by direct electric detection by OCP method without any applied external power source. The limit of detection of both developed method was found in pg/mL range with an acceptable sensitivity and reproducibility. Therefore, the proposed detection scheme offers simplicity and high electrochemical sensitivity for hCG detection using PtNPs-labeled immunocomplex, which can be extended to a simplified and miniaturized electrochemical system for clinical diagnosis.

Finally, the fabrication of micro-nano sized carbon electrode array was studied to approach the application of single molecule detection. Since SPCE was successfully utilized in earlier works, carbon-based film such as pyrolysis photoresist carbon film electrode (PPCE) was considered to be a suitable material for realizing nano-sized carbon electrode array. However, the fabrication of PPCE in micro-nano scale has remained challenges due to poor dry-etching selectivity of the PPCE to EB resist. In order to overcome this, a novel approach in which the direct pyrolysis of SAL601-SR2 electron beam resist after patterning was performed to obtain nano-sized carbon electrode array. By this way, no further dry-etching process is required. The pyrolyzed EB resist exhibited uniform and smooth surface and low resistivity that are important for nano-electrode application. This method enabled simple sub-micrometer fabrication of carbon dot (below 200 nm). However, further optimization is needed to approach the desired dot's size such as pyrolysis temperature. In

short, this work shows the simplified and improved electrochemical assay for protein biomarker detection by OCP technique, and possibility to fabricate sub-micrometer sized carbon electrode array for single molecule isolating and counting application.

4.2 Future perspective

In this work, this fabrication method provides the successful in sub-micrometer fabrication of carbon dot. We expected that this work enables the combination of carbon based nano electrode array with OCP measurement for simplification of electrochemical system and application for biomolecule isolation and counting.

References

[1] F. Ricci, G. Adornetto, G. Palleschi, A review of experimental aspects of electrochemical immunosensors, Electrochimica Acta, 84 (2012) 74-83.

[2] E. Engvall, P. Perlmann, Enzyme-linked immunosorbent assay (ELISA). Quantitative assay of immunoglobulin G, Immunochemistry, 8 (1971) 871-874.

[3] A.K. Sinha, Colorimetric assay of catalase, Analytical Biochemistry, 47 (1972) 389-394.

[4] Y. Wan, Y. Su, X. Zhu, G. Liu, C. Fan, Development of electrochemical immunosensors towards point of care diagnostics, Biosensors and Bioelectronics, 47 (2013) 1-11.

[5] N. Gan, Y. Wu, F. Hu, T. Li, L. Zheng, Y. Cao, One novel nano magnetic Fe3O4/ZrO2/nano Au composite membrane modified amperometric immunosensor for α-fetoprotein in human serum, 2011.

[6] J. Liu, G. Lin, C. Xiao, Y. Xue, A. Yang, H. Ren, W. Lu, H. Zhao, X. Li, Z. Yuan, Sensitive electrochemical immunosensor for α-fetoprotein based on graphene/SnO2/Au nanocomposite, Biosensors and Bioelectronics, 71 (2015) 82-87.

[7] M.K. Sharma, J. Narayanan, S. Upadhyay, A.K. Goel, Electrochemical immunosensor based on bismuth nanocomposite film and cadmium ions functionalized titanium phosphates for the detection of anthrax protective antigen toxin, Biosensors and Bioelectronics, 74 (2015) 299-304.

[8] K. Idegami, M. Chikae, K. Kerman, N. Nagatani, T. Yuhi, T. Endo, E. Tamiya, Gold Nanoparticle-Based Redox Signal Enhancement for Sensitive Detection of Human Chorionic Gonadotropin Hormone, Electroanalysis, 20 (2008) 14-21.

[9] H.A. Videla, Manual of Biocorrosion, CRC press, Inc., Florida, USA, 1996.

[10] M. Ciobanu, J.P. Wilburn, N.I. Buss, P. Ditavong, D.A. Lowy, Miniaturized Reference Electrodes Based on Ag/AgiX Internal Reference Elements. I. Manufacturing and Performance, Electroanalysis, 14 (2002) 989-997.

[11] A.S. Ahammad, Y.-H. Choi, K. Koh, J.-H. Kim, J.-J. Lee, M. Lee, Electrochemical detection of cardiac biomarker troponin I at gold nanoparticle-modified ITO electrode by using open circuit potential, International Journal of Electrochemical Science, 6 (2011) 1906-1916.

[12] B.A. Averill, P. Eldredge, Describing electrochemical cells, Flat World Education, Inc., 2012.
[13] A.J. Bard, L.R. Faulkner, Electrochemical Methods: Fundamentals and Applications, JOHN WILEY & SONS, INC.2001.
[14] B.A. Averill, Describing electrochemical cells, 2012.
[15] C. Zoski, Handbook of Electrochemistry, Elsevier2006.
[16] J. Weng, Analytical Electrochemistry, A John Wiley & Sons, Inc.2000.
[17] Mass transfer polarization.
[18] D.A. Skoog, F.J. Holler, S.R. Crouch, Principles of Instrumental Analysis, Harcourt Brace College, New York, USA, 2007.
[19] P.W. Baker, K. Ito, K. Watanabe, Marine prosthecate bacteria involved in the ennoblement of stainless steel, Environmental Microbiology, 5 (2003) 925-932.
[20] J. Dumańska, K. Maksymiuk, Studies on Spontaneous Charging/Discharging Processes of Polypyrrole in Aqueous Electrolyte Solutions, Electroanalysis, 13 (2001) 567-573.
[21] M. Li, Y.-T. Li, D.-W. Li, Y.-T. Long, Recent developments and applications of screen-printed electrodes in environmental assays—A review, Analytica Chimica Acta, 734 (2012) 31-44.
[22] O.D. Renedo, M.A. Alonso-Lomillo, M.J.A. Martínez, Recent developments in the field of screen-printed electrodes and their related applications, Talanta, 73 (2007) 202-219.
[23] M.A. Alonso-Lomillo, O. Domínguez-Renedo, M.J. Arcos-Martínez, Screen-printed biosensors in microbiology; a review, Talanta, 82 (2010) 1629-1636.
[24] M. Yan, D. Zang, S. Ge, L. Ge, J. Yu, A disposable electrochemical immunosensor based on carbon screen-printed electrodes for the detection of prostate specific antigen, Biosensors and Bioelectronics, 38 (2012) 355-361.
[25] W. Dou, W. Tang, G. Zhao, A disposable electrochemical immunosensor arrays using 4-channel screen-printed carbon electrode for simultaneous detection of Escherichia coli O157:H7 and Enterobacter sakazakii, Electrochimica Acta, 97 (2013) 79-85.
[26] S.F. Chin, L.S. Lim, S.C. Pang, M.S.H. Sum, D. Perera, Carbon nanoparticle modified screen printed carbon electrode as a disposable electrochemical

immunosensor strip for the detection of Japanese encephalitis virus, Microchimica Acta, 184 (2017) 491-497.
[27] S.D. Tallapragada, K. Layek, R. Mukherjee, K.K. Mistry, M. Ghosh, Development of screen-printed electrode based immunosensor for the detection of HER2 antigen in human serum samples, Bioelectrochemistry, 118 (2017) 25-30.
[28] A.J. Gross, A.J. Downard, Regeneration of Pyrolyzed Photoresist Film by Heat Treatment, Analytical Chemistry, 83 (2011) 2397-2402.
[29] N.E. Hebert, B. Snyder, R.L. McCreery, W.G. Kuhr, S.A. Brazill, Performance of Pyrolyzed Photoresist Carbon Films in a Microchip Capillary Electrophoresis Device with Sinusoidal Voltammetric Detection, Analytical Chemistry, 75 (2003) 4265-4271.
[30] L. Moretto, A. Mardegan, M. Cettolin, P. Scopece, Pyrolyzed Photoresist Carbon Electrodes for Trace Electroanalysis of Nickel(II), Chemosensors, 3 (2015) 157.
[31] O. Niwa, D. Kato, Nanocarbon Film-Based Electrochemical Detectors and Biosensors, in: M.d.C. Vestergaard, K. Kerman, I.M. Hsing, E. Tamiya (Eds.) Nanobiosensors and Nanobioanalyses, Springer Japan, Tokyo, 2015, pp. 121-136.
[32] D.J. Fischer, M.K. Hulvey, A.R. Regel, S.M. Lunte, Amperometric detection in microchip electrophoresis devices: Effect of electrode material and alignment on analytical performance, ELECTROPHORESIS, 30 (2009) 3324-3333.
[33] S. T. Larsen, A. Argyraki, L. Amato, S. Tanzi, S. Keller, N. Rozlosnik, R. Taboryski, Pyrolyzed Photoresist Electrodes for Integration in Microfluidic Chips for Transmitter Detection from Biological Cells, 2013.
[34] J.A. Lee, S. Hwang, J. Kwak, S.I. Park, S.S. Lee, K.-C. Lee, An electrochemical impedance biosensor with aptamer-modified pyrolyzed carbon electrode for label-free protein detection, Sensors and Actuators B: Chemical, 129 (2008) 372-379.
[35] F. Wang, S. Hu, Electrochemical sensors based on metal and semiconductor nanoparticles, Microchimica Acta, 165 (2009) 1-22.
[36] X. Luo, A. Morrin, A.J. Killard, M.R. Smyth, Application of Nanoparticles in Electrochemical Sensors and Biosensors, Electroanalysis, 18 (2006) 319-326.
[37] F.W. Campbell, R.G. Compton, The use of nanoparticles in electroanalysis: an updated review, Analytical and Bioanalytical Chemistry, 396 (2010) 241-259.
[38] Y. Li, H.J. Schluesener, S. Xu, Gold nanoparticle-based biosensors, Gold Bulletin, 43 (2010) 29-41.

[39] D. Tang, R. Yuan, Y. Chai, Ultrasensitive Electrochemical Immunosensor for Clinical Immunoassay Using Thionine-Doped Magnetic Gold Nanospheres as Labels and Horseradish Peroxidase as Enhancer, Analytical Chemistry, 80 (2008) 1582-1588.
[40] S. Wu, Z. Zhong, D. Wang, M. Li, Y. Qing, N. Dai, Z. Li, Gold nanoparticle-labeled detection antibodies for use in an enhanced electrochemical immunoassay of hepatitis B surface antigen in human serum, Microchimica Acta, 166 (2009) 269-275.
[41] J. Tang, B. Su, D. Tang, G. Chen, Conductive carbon nanoparticles-based electrochemical immunosensor with enhanced sensitivity for α-fetoprotein using irregular-shaped gold nanoparticles-labeled enzyme-linked antibodies as signal improvement, Biosensors and Bioelectronics, 25 (2010) 2657-2662.
[42] N. Xuan Viet, M. Chikae, Y. Ukita, K. Maehashi, K. Matsumoto, E. Tamiya, P. Hung Viet, Y. Takamura, Gold-linked electrochemical immunoassay on single-walled carbon nanotube for highly sensitive detection of human chorionic gonadotropinhormone, Biosensors and Bioelectronics, 42 (2013) 592-597.
[43] B. Kavosi, A. Salimi, R. Hallaj, F. Moradi, Ultrasensitive electrochemical immunosensor for PSA biomarker detection in prostate cancer cells using gold nanoparticles/PAMAM dendrimer loaded with enzyme linked aptamer as integrated triple signal amplification strategy, Biosensors and Bioelectronics, 74 (2015) 915-923.
[44] J. Zhang, B.P. Ting, M. Khan, M.C. Pearce, Y. Yang, Z. Gao, J.Y. Ying, Pt nanoparticle label-mediated deposition of Pt catalyst for ultrasensitive electrochemical immunosensors, Biosensors and Bioelectronics, 26 (2010) 418-423.
[45] Z. Cui, D. Wu, Y. Zhang, H. Ma, H. Li, B. Du, Q. Wei, H. Ju, Ultrasensitive electrochemical immunosensors for multiplexed determination using mesoporous platinum nanoparticles as nonenzymatic labels, Analytica Chimica Acta, 807 (2014) 44-50.
[46] Y. Li, L. Tian, H. Jia, X. Pang, W. Cao, Q. Wei, An electrochemical immunosensor for ultrasensitive detection of HBsAg based on platinum nanoparticles loaded on natural montmorillonite, Analytical Methods, 7 (2015) 9150-9157.
[47] L. Liu, L. Tian, G. Zhao, Y. Huang, Q. Wei, W. Cao, Ultrasensitive electrochemical immunosensor for alpha fetoprotein detection based on platinum nanoparticles anchored on cobalt oxide/graphene nanosheets for signal amplification, Analytica Chimica Acta, (2017).

[48] J. Todd, B. Freese, A. Lu, D. Held, J. Morey, R. Livingston, P. Goix, Ultrasensitive flow-based immunoassays using single-molecule counting, Clin Chem, 53 (2007) 1990-1995.
[49] D. Jiang, C. Liu, L. Wang, W. Jiang, Fluorescence single-molecule counting assays for protein quantification using epi-fluorescence microscopy with quantum dots labeling, Analytica Chimica Acta, 662 (2010) 170-176.
[50] D.R. Walt, Optical Methods for Single Molecule Detection and Analysis, Analytical Chemistry, 85 (2013) 1258-1263.
[51] L. Wang, G. Xu, Z. Shi, W. Jiang, W. Jin, Quantification of protein based on single-molecule counting by total internal reflection fluorescence microscopy with adsorption equilibrium, Analytica chimica acta, 590 (2007) 104-109.
[52] D. Jiang, L. Wang, W. Jiang, Quantitative detection of antibody based on single-molecule counting by total internal reflection fluorescence microscopy with quantum dot labeling, Analytica chimica acta, 634 (2009) 83-88.
[53] L. Chang, D.M. Rissin, D.R. Fournier, T. Piech, P.P. Patel, D.H. Wilson, D.C. Duffy, Single molecule enzyme-linked immunosorbent assays: theoretical considerations, Journal of immunological methods, 378 (2012) 102-115.
[54] D.M. Rissin, C.W. Kan, T.G. Campbell, S.C. Howes, D.R. Fournier, L. Song, T. Piech, P.P. Patel, L. Chang, A.J. Rivnak, E.P. Ferrell, J.D. Randall, G.K. Provuncher, D.R. Walt, D.C. Duffy, Single-molecule enzyme-linked immunosorbent assay detects serum proteins at subfemtomolar concentrations, Nature biotechnology, 28 (2010) 595-599.
[55] M. Altissimo, E-beam lithography for micro-/nanofabrication, Biomicrofluidics, 4 (2010) 026503.
[56] R.F.W. Pease, Electron beam lithography, Contemporary Physics, 22 (1981) 265-290.
[57] C. Vieu, F. Carcenac, A. Pépin, Y. Chen, M. Mejias, A. Lebib, L. Manin-Ferlazzo, L. Couraud, H. Launois, Electron beam lithography: resolution limits and applications, Applied Surface Science, 164 (2000) 111-117.
[58] Y. Chen, Nanofabrication by electron beam lithography and its applications: A review, Microelectronic Engineering, 135 (2015) 57-72.
[59] K. Nojiri, Dry Etching Technology for Semiconductors, 2015.

[60] M. Madou, Fundamentals of Microfabrication: The Science of Miniaturization, Second Edition, 1997.
[61] R. C. Jaeger, Introduction to Microelectronic Fabrication / R.C. Jaeger, 2017.
[62] A.P. Nayak, L. VJ, M.S. Islam, Wet and Dry Etching.
[63] H.J. Lee, A.W. Wark, R.M. Corn, Microarray methods for protein biomarker detection, The Analyst, 133 (2008) 975-983.
[64] N. Rifai, M.A. Gillette, S.A. Carr, Protein biomarker discovery and validation: the long and uncertain path to clinical utility, Nature biotechnology, 24 (2006) 971-983.
[65] P. Berger, C. Sturgeon, Pregnancy testing with hCG – future prospects, Trends in Endocrinology & Metabolism, 25 (2014) 637-648.
[66] M. Montagnana, T. Trenti, R. Aloe, G. Cervellin, G. Lippi, Human chorionic gonadotropin in pregnancy diagnostics, Clinica Chimica Acta, 412 (2011) 1515-1520.
[67] U.-H. Stenman, H. Alfthan, Determination of human chorionic gonadotropin, Best Practice & Research Clinical Endocrinology & Metabolism, 27 (2013) 783-793.
[68] U.-H. Stenman, A. Tiitinen, H. Alfthan, L. Valmu, The classification, functions and clinical use of different isoforms of HCG, Human Reproduction Update, 12 (2006) 769-784.
[69] U.L.F.H. Stenman, H. Alfthan, T. Ranta, E. Vartiainen, J. Jalkanen, M. SeppÄLÄ, Serum Levels of Human Chorionic Gonadotropin in Nonpregnant Women and Men Are Modulated by Gonadotropin-Releasing Hormone and Sex Steroids*, The Journal of Clinical Endocrinology & Metabolism, 64 (1987) 730-736.
[70] S. Madersbacher, R. Klieber, K. Mann, C. Marth, M. Tabarelli, G. Wick, P. Berger, Free alpha-subunit, free beta-subunit of human chorionic gonadotropin (hCG), and intact hCG in sera of healthy individuals and testicular cancer patients, Clinical Chemistry, 38 (1992) 370-376.
[71] A.G. Rushworth, A.H. Orr, K.D. Bagshawe, The concentration of HCG in the plasma and spinal fluid of patients with trophoblastic tumours in the central nervous system, British Journal of Cancer, 22 (1968) 253-257.
[72] U.H. Stenman, Testicular cancer: The perfect paradigm for marker combinations, Scandinavian Journal of Clinical and Laboratory Investigation, 65 (2005) 181-188.
[73] U.-H. Stenman, H. Alfthan, K. Hotakainen, Human chorionic gonadotropin in cancer, Clinical Biochemistry, 37 (2004) 549-561.

[74] E. Engvall, P. Perlmann, Enzyme-linked immunosorbent assay (ELISA) quantitative assay of immunoglobulin G, Immunochemistry, 8 (1971) 871-874.
[75] R.M. Lequin, Enzyme Immunoassay (EIA)/Enzyme-Linked Immunosorbent Assay (ELISA), Clinical Chemistry, 51 (2005) 2415.
[76] S. Paulie, H. Perlmann, Enzyme-Linked Immunosorbent Assay, eLS, John Wiley & Sons, Ltd2001.
[77] Overview of ELISA.
[78] Competitive ELISA: Basic Principles.
[79] H. Zhou, J.H. Park, F.-R.F. Fan, A.J. Bard, Observation of Single Metal Nanoparticle Collisions by Open Circuit (Mixed) Potential Changes at an Ultramicroelectrode, Journal of the American Chemical Society, 134 (2012) 13212-13215.
[80] D.M. Rissin, C.W. Kan, T.G. Campbell, S.C. Howes, D.R. Fournier, L. Song, T. Piech, P.P. Patel, L. Chang, A.J. Rivnak, E.P. Ferrell, J.D. Randall, G.K. Provuncher, D.R. Walt, D.C. Duffy, Single-molecule enzyme-linked immunosorbent assay detects serum proteins at subfemtomolar concentrations, Nature biotechnology, 28 (2010) 595.
[81] S.H. Kim, S. Iwai, S. Araki, S. Sakakihara, R. Iino, H. Noji, Large-scale femtoliter droplet array for digital counting of single biomolecules, 2012.
[82] A.L. Jung, L. Kwang-Cheol, P. Se Il, S.L. Seung, The fabrication of carbon nanostructures using electron beam resist pyrolysis and nanomachining processes for biosensing applications, Nanotechnology, 19 (2008) 215302.

ACHIEVEMENTS

Publications

1. K. Charoenkitamorn, P. T. Tue, K. Kawai, O. Chailapakul, Y. Takamura, Sensors, 18 (2018) 444.
   "Electrochemical Immunoassay using Open Circuit Potential Detection labeled by Platinum Nanoparticles"
2. K. Charoenkitamorn, P. T. Tue, M. Chikae, O. Chailapakul, Y. Takamura, Electroanalysis, under revision.
   "Gold Nanoparticles Labeled Electrochemical Immunoassay using Open Circuit Potential for Human Chorionic Gonadotropin Detection"

Conferences

1. The 78th Japan Society of Applied Physics (JSAP) Autumn Meeting 2017 (September 5-8, 2017)
   "A simple platinum nanoparticles based electrochemical immunoassay for sensitive detection of human chorionic gonadotropin hormone using open circuit potential"

ACKNOWLEDGEMENTS

I would like to express my deep appreciation to my advisor, Professor Yuzuru Takamura for providing the useful suggestions, training and teaching the theoretical background and technical skills during my research. As well with Assistant Professor Phan Trong Tue for his valuable suggestions, advice and correcting to my thesis from the beginning up to completion of my writing, and the members of examination committee, Professor Takahiro Hohsaka (JAIST), Associate Professor Masashi Akabori (JAIST), Associate Professor Yuichi Hiratsuka (JAIST), and Associate Professor Takahiro Yamaguchi (Kanazawa University).

I would also especially like to thank the financial supports for my study and research here, the great collaboration between Japan Advanced Institute of Science and Technology (JAIST) and Chulalongkorn University (CU, Thailand).

In addition, a thank you to members of Takamura Laboratory, School of Materials Science, Japan Advanced Institute of Science and Technology for the suggestions and spiritual supports throughout this research.

I would like to thanks my colleagues in Electrochemistry and Optical Spectroscopy Center of Excellence (EOSCE), Department of Chemistry, Faculty of Science, Chulalongkorn University, and all good friends for the suggestions and supports throughout this research.

Lastly, I am very grateful to my family; my parents, for their love and understanding. For my siblings, thank you very much indeed for encouraging and supporting me during the whole period of my study and research here, Japan Advanced Institute of Science and Technology (JAIST).

2017, November 22

Kanokwan CHAROENKITAMORN